UNIVERSITY *of the*
WESTERN CAPE

ASSESSING THE CHANGE IN HYDRO-GEOCHEMICAL PROPERTIES OF FLY ASH OVER TIME WHEN DISPOSED INTO OPENCAST COAL MINES IN MPUMALANGA, SOUTH AFRICA.

By

Angelo Gerald Johnson

Thesis submitted in fulfilment of the requirements for the degree of

Master of Science

UNIVERSITY *of the*
WESTERN CAPE

The Department of Earth Sciences

Faculty of Natural Sciences

The University of the Western Cape

Supervisor: Dr. Jaco Nel

Co-supervisor: Dr. Thokozani Kanyerere

https://etd.uwc.ac.za

Declaration

I declare that "**Assessing the change in hydro-geochemical properties of fly ash over time when disposed into opencast coal mines in Mpumalanga, South Africa"** is my own work, that it has not been submitted for any degree or examination in any other university, and that all the sources I have used or quoted have been indicated and acknowledged by complete references.

Full Name: Angelo Gerald Johnson

Date: 30 November 2018

https://etd.uwc.ac.za

Acknowledgements

I would like to thank and praise the Almighty God for the blessings, courage and perseverance He bestowed upon me during my journey as a Masters candidate. I dedicate my thesis to my late grandfather, hero and inspiration Augustus Jeremiah (Boy) Engelbrecht. Most of all, overcoming the anxiety that comes with completing a master's degree, it was all done in the name of science. I would also like to thank the following people who played a major role in my life and contributed to this project:

- My academic father, supervisor and mentor Dr. Jaco Nel for guiding me in my scientific thinking throughout this project. You introduced me to a world of opportunity in the field of geohydrology. Most of all, thanks for the friendship and the braais.
- My co-supervisor Dr. Thokozani Kanyerere for his academic guidance and opportunities. Thanks for introducing me to Dr. Nel.
- SANParks and my supervisor Mr. Willem Louw for the opportunity of employment as Junior Scientist under the UNDP/GEF5 project.
- ESKOM and Kelley Reynolds-Clausen for funding this project and allowing me to do my science and figure out solutions for their Coal Ash problem. Kelley you are truly appreciated.
- Marlese Nel I am forever grateful for your hospitality. You're patience in reviewing my scientific papers are truly appreciated.
- Johan and Anneline Fourie, owners of Metron laboratories for analysing my water samples.
- My colleagues in the department of Earth Science at UWC: Annalisa Vicente, Phumlani Mqondeki, Vincent Banda, Nangamso Tuswa, Pamela Sekese. Thanks for your support guys! Also thanks to Victor Delicado for the assistance in the field, I also enjoyed the stays at your place.
- My friends and family for their emotional support when times were tough, also for some financial support when I couldn't carry myself. All of you are highly appreciated.
- Last but not least, my beautiful 3 sisters (Elizma, Mikyla and Andrea) for always believing in me and motivating me to become the best I can be. My strong and supportive parents (Paul and Audrey) for supporting all my decisions since day 1.

Without all of you, I would not have come this far and with your continuous support I promise this is not yet the end!

UNIVERSITY of the
WESTERN CAPE

https://etd.uwc.ac.za

Abstract

Eskom supplies to 95% of South Africa's energy needs and it primarily comes from coal combustion at their coal–fired power stations. Large volumes of fly ash are generated at these coal-fired power stations as a by-product of the coal combustion process. Fly ash is disposed onto landfills at the respective power stations and these landfills are currently running out of storage space. Subsequently, there are concerning environmental impacts upon the natural water environment resulting from coal mining. More specifically, the discharge of acid mine (AMD) water from historical coal mines impact negatively on the water quality in the nearby rivers and dams in the Witbank area.

Therefore, as a consequence of the limited space at fly ash landfills, Eskom has embarked on finding alternative ways to re-use fly ash in different applications such as: soil amelioration and land reclamation, road construction as well as brick and cement development. This study focussed on the feasibility of disposing fly ash into the backfill of historical and future coal mines with the intention to firstly reduce fly ash disposal at existing landfills and secondly to improve the decant water quality of the coal mines in the Witbank area.

Globally, fly ash has been successfully used in mine backfilling and AMD treatment in countries such as United States of America and India, due to cementitious properties of their fly ash. However, there is limited knowledge on how South African fly ash would behave under backfilled conditions of opencast coal mines where it will be exposed to acidic water environments. This is due to the fact that South African fly ash is considered a Level 3 type hazardous waste, due to its heavy metal concentrations. This waste classification is unique and the strictest compared to global classifications and these methodologies specify that fly ash should be disposed onto lined waste disposal sites due to the potential leaching of heavy metals from these waste sites. It is important to understand the hydrogeological and hydro-geochemical properties of fly ash over time once it is exposed to acid mine water.

Field and laboratory tests were conducted to understand these hydrogeological and hydro-geochemical properties of fly ash. Falling head hydraulic tests were conducted at two existing ash landfill sites to determine the hydraulic conductivity (K) of ash of different age. The results exhibit a decreasing trend in K with increasing age. This is due to the pozzolanic nature of fly ash and secondary mineralization of gypsum which causes the fly ash to harden in the presence of water from irrigation for dust suppression together with precipitation over time.

UNIVERSITY of the
WESTERN CAPE

https://etd.uwc.ac.za

Laboratory testing included the use of constant head Darcy column tests to determine the change in K and geochemical properties of the leachate over time. Natural AMD with a pH of 2.5 and a metal composition was used as influent and the leachate were routinely collected and analysed for metal concentrations. The hydraulic conductivity of the fly ash showed a decreasing trend over time. During the placement of coal ash, the moisture allows pozzolanic reactions to solidify the coal ash and lowers the K, towards 10^{-1} m/d, relative to fresh ash. Secondary mineralization of calcium minerals, in the coal ash contributes to a further decrease in the K, by another order of magnitude from 10^{-1} m/d towards 10^{-2} m/d. Sulphate and iron minerals from the AMD also played a major role in the decreasing K as they accumulate in void spaces and having a clogging effect, decreasing the K to 10^{-3} m/d. The alkaline nature of the coal ash initially neutralizes the acidic levels of AMD from an inflow pH = 2.5 to an outflow pH = 11. Acidification of the outflow towards a pH = 4 was observed, due to large volumes of AMD (>80 000 mL) flowing through short coal ash columns. The K decreased to 3 orders of magnitude, from an initial 10^{-1} m/d to 10^{-3} m/d, with the AMD iron (>150 mg/L) and sulphate concentration (>2000 mg/L) playing the dominant role in reducing the hydraulic conductivity.

From the geochemical leach test results, it was observed that most of the leachate water was of a better quality than the influent AMD water quality. The outflow pH (pH = 11 to pH = 4) was higher than the pH of the inflow AMD (pH = 2.5). Overall EC reduced in discharge compared to inflow AMD (EC_{inflow}: 535 – 545 mS/m versus $EC_{outflow}$: 350 – 490 mS/m), although Na and K in the leachate exhibited higher concentrations (10^{+2} mg/L) compared to the AMD inflow concentrations (10^{+1} mg/L). However, most of the other chemical elemental concentrations such as Fe (10^{-2} – 10^{+1} mg/L), Si (10^{-2} – 10^{0} mg/L), Al (10^{-2} – 10^{+1} mg/L), Mn (10^{-2} – 10^{+1} mg/L), Cr (10^{-3} – 10^{0} g/L) and SO_4 (10^{+2} – 1^{+3} mg/L) in the discharge showed lower concentrations when compared to the inflow Fe (10^{+2} mg/L), Si (10^{0} mg/L), Al (10^{+1} mg/L), Mn (10^{+1} mg/L), Cr (10^{-2} mg/L) and SO_4 (10^{+3} mg/L) concentrations. These results show how fly ash backfill may impact on the current coal mining environment.

Overall, the laboratory hydraulic conductivity and geochemical testing showed promising results for fly ash backfilling. Based on this research, fly ash can be used to alter the existing coal mining environment as it is currently known in the Witbank area. The topography, hydraulic conductivity and the water table within the backfill can be altered to improve decant water quality of ash backfilled coal mines.

https://etd.uwc.ac.za

Table of Contents

Declaration ii

Acknowledgements iii

Abstract iv

Table of Contents vi

List of Figures ix

List of Tables xii

List of Abbreviations and Acronyms xiii

Metric Units of measurement xiii

List of Definitions xiii

1 INTRODUCTION 1

1.1 Background 1

1.2 Problem Statement 2

1.3 Aims and Objectives 3

1.4 Research question 3

1.5 Thesis Structure 3

1.6 Research Framework 4

2 LITERATURE REVIEW 5

2.1 Introduction 5

2.2 Data Collection Methods 5

2.2.1 Field component 5

2.2.2 Laboratory component 6

2.3 Characteristics of Fly Ash 8

2.3.1 Pozzolanic binders of fly ash 8

2.3.2 Physical properties of fly ash 8

2.3.3 Chemical properties of fly ash 9

2.3.4 Hydraulic conductivity of fly ash 10

UNIVERSITY of the
WESTERN CAPE

https://etd.uwc.ac.za

2.4 Coal Mining Practices and Impacts....12
2.5 Conclusion....15
3 MATERIALS AND METHODS....16
3.1 Materials....16
3.1.1 Fly ash....16
3.1.2 Acid Mine Drainage (AMD)....18
3.2 Field Methods....18
3.2.1 In-situ hydraulic conductivity testing....18
3.3 Laboratory Methods....20
3.3.1 Hydraulic conductivity testing....20
3.3.2 Geochemical testing....23
3.3.3 Scanning Electron Microscopy (SEM)....23
3.4 Conclusion....24
4 RESULTS AND DISCUSSION....25
4.1 Fly Ash Characteristics....25
4.1.1 Chemical elemental composition and classification....25
4.1.2 Moisture content of fly ash....25
4.1.3 Particle size ratio of fly ash....26
4.1.4 Qualitative external elemental composition....29
4.2 AMD Water Chemistry....31
4.3 Field Hydraulic Conductivity of Ash....31
4.3.1 Kendal power station (K-Ash)....31
4.3.2 Tutuka power station (T-Ash)....36
4.4 Laboratory Hydraulic Conductivity of Fly Ash....40
4.4.1 Hydraulic conductivity of K-Ash and T-Ash at 40% moisture content....41
4.4.2 Hydraulic conductivity of K-Ash and T-Ash at 50% moisture content....43
4.4.3 Hydraulic conductivity of K-Ash and T-Ash at 60% moisture content....44

UNIVERSITY of the
WESTERN CAPE

https://etd.uwc.ac.za

4.4.4 The relationship between hydraulic conductivity and moisture content for K-Ash and T-ash columns 48
4.5 Laboratory Geochemistry 49
4.5.1 Acid Mine Drainage 50
4.5.2 Fly ash environmental geochemistry 51
4.5.3 Leachate chemistry analysis 54
4.6 Conclusion 63
5 EXPECTED MINE BACKFILL CHANGES UNDER DIFFERENT FLY ASH DISPOSAL SCENARIOS 64
5.1 Topographic 64
5.2 Hydraulic conductivity (K) in backfill 64
5.3 Water table in backfill 65
5.4 Post Closure Coal Mine Scenarios 66
5.4.1 Base Case: Coal mine backfill without fly ash 66
5.4.2 Fly ash monolith above water table 67
5.4.3 Fly ash monolith below water table 68
5.5 Conclusion 69
6 CONCLUSIONS AND RECOMMENDATIONS 70
6.1 Conclusion 70
6.2 Recommendations 71
7 REFERENCES 72
APPENDIX A: Darcy column test data. 76
APPENDIX B: Falling head hydraulic test data. 93
APPENDIX C: Leachate samples quality data. 103

UNIVERSITY of the
WESTERN CAPE

https://etd.uwc.ac.za

List of Figures

FIGURE 1.1. Research framework....4
FIGURE 2.1. A schematic depiction of a constant-head permeameter (after (Fetter 2001))...7
FIGURE 2.2. Schematics of (a) unamended and (b) fly ash amended mine tailings (Alhomair et al., 2017)....11
FIGURE 2.3. A conceptual model of an open cast coal mine (Lupankwa et al., 2008)....14
FIGURE 3.1. Fly ash being disposed of at Kendal and Tutuka power stations 16
FIGURE 3.2. Collecting AMD from the Driefontein Pit Lake for laboratory testing....18
FIGURE 3.3. Falling head hydraulic test procedure on fly ash dumps where (A) auger holes are drilled, (B) water injected into the hole with piezometer installed and, (C) falling head is recorded with a water level recording instrument. 19
FIGURE 3.4. A depiction of the caps used in the column setup where, A) Top view, B) Side view and C) Bottom view. 21
FIGURE 3.5. A depiction of the Darcy column testing setup in the laboratory....22
FIGURE 3.6. Samples from 4 columns prepared for SEM imaging after hydraulic conductivity testing. 24
FIGURE 4.1. SEM images of (A) fly ash spheres and sizes 28
FIGURE 4.2. SEM images of (B) Iron-rich material 28
FIGURE 4.3. SEM images of (C) calcium-rich material 28
FIGURE 4.4. SEM images of (E) agglomerated particles and irregular shaped amorphous particles 28
FIGURE 4.5. External elemental composition of Fe and Ca minerals by weight percentage on Fly Ash particles from the K50 column. 30
FIGURE 4.6. External elemental composition of Fe and Ca minerals by weight percentage on Fly Ash particles from the T50 column. 30
FIGURE 4.7. External elemental composition of Fe and Ca minerals by weight percentage on Fly Ash particles from the K60b column. 30
FIGURE 4.8. External elemental composition of Fe and Ca minerals by weight percentage on Fly Ash particles from the T60b column. 30
FIGURE 4.9. The hydraulic conductivity determined for KF-H4 using the Bouwer and Rice solution. 32
FIGURE 4.10. The hydraulic conductivity determined for K5-H4 using the Bouwer and Rice solution. 32

UNIVERSITY of the WESTERN CAPE

https://etd.uwc.ac.za

FIGURE 4.11. The hydraulic conductivity determined for K10-H3 using the Bouwer and Rice solution. 33
FIGURE 4.12. The hydraulic conductivity determined for K15-H1 using the Bouwer and Rice solution. 34
FIGURE 4.13. The hydraulic conductivity determined for K20-H3 using the Bouwer and Rice solution. 34
FIGURE 4.14. In-situ hydraulic conductivity of ash of different age at Kendal Power Station ash dump. 35
FIGURE 4.15. The hydraulic conductivity determined for TF-H2 using the Bouwer and Rice solution. 36
FIGURE 4.16. The hydraulic conductivity determined for T1-H2 using the Bouwer and Rice solution. 37
FIGURE 4.17. The hydraulic conductivity determined for T5-H3 using the Bouwer and Rice solution. 37
FIGURE 4.18. The hydraulic conductivity determined for T20-H3 using the Bouwer and Rice solution. 38
FIGURE 4.19. The hydraulic conductivity determined for T30-H2 using the Bouwer and Rice solution. 39
FIGURE 4.20. In-situ hydraulic conductivity of ash of different age at Tutuka Power Station ash dump. 40
FIGURE 4.21. The hydraulic conductivity of the K40 column pre-cured to 40% moisture content. 41
FIGURE 4.22. The hydraulic conductivity of the T40 column pre-cured to 40% moisture content. 42
FIGURE 4.23. The pH of the K40 and T40 leachate over time. 42
FIGURE 4.24. The change in hydraulic conductivity of fly ash over time plotted with the change in pH of the discharge of fly ash pre-cured to 40% moisture content. ... 43
FIGURE 4.25. The change in hydraulic conductivity of fly ash over time plotted with the change in pH of the discharge of fly ash pre-cured to 50% moisture content. ... 44
FIGURE 4.26. The change in hydraulic conductivity of fly ash over time plotted with the change in pH of the discharge of fly ash pre-cured to 60% moisture content. ... 45
FIGURE 4.27. The change in hydraulic conductivity of fly ash over time plotted with the change in pH of the discharge of fly ash pre-cured to 60% moisture content 47

UNIVERSITY of the
WESTERN CAPE

https://etd.uwc.ac.za

FIGURE 4.28. The relationship between the hydraulic conductivity vs the various moisture content of K-Ash columns. 48
FIGURE 4.29. The relationship between the hydraulic conductivity vs the various moisture content of the T-Ash columns. 49
FIGURE 4.30. Stability diagram for the Al-H2O system at standard conditions (activity Al = $1e^{-3}$). 52
FIGURE 4.31. Stability diagram for the Cr-H2O system at standard conditions (activity Cr = $1e^{-5}$). 52
FIGURE 4.32. Stability diagram for V at standard conditions (activity Al = $1e^{-5}$).....53
FIGURE 4.33. Stability diagram for the B-H2O system at standard conditions (activity Al = $1e^{-5}$). 53
FIGURE 4.34. The EC concentration of influent AMD compared to the temporal trend in EC of the effluent for K-Ash.....54
FIGURE 4.35. The EC concentration of influent AMD compared to the temporal trend in EC of the effluent for T-Ash. 55
FIGURE 4.36. A comparison between influent AMD and leachate Si concentrations.....56
FIGURE 4.37. A comparison between influent AMD and leachate Al concentrations. 57
FIGURE 4.38. A comparison between influent AMD and leachate Fe concentrations. 58
FIGURE 4.39. A comparison between influent AMD and leachate S as SO_4 concentrations. 58
FIGURE 4.40. A comparison between influent AMD and leachate Ca concentrations.....59
FIGURE 4.41. A comparison between influent AMD and leachate Mg concentrations.....60
FIGURE 4.42. A comparison between influent AMD and leachate Na concentrations. 60
FIGURE 4.43. A comparison between influent AMD and leachate K concentrations. 61
FIGURE 4.44. A comparison between influent AMD and leachate Mn concentrations.....61
FIGURE 4.45. A comparison between influent AMD and leachate Cr concentrations. 62
FIGURE 4.46. The hydraulic conductivity of K-Ash and T-Ash columns 63
FIGURE 5.1. Conceptual depiction of an opencast coal mine backfilled without fly ash. 67
FIGURE 5.2. Conceptual depiction of an opencast coal mine backfilled with fly ash above the water table. 68
FIGURE 5.3. Conceptual depiction of an opencast coal mine backfilled with fly ash below the water table. 69

UNIVERSITY of the
WESTERN CAPE

https://etd.uwc.ac.za

List of Tables

TABLE 2.1. The particle general particle size of fly ash found in different literature studies. 9

TABLE 3.1. Field testing set-ups.....19

TABLE 3.2. Laboratory Column Setup. 22

TABLE 4.1. The chemical composition of major and minor oxides by weight percentage (%) of two types of fly ash based on X-ray fluorescence (XRF) analysis. 25

TABLE 4.2. Composition of sand-silt-clay by weight percentage ratio of Fly Ash. 26

TABLE 4.3. Composition of the chemical concentrations of Acid Mine Drainage used as influent. 31

TABLE 4.4. A comparison in hydraulic conductivity of fly ash cured for 3 and 28 days respectively. 40

UNIVERSITY of the
WESTERN CAPE

https://etd.uwc.ac.za

List of Abbreviations and Acronyms

AMD	Acid Mine Drainage
ASTM	American Society of Testing Methods
CSA	Canadian Standards Association
DEA	Department of Environmental Affairs
DWAF	Department of Water Affairs and Forestry
EC	Electrical Conductivity
EIA	Environmental Impact Assessment
ICP	Inductively Coupled Plasma
K	Hydraulic Conductivity
K-Ash	Fly Ash obtained from Kendal power station
LEAF	Leaching Environmental Assessment Framework
NEMA	National Environmental Management Act
SEM	Scanning Electron Microscope
T-Ash	Fly Ash obtained from Tutuka power station
USEPA	United States Environmental Protection Agency

Metric Units of measurement

L/s	Litre per second
mg/L	Milligram per Litre
mS/m	Millisiemens per metre
Mt	Megaton / 1 million ton
µm	Micrometre

UNIVERSITY of the
WESTERN CAPE

List of Definitions

Effluent/Leachate	Water that has percolated through a solid and leached out some of the constituents.
Electrical Conductivity	EC or Electrical Conductivity of water is its ability to conduct an electric current. Salts or other chemicals that dissolve in water can break down into positively and negatively charged ions. These free ions in the water conduct electricity, so the water electrical conductivity depends on the concentration of ions. (AQUAREAD, 2019)
Influent/Leachant	Water used as inflow for column tests

https://etd.uwc.ac.za

1 INTRODUCTION

1.1 Background

Coal mining in South Africa has been taking place since the late 1800's in three provinces: Mpumalanga (Witbank), Kwa-Zulu Natal and recently Limpopo (Waterberg Coalfield). More specifically coal mining commenced in 1894 in the Witbank area, supplying coal to the growing gold and diamond mining industries (McCarthy, 2011). In 2017, South Africa was the 6th biggest coal exporter internationally, exporting coal to China, India and European countries. Domestically, coal-fired power stations are the biggest user of coal to supply to the country's energy needs. Eskom generates about 95% of South Africa's electricity and it primarily comes from coal-fired power stations (Stats SA, 2008). Consequently, the coal-fired power stations generally produce approximately 25 Megaton (Mt) of fly ash annually, through the coal combustion process (Eskom, 2017). Fly ash is considered a waste product for the power stations and is currently disposed onto waste dumps, with limited space to expand.

Of the total amount of fly ash being produced per annum, only 7% is re-used in the cement and brick making industry. Consequently, as part of Eskom's drive to find more alternative beneficial use options for fly ash, this study is focused on the feasibility of using fly ash to backfill historical and potentially future coal mines in the Witbank area, Mpumalanga. Hydrogeological and hydro-geochemical characterisation will be required to determine and estimate these potential impacts.

UNIVERSITY of the
WESTERN CAPE

According to Department of Environmental Affairs (2010), fly ash is currently considered as a Level 3 type of waste, due to its heavy metal concentrations. At a global scale, this hazardous classification of fly ash is unique and the waste type classification is the strictest. The waste classification methodologies follow the leaching methodology on a crushed fine ash sample. Subsequently, the National Environmental Management Act (NEMA) specifies that in order to classify ash, a full Inductively Coupled Plasma (ICP) analysis and complete leaching (varying protocols) of ash are required. These methodologies specifies that ash needs to be disposed of on lined waste disposal sites. However, historic waste disposal sites do not show the leaching of contaminants as predicted by the waste classification methodology, indicating an obvious mismatch between what is predicted by the method and observed in practice.

Therefore, the overall aim of the project is to improve the understanding of the hydrogeological and geochemical processes of a fly ash monolith backfill with reference to acid mine drainage and mine decant water quality. The intention is to set up laboratory experiments that would be

https://etd.uwc.ac.za

more representative of field conditions where fly ash will be exposed to acid mine drainage in coal mining environments. The outcome of this study will be to conclude whether fly ash can be disposed in opencast coal mines in the Witbank area and, how this application would impact on the current coal mining environment.

1.2 Problem Statement

The current fly ash disposal method is not an optimal solution for disposal, due to landfill space limitations and tipping costs (Daniels et al., 2002). More specifically, many of Eskom's coal-fired power stations are currently running out of ash storage space (Reynolds-Clausen and Singh, 2016).

Therefore, disposing fly ash as a monolith into the backfill of old and future opencast coal mines is a potential alternative way of reducing ash deposition on ash dumps and might potentially mitigate the generation and impacts of acid mine drainage (AMD). However, in order to determine the feasibility of fly ash backfill, it is important to understand the hydro-geochemical properties of fly ash once it is exposed to the opencast coal mining environment. The literature shows that various studies have been done on the hydraulic and geochemical properties of ash. These studies include: use of ash as amended mine tailings (Alhomair, 2017), hydraulic properties (Kostas et al., 2000; Sivapullaiah and Lakshmikantha, 2004; October, 2011), physical properties (October 2011; Muchingami 2013) and the chemical properties of fly ash (Campbell, 1999; Vadapalli *et al.*, 2007; Akinyemi *et al.*, 2013)

UNIVERSITY of the
WESTERN CAPE

Several historical coal mines in the Witbank area of the Mpumalanga province have been generating AMD. The AMD discharges from these old mine sites and it has been revealed that it has led to the deterioration in the water quality in many surface streams (Geldenhuis and Bell, 1998). McCarthy (2011) found that the high salinity and sulphate concentrations (exceeding 200 mg/L which is above the recommended DWAF 1996 standard for domestic use) in the Middelburg and Witbank dams is a direct consequence of these acidic waters discharging from the old mine sites and into the streams. It is postulated that fly ash backfilling can be used to reduce these negative impacts of AMD on surface water bodies, while reducing Eskom ash disposal footprints.

However, there is limited knowledge on how South African fly ash would behave under backfilled conditions into an AMD generating opencast mine and the impact on the immediate environment surrounding the mine sites. Thus, there is a need to assess the hydraulic and

https://etd.uwc.ac.za

geochemical properties of fly ash to comprehend how fly ash backfill would potentially impact on the natural water environment (groundwater and surface water).

1.3 Aims and Objectives

The aim of this study is to investigate the temporal change in hydro-geochemical properties of fly ash if disposed as a monolith within opencast coal mines. This will provide knowledge and understanding on how the hydraulic and geochemical properties of fly ash will impact on the mining environment. The objectives of this study therefore are to:

- Assess the temporal change in hydraulic conductivity of fly ash at both field and laboratory scale.
- Evaluate the chemical changes of AMD flowing through fly ash.
- Evaluate how fly ash disposal will influence the current mining backfill impacts.

1.4 Research question

What are the hydraulic and geochemical properties of fly ash that need to be understood to demonstrate or predict how fly ash would potentially impact on the natural water environment (groundwater and surface water)?

1.5 Thesis Structure

Chapter 1 introduces the research and the importance of conducting the study. Chapter 2 entails a desktop study on the important components of this research. These components include: a) challenges of a relentless growing fly ash production and its problems with space and costs associated with the current fly ash disposal sites, b) characteristics of fly ash including the physical and chemical properties, hydraulic conductivity and geochemical research that has been conducted on fly ash and c) the data collection methods with regards to the laboratory and field tests that are typically conducted to study the hydraulic and geochemical properties of fly ash. The materials and methods used in this research are explained in Chapter 3 and elaborates on the field and laboratory experiments that were conducted to achieve the research objectives. Chapter 4 entails the analysis and discussion of the field and laboratory data and results. In Chapter 5, a combination of the field and laboratory test results and analysis are used to generate potential conceptual backfill scenarios of fly ash into opencast coal mines and that will prevent negative impacts. It includes scenarios of fly ash disposed as a monolith in various locations within the backfill of opencast coal mines. Conclusions of the study and further recommendations are made in Chapter 6.

UNIVERSITY of the WESTERN CAPE
https://etd.uwc.ac.za

1.6 Research Framework

FIGURE 1.1 depicts the process that was followed in the study. Firstly, the topic (Assessing the change in hydro-geochemical properties of fly ash over time when disposed into opencast coal mines) for the research was chosen and a desktop study followed to gather information regarding the hydraulic and geochemical properties of fly ash. Thereafter, field and laboratory testing methods were chosen in order to generate hydraulic and geochemical data. Lastly, the hydraulic and geochemical data that was obtained through the field and laboratory testing, was used to conceptualise potential mine backfilling scenarios with fly ash. Ultimately, the data was used to conclude whether it is feasible to backfill opencast coal mines with fly ash.

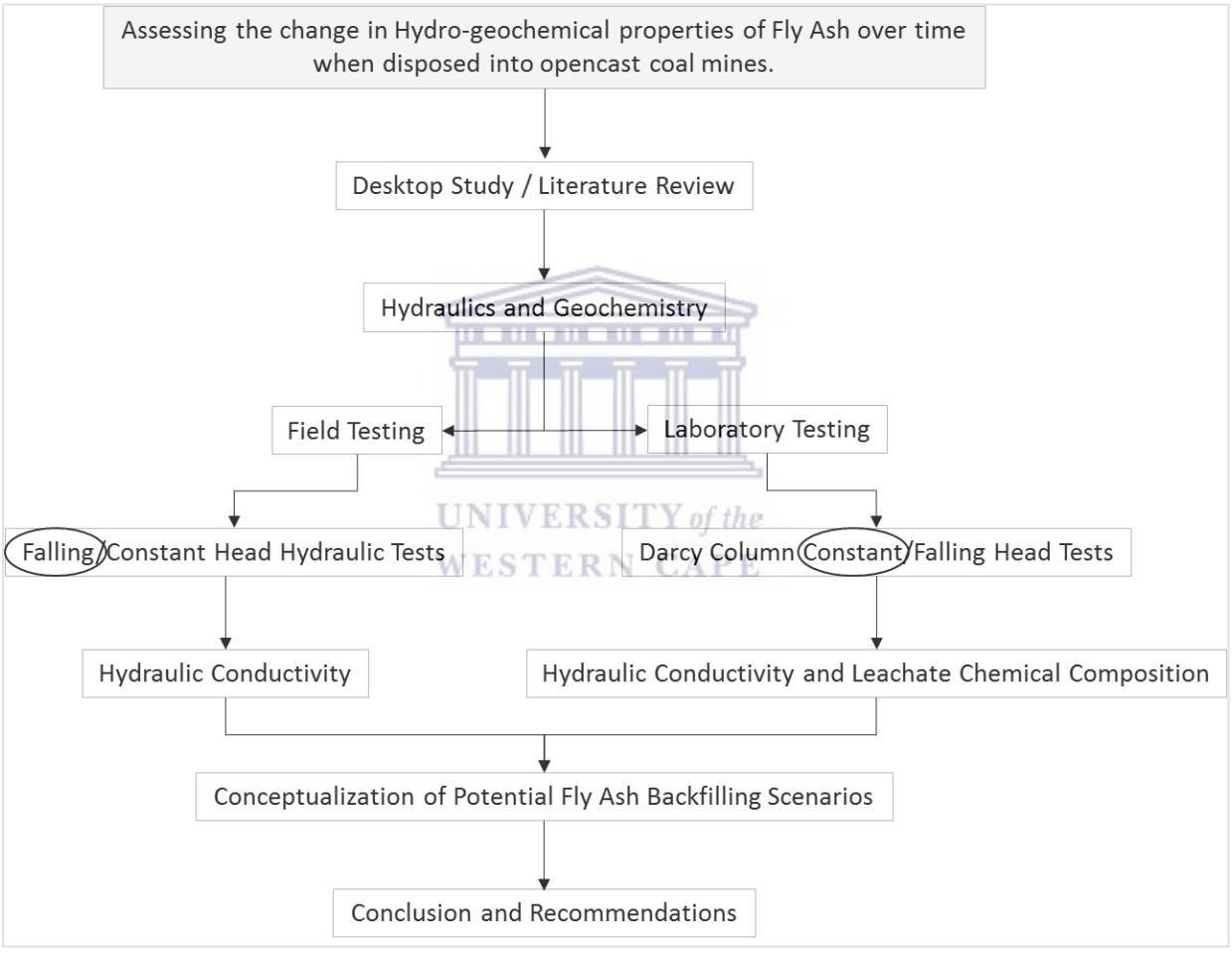

FIGURE 1.1. *Research framework*

https://etd.uwc.ac.za

2 LITERATURE REVIEW

2.1 Introduction

This chapter introduces the desktop study which was conducted with regards to the research that has been done on fly ash. The literature reviewed entailed the physical, hydrogeological and geochemical characteristics of fly ash. Lastly, a review was done on the current coal mining closure practices and its impacts on the environment.

2.2 Data Collection Methods

2.2.1 Field component

2.2.1.1 Hydraulic Conductivity Testing

According to Fetter (2001), the Bouwer and Rice slug-test method is a useful method when determining the permeability of unconfined geological material. The method suggests that a volume of water is removed from a well or borehole, after which the rate of the rise in water level is measured. Alternatively, a volume of water can also be injected to the well and the subsequent rate in the fall of water level can be measured. The rate at which the water level falls or rises, is directly linked to the transmissivity or hydraulic conductivity of the aquifer. Moreover, there are multiple slug test methods which are designed for different applications depending on the aquifer type. The methods used for confined aquifers are, (i) Cooper's (1967) method, (ii) Uffink's (1979, 1980) method for oscillation tests, (iii) Cooper-Bredehoeft-Papadopulos (1967) method, (iv) Hvorslev (1956) Slug-Test method, and (v) Van der Kamp (1976) method. Additionally, the Bouwer and Rice (Bouwer and Rice, 1976; Bouwer, 1989) slug-test method was designed for unconfined aquifers. The test can be performed on open boreholes and screened wells. The Bouwer and Rice (1976) equation:

$$K = \frac{r_c^2 \ln(R_e / r_w)}{2d} \frac{1}{t} - ln \frac{h_o}{h_t} \qquad \textit{Equation 1}$$

Where:

K = Hydraulic conductivity (m/d)

r_c = radius of the casing where the rise of the water level is measured (m)

R_e = radial distance over which the difference in head is dissipated (m)

h_o = Head in piezometer at $t_o = 0$ (m)

h_t = Head in piezometer at $t > t_o$ (m)

r_w = effective radius of piezometers (m)

d = length of open section of piezometer through which water can enter (m)

https://etd.uwc.ac.za

t = the time since H = H_0 (s)

2.2.2 Laboratory component

2.2.2.1 Hydraulic conductivity testing

Darcy's law is commonly applied in laboratory experiments to determine the saturated hydraulic conductivity of geological material, using constant head hydraulic test data. The law can be described as a simple proportional relationship between the instantaneous discharge rate (Q) through a porous medium, hydraulic conductivity (K), hydraulic gradient (I) and cross-sectional area (A). The hydraulic conductivity of a geological material, is one of the most important physical parameters studied by hydrogeologists. It is considered that the hydraulic conductivity is the permeability of a given rock with respect to water (Younger, 2007).

A permeameter is a device used in the laboratory to measure hydraulic conductivity of a given hydrogeological material. There are two types of permeameters namely (a) a constant-head permeameter and (b) a falling head permeameter. The constant-head permeameter is mainly used to measure hydraulic conductivity of non-cohesive sediments, such as sand, whereas, falling-head permeameters are used to measured cohesive materials usually having low conductivities (Fetter, 2001). For this study, the constant-head permeameter was chosen in accordance with the ASTM standard method A and the USEPA method 1314 (USEPA, 2012; ASTM, 2016).

UNIVERSITY of the
WESTERN CAPE

A constant head permeameter is illustrated in FIGURE 2.1. To determine the hydraulic conductivity from the test setup, the following parameters are measured and substituted into Darcy's equation:

$$Q = KIA \qquad \textit{Equation 2}$$

Where:

- Q: The volume of water discharging from the column per unit time t and the units of measurement are in cubic meter per day (m^3/d).
- K: The hydraulic conductivity measured in meters per day (m/d)
- I: Hydraulic gradient (Δ H) measured as the difference in head ($H_1 - H_2$) in meters over the length (L) of the sample in meters (m/m).
- A: The cross-sectional area (A) of the sample measured in square meters (m^2).

https://etd.uwc.ac.za

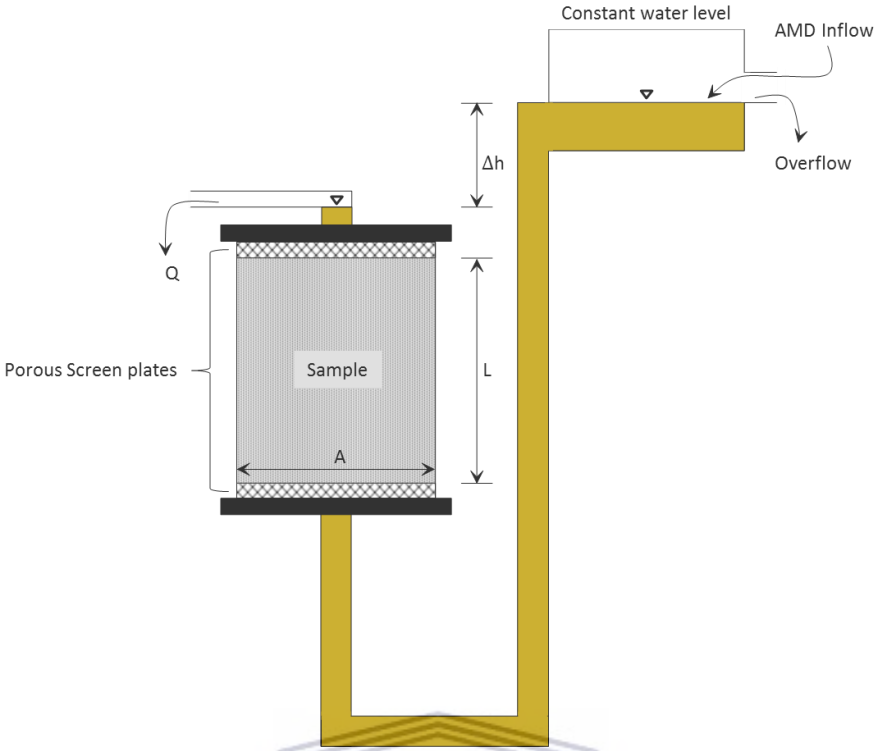

FIGURE 2.1. *A schematic depiction of a constant-head permeameter* after (Fetter, 2001).

UNIVERSITY of the
WESTERN CAPE

2.2.2.2 Chemical leachate testing

There are two leaching test methods commonly used in laboratories to evaluate the leaching behaviour of waste materials: One method is the batch leaching procedure where a solid sample is placed into a container together with a leaching liquid (usually water), the container is then shaken for a certain period of time after which a sample of the fluid is extracted and tested for any contaminants leaching from the solid sample. The second method is the column testing procedure where the sample material is placed into a cylindrical column and a certain leaching fluid is forcefully leached through or around the material in the column (FIGURE 2.1). The effluent of the column is ultimately analysed for contaminants. The batch leaching procedure entails a single extraction, meaning that the sample is shaken up only once and the leachate is extracted for chemical analysis, whereas, the column testing procedure entails multiple extraction of leachate over a period of time whilst the waste material is leached with a liquid. Distilled or deionised water is the standard liquid used in these leaching tests (Ecology, 2003).

https://etd.uwc.ac.za

2.3 Characteristics of Fly Ash

2.3.1 Pozzolanic binders of fly ash

Binders are defined as adhesive substances that create solid bonds between adjacent materials. In fly ash, solid bonds form through chemical reactions between calcium with water. These bonds are referred to as pozzolanic bonds.

The formation of cementitious or pozzolanic gels (Tastan et al., 2011):

$$CaO + H_2O \Rightarrow Ca(OH)_2 \qquad \text{Reaction (1)}$$

$$Ca(OH)_2 \Rightarrow Ca^{2+} + 2[OH]^- \qquad \text{Reaction (2)}$$

$$Ca^{2+} + 2[OH]^- + SiO_2 \Rightarrow CSH \qquad \text{Reaction (3)}$$

$$Ca^{2+} + 2[OH]^- + Al_2O_3 \Rightarrow CASH \qquad \text{Reaction (4)}$$

The $Ca(OH)_2$ (calcium hydroxide) mineral is commonly known as portlandite and forms during the reaction between CaO and water, where calcium silicate hydrate gel (CSH) and calcium aluminate silicate hydrate gel (CASH) are known as cementitious solid end products. The South African fly ash however, consists only of the natural pozzolanic properties and is not self-cementing, due to its low calcium content. Therefore, from abovementioned reactions where pozzolanic and cementing bonds form, only the formation of $Ca(OH)_2$ in reaction (1) is applicable when studying the fly ash from the South African coal-fired power stations.

UNIVERSITY of the
WESTERN CAPE

2.3.2 Physical properties of fly ash

The physical and chemical properties of fly ash particles are a function of the coal combustion conditions, the mineral matter of the coal, and post-combustion cooling (Kutchko and Kim, 2006). Particle Size Distribution of fly ash varies from time to time depending on the coal burning conditions in the power station. Particle size distribution analysis from a South African power station showed that the fly ash particle size distribution was <25 µm (38%), 25-75 µm (42%) and 75-150 µm (14%) (Vadapalli et al., 2007). Confirming that fly ash predominantly consists of particle sizes smaller than 75 µm, with some particle being greater than 75 µm in size.

The literature was consistent in reporting these particle sizes as shown in TABLE 2.1:

https://etd.uwc.ac.za

TABLE 2.1. The particle general particle size of fly ash found in different literature studies.

Source:	Particle size range (µm)	Fly Ash location
Mahlaba et al., 2011	< 20 to 100	South Africa
Kutchko and Kim, 2006	1 to 100	USA
Campbell, 1999	< 1 to 400	South Africa
Fisher et al., 1978	1 to 70	USA
Zhang, 2014	1 to 100	USA

2.3.3 Chemical properties of fly ash

Fly ash consists of a wide range of chemical elements. These elements are: Aluminium (Al), Silica (Si), Calcium(Ca), Iron (Fe), Magnesium (Mg), Phosphorus, (P), Potassium (K), Sodium (Na), Manganese (Mn) and Sulphur (S) (Mahlaba et al., 2011; Hung and Hai, 2014; Zhang, 2014). In literature, silicon, aluminium, iron and calcium are the most mentioned elements related to fly ash and fly ash is also classified according to the abundance and ratios of these elements. South African fly ash is commonly known for its silica-alumina-iron ratio of above 70% weight composition of the total weighting mass, whereas, calcium is less abundant ranging between 5 and 10% weight by total mass (Akinyemi et al., 2013; Jung, 2016).

Prasad and Mondal (2008) tested the heavy metal leaching characteristics of two fly ashes with similar CaO content as the South African fly ash, using the batch leaching procedure instead of the column leaching test. Their objective was to assess the leaching behaviour of fly ash by means of a standardized procedure that was developed by Van Der Sloot (USEPA, 2014). The study found that all the heavy metals leached out of the two ashes, with Fe showing the highest leach ability.

Moghal (2013) conducted a similar study in order to characterise the geotechnical and physico-chemical properties of two low lime fly ashes with reference to acidic distilled water. The study concluded that higher concentrations of heavy metals are extracted at lower pH values compared to higher pH conditions. The cumulative percentage leached also showed that the heavy metal concentrations increased with increasing liquid solid ratio.

Overall, the abovementioned studies concluded that fly ash will impact negatively on the environment due to heavy metals leaching from the ash. However, the leaching method used in those studies are not a practical method to simulate the natural conditions of fly ash at field scale. This is due to the fact that there are maximum particle surface area exposed to react with water during the shaking phase of the testing method. Hence the probability of heavy metals leaching from ash is high, whereas, fly ash would be disposed of in the form of a monolithic

UNIVERSITY of the WESTERN CAPE
https://etd.uwc.ac.za

structure. Therefore the column testing method would be more applicable, where water will percolate through the ash. Thus the findings in the studies by Prasad and Mondal (2008) and Moghal (2013) are not relevant to a real fly ash disposal site as these sites do not show these leaching behavioural patterns.

2.3.4 Hydraulic conductivity of fly ash

The factors that have been shown to influence hydraulic conductivity of fly ash include (i) pozzolanic properties, (ii) curing time, and (iii) the chemical composition of the water that is used in the leaching test. The hydraulic conductivity of fly ash has been evaluated for various applications. Some of these applications include (a) the use of fly ash in earth work construction and, (b) use of fly ash to neutralise acidic mine water and, (c) utilisation of fly ash as a landfill barrier material.

2.3.4.1 Pozzolanic properties affecting hydraulic conductivity

Alhomair (2017) tested the hydraulic conductivity of fly ash mixed with mine tailings as an aim to determine whether fly ash amended mine tailings would be acceptable to use in earthwork construction applications. FIGURE 2.2 depicts how the fly ash was mixed with mine tailings, compacted and cured for 7 and 28 days respectively and tap water was used as a solvent. Class C fly ash was used in the study and it was established that the majority of cementitious bonding formations occurred within the first 7 days of curing and thereafter the effect of curing become negligible. He found that there are no significant differences in K-values with respect to the different curing periods. The hydraulic conductivity of fly ash amended tailings ranged between 10^{-1} m/d to 10^{+2} m/d. These K-values are unusually high for fly ash but it should be noted that the fly ash was mixed with loosely unconsolidated material that is very heterogeneous in size.

UNIVERSITY of the
WESTERN CAPE

https://etd.uwc.ac.za

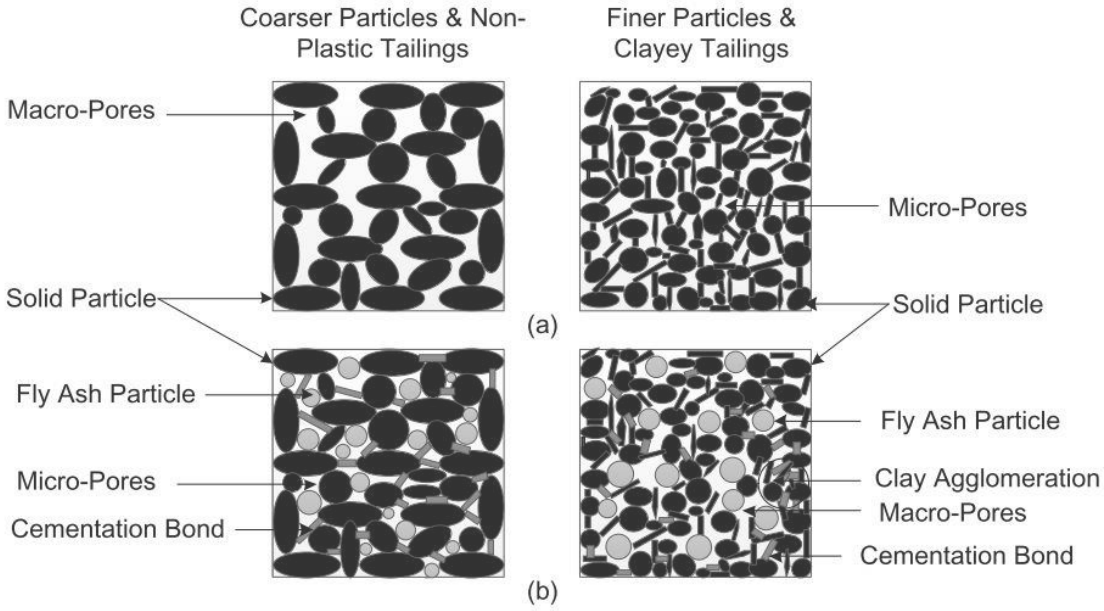

***FIGURE 2.2**. Schematics of (a) unamended and (b) fly ash amended mine tailings* (Alhomair *et al.*, 2017).

UNIVERSITY of the WESTERN CAPE

Kostas et al. (2000) investigated the hydraulic performance of permeable reactive barriers (PRB's) for the decontamination of acidic mine waters. Class C fly ash and red mud was used as reactive mediums and were mixed to various ratios with sand respectively in the experimental set-up. The objective of the study was to enhance permeability in these fine reactive mediums. The sand mixtures thus ensured heterogeneity and consequently enhanced permeability. Moreover, the sand/fly ash and sand/red mud mixtures were leached with synthetic acid mine drainage water and the pore volumes in the sand/fly ash mixture decreased due to pozzolanic and cementitious bonds forming between the reaction of fly ash particles and AMD. Besides the pozzolanic and cementitious bonds, the chemical reaction between fly ash and AMD also played a major role in the decreased hydraulic conductivity. Overall, the permeation of the sand/fly ash mixtures with AMD showed decreasing hydraulic conductivity ranging between 10^{-1} m/d to 10^{-4} m/d from highest to lowest. The 80/20 ratio of sand/fly ash mixture showing highest hydraulic conductivity compared to the lowest hydraulic conductivity of the 20/80 ratio of the sand/fly ash mixture. This is due to greater volumes of fly ash in the 20/80 ratio of sand/fly ash.

Nhan et al. (1996) evaluated the potential to use fly ash as a landfill barrier. They studied the hydraulic properties of a class F fly ash mixed with lime kiln dust and calcium bentonite. The

https://etd.uwc.ac.za

calcium and lime components were added to the fly ash to increase the workability in the compaction of the mixture and therefore to obtain low hydraulic conductivity. The fly ash-calcium-lime kiln mixture was mixed to a ratio of 70-10-20 by dry weight percentage and a synthetic leachate with pH of 3.98 were used. The average hydraulic conductivity determined for 30 barrier samples was measured at 10^{-3} m/d.

Besides pozzolanic bonds, other geochemical reactions have a direct impact on the hydraulic conductivity of fly ash (Kostas et al., 2000). For example, the secondary mineralization of gypsum results in the pore spaces to decrease and thus causes the hydraulic conductivity to decrease. Gypsum is formed in the reaction between calcium and sulphate rich water and the formation of the mineral is presented in reaction (5).

Gypsum formation (Zarga et al. 2013):

$$SO_4^{2-} + Ca^{2+} + 2H_2O \leftrightarrows CaSO_4 \cdot 2H_2O \qquad \text{Reaction (5)}$$

2.3.4.2 Chemical composition of water affecting hydraulic conductivity

Jarosite is a hydrous sulphate of potassium and iron and is formed in ore deposits. It is an abundant mineral in acid mine water and the mineral is insoluble in water. It is expected that the mineral does not leach through fly ash and thus will clog up the ash if AMD is leached through it. Hence, jarosite causes the hydraulic conductivity of fly ash to decrease over time and the rate at which it would affect the hydraulic conductivity is dependent on the abundance of the jarosite mineral present in the AMD water (Adam et al., 2000; Murray et al., 2014).

UNIVERSITY of the
WESTERN CAPE

Formation of jarosite:

$$K^+ + 3Fe^{+3} + 2SO_4^{-2} + 6H_2O = KFe_3(SO_4)_2(OH)_6 + 6H^+ \qquad \text{Reaction (6)}$$

2.4 Coal Mining Practices and Impacts

In South Africa, the coal industry is one of the biggest contributors to the country's GDP from a mining perspective. Coal sales totalled at R130 billion in 2017 compared to the R112 billion in 2016. Among the three leading industries in the sector, the coal industry recorded growth in employment whereas gold and platinum shed jobs (Minerals Council South Africa, 2018). Though the industry contributed to the GDP, there are concerning environmental impacts upon the natural water environment resulting from the coal mining activity (Chelin, 2000). According to Younger and Wolkersdorfer (2003), mining activity can have significant impacts

https://etd.uwc.ac.za

on the natural water environment. Mining inevitably changes the natural water environment through:

- natural strata extraction
- the processing of minerals and disposal of mining wastes back into mine voids
- dewatering of mining pits
- post-closure mine flooding and uncontrolled discharge of polluted waters

There are many historic coal mines in the Witbank area. Most of these old mine sites are abandoned, some of the underground mines have collapsed and most of them are decanting acidic water into the neighbouring water bodies (Bell et al., 2001). The water that is discharging from these old mine sites is highly saline, very acidic with a pH of 2.5 and contains elevated levels of sulphate concentrations. Furthermore, the rising salinity and sulphate concentration of the water in the Middelburg and Witbank dams (exceeding the 200 mg/L which is the maximum for domestic water use purposes) is an indication of the post-closure mining activity having a negative impact on the water resources surrounding the mining area (McCarthy, 2011).

Acid mine drainage (AMD) is generated when the pyrite minerals from the mining spoils are exposed to oxygen and water from natural recharge. Pyrite is the most abundant sulphide mineral and is found in coal-bearing rocks. When the mineral undergoes oxidation in the presence of water, AMD will be generated. FIGURE 2.3 depicts an operational opencast coal mine and indicates the oxidation phase of the mining spoils where AMD is generated. The chemical process are shown in reaction (7):

$$\underset{Pyrite}{4FeS_2\,(s)} + \underset{Oxygen}{15O_2\,(g)} + \underset{Water}{14H_2O\,(l)} \rightarrow \underset{Yellow\ Boy}{4Fe(OH)_3\,(s)} + \underset{Sulfate}{8SO_4^{2-}(aq)} + \underset{Acid}{16H^+(aq)} \quad \text{Reaction (7)}$$

https://etd.uwc.ac.za

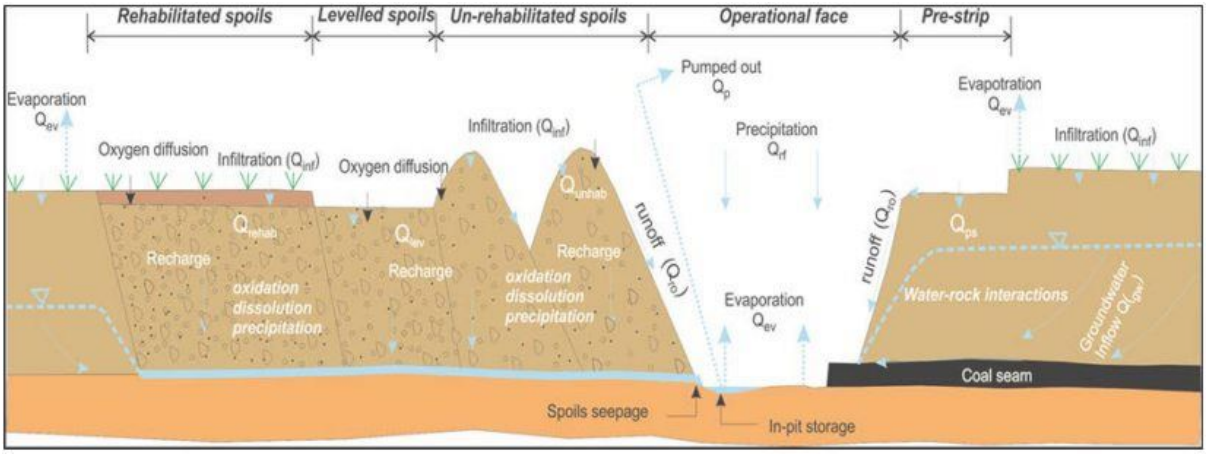

FIGURE 2.3. *A conceptual model of an open cast coal mine* (Lupankwa et al., 2008).

The management options on the prevention or remediation methods of AMD generation by mining activities is a costly process and in most cases, not feasible. According to Norton and Associates (1995), the remediation methods for large scale problems must be low cost, preferably passive, environmentally acceptable, relatively labour free and unobtrusive. Furthermore, they summarized the best environmental options available for sustainable post closure mining activities to be:

- set up of environmental management systems prior to closure in order to deal with main groundwater issues
- continuation of pumping at lower volumes at shallow layers in the strata to prevent groundwater from surfacing
- to use cheap and effective passive water treatments such as wetlands to treat surface issues
- to protect surface structures from acidic waters
- to control or prevent methane migration with groundwater rebound in abandoned coalfield
- to use expensive chemical or biochemical methods to treat groundwater and surface water bodies
- to use reactive hydraulic barrier methods to try and prevent oxygen ingress into the backfill

Though there are costly management practices in place to prevent or mitigate the generation of AMD and thus protect water resources surrounding mining activities. The option of

https://etd.uwc.ac.za

investigating the feasibility of using fly ash to challenge these post closure coal mining constraints should be considered.

2.5 Conclusion

Concluding this chapter, adequate and appropriate literature has been reviewed to understand what research has been done to better understand the hydro-geochemical properties of fly ash. In reviewing the literature, the author have come across gaps in knowledge, specifically the limited understanding there are in South Africa with regards to the changing hydro-geochemical properties of fly ash once it is exposed to AMD in an opencast coal mine environment.

UNIVERSITY of the
WESTERN CAPE

https://etd.uwc.ac.za

3 MATERIALS AND METHODS

This chapter introduces the materials and methods used in the field as well as the laboratory. In the field, hydraulic falling head tests were conducted on ash of different age to determine the change in hydraulic conductivity over time. Materials used in the laboratory included fly ash from two power stations and natural AMD from an historic coal mining site in Mpumalanga. Laboratory hydraulic conductivity tests were done with the use of Darcy constant hydraulic head experiments. The effluent was collected from the hydraulic conductivity experiments and analysed for chemical elemental composition to evaluate the potential influence of fly ash on decant mine water quality.

3.1 Materials

3.1.1 Fly ash

3.1.1.1 Sample collection

Fly ash from two different power stations was used in this study. Fly ash A (K-Ash) was collected from Kendal Power Station, a 4000MW plant situated approximately 40km southwest of Witbank in Mpumalanga, and fly ash B (T-Ash) was obtained from Tutuka Power Station, which is a 3654MW plant situated approximately 25 km northeast of Standerton in Mpumalanga, South Africa.

Fly ash from the Kendal and Tutuka power stations is dry dumped and conditioned to 15% moisture content through irrigation for dust suppression. The ash was collected directly from the conveyor belt at the respective ash waste dumps and placed in 25L buckets, sealed and transported to the laboratory for testing. FIGURE 3.1 depicts the dumping of the ash onto ash dumps via conveyor belts.

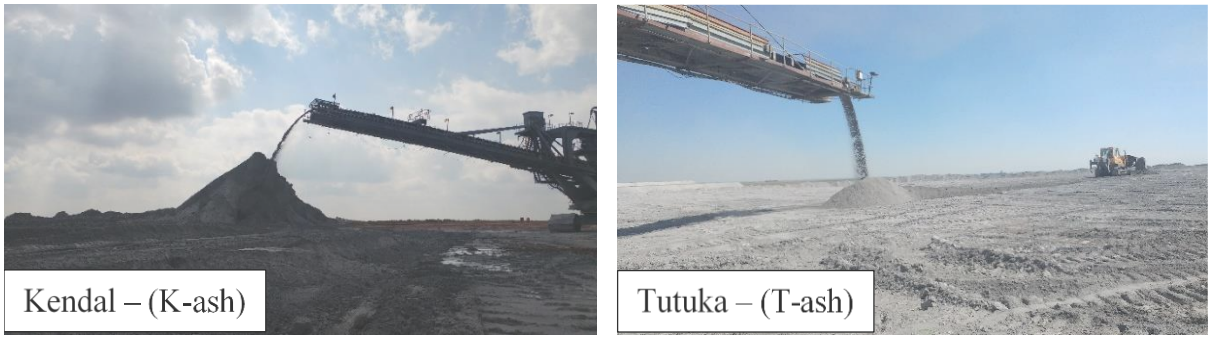

***FIGURE 3.1**. Fly ash being disposed of at Kendal and Tutuka power stations*

https://etd.uwc.ac.za

3.1.1.2 Chemical elemental composition and classification

The chemical composition (major and minor oxides) of the fly ash was measured with an X-ray fluorescence (XRF) spectrometer at Metron Laboratory (Pty) Ltd, a South African National Accreditation System (SANAS) laboratory.

3.1.1.3 Moisture content

The moisture content of K-Ash and T-Ash was measured in the laboratory. A foil container was weighed to an accuracy of 0.01g before placing a small portion of the ash in it. Once the combined weight of the container and the ash sample was recorded, the samples were placed in an oven and dried at 105˚C for 24hours. Samples were weighed for a second time. Moisture content of the ash was calculated as follows:

$$\emptyset = \frac{WetAsh - DryAsh}{DryAsh} \qquad \textit{Equation 3}$$

Where $\emptyset$ = moisture content

3.1.1.4 Particle size ratios

The particle size ratios was determined in the laboratory using the sedimentation principle. In order to use the sedimentation principle, where the largest particles will settle first and the silt and clay fraction will settle over a longer time period, the particles need to be separate i.e. loose from one another. This implies that the organic matter binding the clay-sized particles be destroyed because the clay particles may behave like larger particles, settling first and thereby giving a skew representation of the grain size distribution.

UNIVERSITY of the
WESTERN CAPE

Sedimentation principles: Settling speed of particles is derived from Stoke's law and is influenced by the size of the particle, its density and the properties of the fluid. The method that follows involves the settling of particles through 10cm of liquid.

If sand, silt and clay are initially uniformly distributed through a column of liquid, and allowed to settle at 20°C, then after 32 seconds sand particles larger than 60μm initially at the liquid surface have settled beyond 10cm and 60μm particles initially at the surface have reached 10cm. The concentration of silt and clay at 10cm depth has not changed and can be sampled with a pipette. The sample comes from around the pipette tip not only from the 10cm depth and therefore slight errors are involved.

https://etd.uwc.ac.za

3.1.2 Acid Mine Drainage (AMD)

Natural AMD water was collected from Driefontein, an old coal mine site in the Witbank area in Mpumalanga. According to Bell et al., (2001) the Driefontein pit lake is a product of a collapsed historical underground coal mine that collapsed due to multiple pillar failure. As a result the voids filled up with water and decanted to form the pit lake. The water in the pit lake is of an acidic nature resulting from the reaction between water, oxygen and pyrite minerals in unmined coal and host rocks. FIGURE 3.2 depicts how samples were collected in 25lt buckets, sealed and transported to the laboratory. The AMD was used as the leaching solvent in the laboratory for hydraulic conductivity and geochemical testing.

UNIVERSITY of the
WESTERN CAPE

***FIGURE 3.2**. Collecting AMD from the Driefontein Pit Lake for laboratory testing*

The water quality of the AMD was measured in the laboratory, using the inductively coupled plasma mass spectrometry (ICP-MS) method. The machine used in the analysis for this study have detection limits for Cr<0.01, Fe<0.06 and Al<0.06 mg/L. The focus and analysis was on specific inorganic elements and metals, due to their elevated concentrations in nearby water bodies of the Witbank coal mining area.

3.2 Field Methods

3.2.1 In-situ hydraulic conductivity testing

Falling head hydraulic tests was applied on both Kendal and Tutuka ash dumps. These tests were conducted to determine the field hydraulic conductivity of fly ash related to age. TABLE 3.1 shows that approximately 5 holes per ash dump age was tested and the age of fly ash ranged from freshly dumped ash to fly ash that was dumped up to 30 years ago.

https://etd.uwc.ac.za

TABLE 3.1. Field testing set-ups

Power Station	Age of Ash(years)	Number of holes tested
Kendal	Fresh	5
	5	5
	10	5
	15	5
	20	4
Tutuka	Fresh	5
	1	5
	5	5
	20	4
	30	5

Shallow holes were augured into the ash dumps. A 1 meter long piezometer with a 0.3 meter perforated screen was placed into each hole to prevent the holes from collapsing and a water level recording instrument (Solinst Levelogger, model 3000) was installed. Water was injected into each hole at least three times to ensure saturated conditions. The holes were injected instantaneously with water and allowed to infiltrate into the fly ash while measurements of head were recorded (FIGURE 3.3). The rate of infiltration is related to the hydraulic conductivity of the fly ash. Data derived from these holes was interpreted using the Bouwer and Rice Equation 1 (Fetter, 2001; Kruseman and de Ridder, 1994):

UNIVERSITY of the
WESTERN CAPE

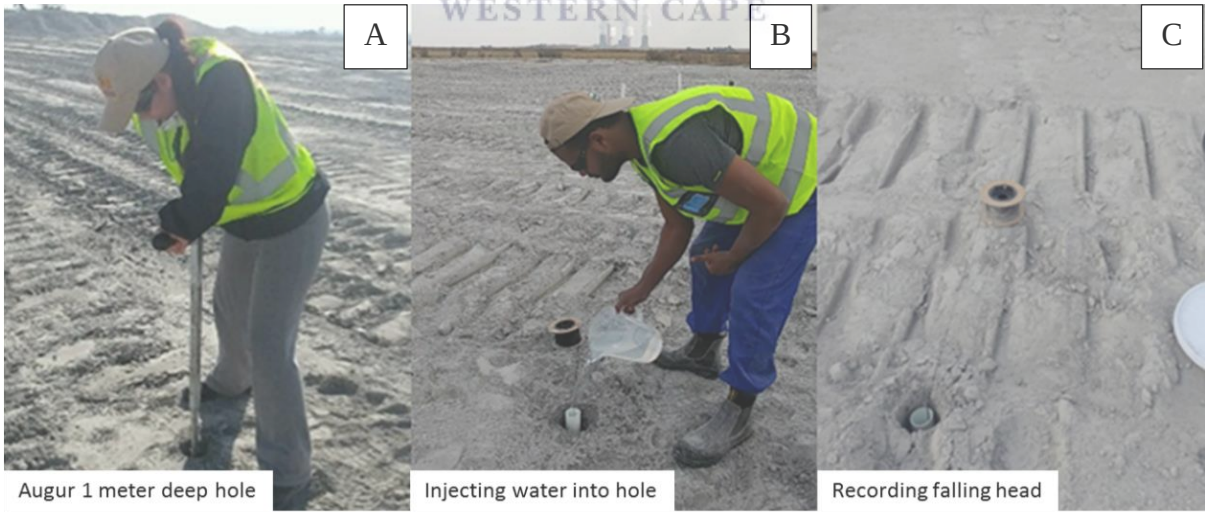

FIGURE 3.3. Falling head hydraulic test procedure on fly ash dumps where (A) auger holes are drilled, (B) water injected into the hole with piezometer installed and, (C) falling head is recorded with a water level recording instrument.

https://etd.uwc.ac.za

The data from the falling head hydraulic tests is analysed using the AQTESOLVE PRO version 4.0 software. For the Bouwer and Rice slug test method, the software assumes: (a) aquifer has infinite areal extent, (b) aquifer is homogeneous and uniform in thickness, (c) aquifer potentiometric surface is initially horizontal, (d) a volume of water, V, is injected instantaneously from the control well, (e) aquifer is either confined or unconfined and, (f) the flow is steady.

3.3 Laboratory Methods

In the laboratory, the hydraulic and chemical leachate properties of fly ash were assessed. The hydraulic properties were determined through the use of a Darcy column setup and the effluent from the column testing was sent to the laboratory for chemical analysis. After the hydraulic conductivity column testing, fly ash samples from four columns were analysed under the Scanning Electromagnetic Microscope (SEM) to evaluate the particle morphology and external chemical elemental composition. The laboratory testing period lasted approximately 6 months (from September 2017 to February 2018) and the fly ash was leached continuously with AMD throughout the testing period.

3.3.1 Hydraulic conductivity testing

The flow-through leaching test is used to assess the leaching behaviour of fly ash. However, Method 1314 from the LEAF methodology was modified in the laboratory test set-up with the aim of achieving the closest field conditions. Therefore, instead of using distilled water, AMD water was used as the leaching liquid due to the high probability of fly ash being backfilled into AMD environments. Furthermore, the fly ash was not packed into the columns as according to the ASTM D 4874 leaching standard but, the fly ash were rather mixed to a slurry of various moisture content and poured into the columns.

The experimental set-up is shown in FIGURE 3.5 and the various column specifications are listed in TABLE 3.2. The setup consisted of a permeameter apparatus where the headwater reservoir had an AMD inlet and an overflow outlet which ensured constant hydraulic head conditions. The column design consisted of bottom and top caps and fitted with porous screen plates between caps and fly ash sample to prevent fly ash from clogging the piping system. The cap design are depicted in FIGURE 3.4 and consisted of the following:

- O-ring grooves as gaskets between cap and column to ensure no leaking takes place on the sides (FIGURE 3.4 (B))

UNIVERSITY of the WESTERN CAPE
https://etd.uwc.ac.za

- Threaded holes where connectors to piping were screwed in and thread seal tape was used as gaskets to prevent leakage (FIGURE 3.4 (C))
- 8 holes drilled at 45 degree angles from the inlet to ensure fully saturation of ash through the column from the bottom upwards (FIGURE 3.4 (A))

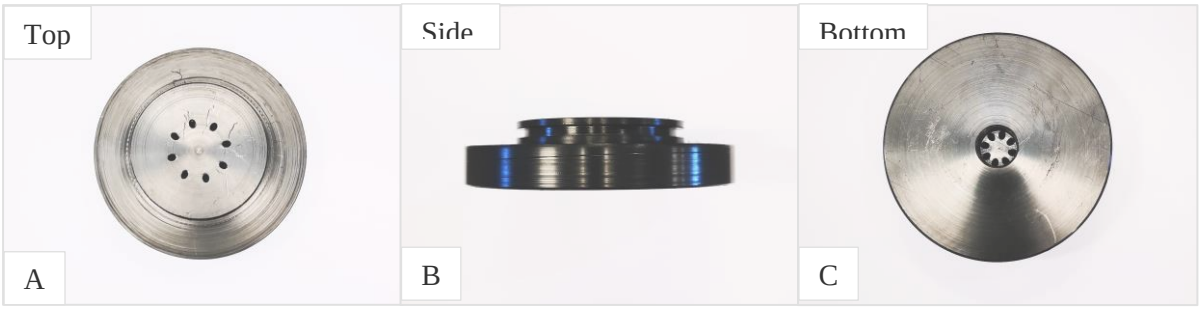

FIGURE 3.4*. A depiction of the caps used in the column setup where, A) Top view, B) Side view and C) Bottom view.*

A total of 8 columns packed with fly ash was connected to the headwater reservoir through a piping system. The hydraulic conductivity test was performed by introducing AMD water to the fly ash columns under constant hydraulic gradient (Δ H) conditions. The AMD moves from head 1 (H_1) down the piping and upwards through the ash sample in the column until it eventually discharges at head 2 (H_2) (FIGURE 3.5). The upwards movement of AMD through the ash sample ensures fully saturated conditions as the distribution of AMD spreads evenly through the cross-sectional area (A) of the column. At outflow, the discharge (Q) is measured as length cubed per unit time (FIGURE 3.5). Initially the discharge was measured 4-8 times a day during the first two weeks of testing. Thereafter, discharge was measured 2 times a day as the flow rates decreased until week 5 of testing. Final flow measurements were measured once every 3 days. The hydraulic conductivity (K) is then calculated through applying the measured parameters into Darcy's equation (Equation 2):

Furthermore, the fly ash was prepared to varying moisture content before hydraulic conductivity testing commenced. The fly ash was mixed to a slurry at 40%, 50% and 60% saturation respectively to evaluate the effect of moisture content during curing on the hydraulic conductivity. The slurry was then placed into 2 sets of columns and left to cure for 3 and 28 days respectively. The different curing times are known to have an effect on the strength of ash and therefore also expected to have an effect on the hydraulic conductivity. This is due to the reaction time for pozzolanic bonds to form while the fly ash sets over the cured waiting period.

UNIVERSITY of the
WESTERN CAPE

https://etd.uwc.ac.za

After the cured waiting period, the ash columns were leached with AMD to determine the change in hydraulic conductivity as well as the chemical leachate of ash over time.

TABLE 3.2. Laboratory Column Setup.

Power Station	Column Name	Pre-Cured Moisture Content (%)	Cured Waiting Time (days)	Column Length (m)	Cross-Sectional Area (m^2)	Hydraulic Gradient (m/m)
Kendal	Kash50	50	3	0.2	0.006362	2.5
	Kash60	60				
	K40	40	28			
	K50	50				
	K60	60				
	K60b	60		0.5		1.15
Tutuka	Tash50	50	3	0.2		2.5
	Tash60	60				
	T40	40	28			
	T50	50				
	T60	60				
	T60b	60		0.5		1.15

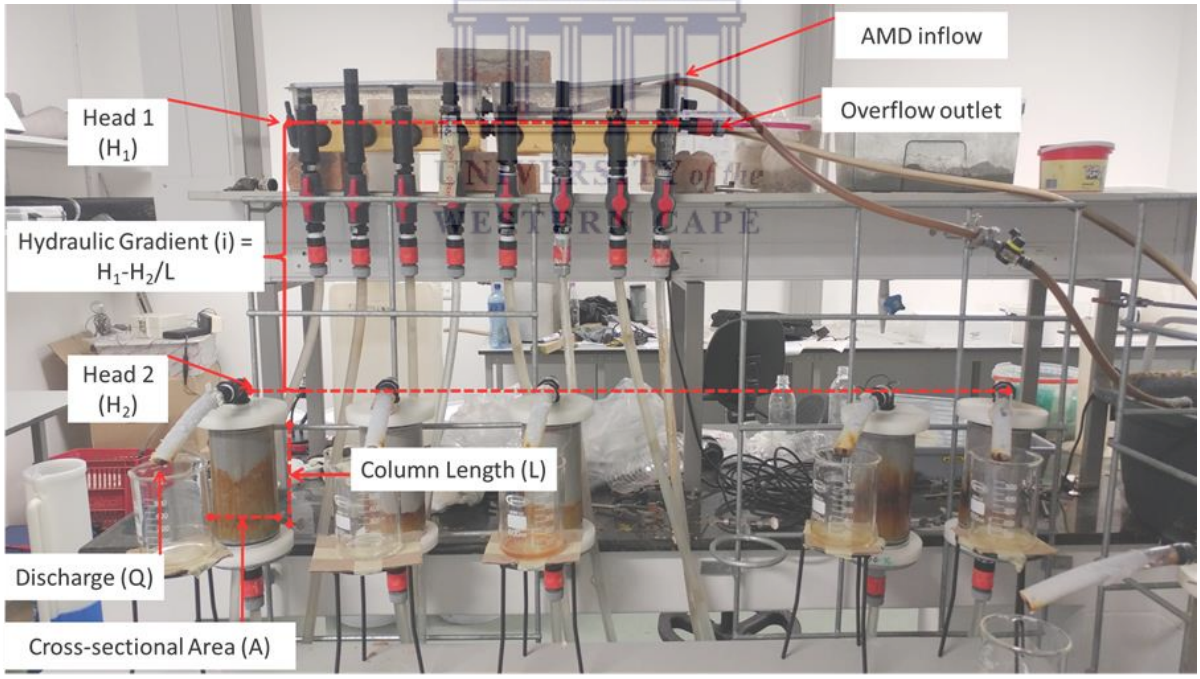

***FIGURE 3.5.** A depiction of the Darcy column testing setup in the laboratory.*

https://etd.uwc.ac.za

3.3.2 Geochemical testing

The influent and effluent from the hydraulic column tests was monitored for pH and EC throughout the duration of the experiment. Influent and effluent samples were routinely collected in clean plastic bottles and sealed to prevent evaporation. After-sample collection, the samples were transported to Metron Laboratory (Pty) Ltd, a SANAS accredited laboratory in Vanderbijlpark, Gauteng province of South Africa. The data was analysed to compare elemental composition of influent water against the effluent water. The chemical elements that were analysed included the concentrations of Iron (Fe), Sulphur (S as SO_4), Calcium (Ca), Magnesium (Mg), Sodium (Na), Potassium (K), Aluminium (Al), Silicon (Si), Chromium (Cr) and Manganese (Mn). According to Cogho and Niekerk (2009), there are significantly high concentrations (above domestic use standards) of these chemical elements found in streams, rivers and dams nearby old mine sites in the Witbank area. The analysis was conducted to investigate the potential influence fly ash will have on these problem elements in mine decant water quality.

3.3.3 Scanning Electron Microscopy (SEM)

After the hydraulic conductivity testing, the fly ash from 4 columns in the experimental set-up was prepared and sent for Scanning Electron Microscopy (SEM) analysis. The analysis were conducted in the Physics Department at the University of the Western Cape, South Africa. The SEM provides detailed imaging data about the morphology and surface texture of different fly ash particles, as well as a qualitative external elemental composition of the particles. The scanning electron microscope used for this study was a Zeiss Auriga. As shown in FIGURE 3.6, samples were taken from the bottom, middle and top of each column and sent away for testing. The samples were adhered to a carbon-based adhesive which was placed onto an aluminium SEM stub. Furthermore, the samples were coated with a 10-20nm layer of carbon (C) and gold (Au) to ensure sufficient conductivity during analysis. According to Kutchko and Kim (2006), the analysis can determine the particle morphology, external surface structure and external elemental distribution of the fly ash particles. For this study, the analysis was done only to determine the particle morphology and external elemental distribution of fly ash after it was leached with AMD.

https://etd.uwc.ac.za

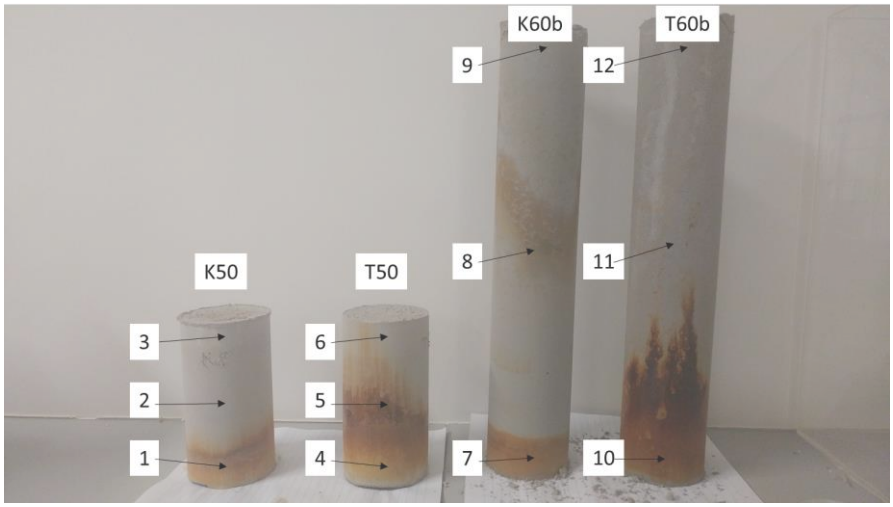

FIGURE 3.6. *Samples from 4 columns prepared for SEM imaging after hydraulic conductivity testing.*

3.4 Conclusion

The methods used in this study provided a platform to achieve all research goals that were set out. The tools used in the methodology was appropriate and the research objectives could be met to ultimately achieve the overall aim of the research. Temporal changes in hydraulic and geochemical properties of fly were successfully obtained from field and laboratory experiments, ultimately the author could use it for analysis.

UNIVERSITY of the
WESTERN CAPE

https://etd.uwc.ac.za

4 RESULTS AND DISCUSSION

4.1 Fly Ash Characteristics

4.1.1 Chemical elemental composition and classification

The chemical composition of K-Ash and T-Ash are listed in TABLE 4.1 and the fly ash was classified based on the ASTM C618 method (Fox, 2017).

TABLE 4.1. *The chemical composition of major and minor oxides by weight percentage (%) of two types of fly ash based on X-ray fluorescence (XRF) analysis.*

	Component	Chemical Formula	K-Ash (weight %)	T-Ash (weight %)
Major Oxides	**Aluminium oxide**	Al_2O_3	32.8	30.4
	Silicon dioxide	SiO_2	49.3	52.9
	Calcium oxide	CaO	6.9	5.3
	Iron oxide	Fe_2O_3	3.00	4.65
Minor Oxides	**Chromium oxide**	Cr_2O_3	0.018	0.025
	Potassium oxide	K_2O	0.694	0.752
	Magnesium oxide	MgO	1.28	1.14
	Manganese oxide	MnO	0.025	0.035
	Sodium oxide	Na_2O	0.312	0.345
	Phosphorus pentoxide	P_2O_5	0.425	0.329
	Titanium dioxide	TiO_2	1.37	1.27
	Loss on ignition		3.88	2.88

UNIVERSITY of the
WESTERN CAPE

The fly ash from both power stations shows characteristics of a Class F fly ash, making it a natural pozzolanic material. Both have an $SiO_2 + Al_2O_3 + Fe_2O_3$ weight above 70%, with a low CaO (CaO < 10 wt.%) content which is common for South African fly ash, whereas, a Class C fly ash would have 50 - 70 weight percentage of $SiO_2 + Al_2O_3 + Fe_2O_3$ with high CaO (CaO > 10 wt.%) content (TABLE 4.1). According to EN 197-1 standards, K-Ash and T-ash are classified as siliceous fly ash due to their CaO < 10weight % content. The Class F fly ash is pozzolanic in nature, meaning it hardens over time when exposed to water and the Class C fly ash has self-cementing properties due to high CaO content (BS EN 197-1, 2011).

4.1.2 Moisture content of fly ash

The moisture content of the fly ash from both power stations was measured in the laboratory using Equation 3. The K-Ash has a moisture content of 18%, whereas, T-Ash has a moisture content of 17%.

https://etd.uwc.ac.za

4.1.3 Particle size ratio of fly ash

4.1.3.1 Settling tube method

The sand-silt-clay ratio of K-Ash and T-Ash was determined in the laboratory using the sedimentation principle and the results are listed in TABLE 4.2. K-Ash and T-Ash showed similar sand content with 32% measured for both, whereas, the clay-silt ratios differed with K-Ash having 5% clay and 63% silt content and T-Ash with only 2% clay and 66% silt. This means that the abundance of the fines in the K-Ash are higher compared to fines in the T-Ash.

***TABLE 4.2**. Composition of sand-silt-clay by weight percentage ratio of Fly Ash.*

Sample Name	Sand Size Particles (%)	Silt Size Particles (%)	Clay Size Particles (%)
K-Ash	32	63	5
T-Ash	32	66	2

4.1.3.2 Scanning electron microscope

Fly ash from the K50, T50, K60b and T60b columns were analysed under the SEM after hydraulic conductivity testing. The SEM analysis provided data on the morphology and the visible external elemental distribution of fly ash particles after leaching.

The morphology of fly ash particles is dominated by the temperature and cooling rates of the coal combustion process. The overall particles consisted of solid spheres and ranged in sizes approximately between 1 to 100 µm (FIGURE 4.1). Apart from solid spheres, there are also agglomerated and irregular shaped amorphous particles present in the particle make-up. According to Kutchko and Kim (2006), these agglomerated and irregular amorphous particles may have formed due to rapid cooling and inter-particle contact.

In total, 12 fly ash samples from 4 columns were analysed under the SEM to determine the physical size as well as the external elemental distribution. FIGURE 3.6 depicts that a sample from the bottom, middle and top of each column was taken for SEM analysis. The data is shown below.

Bottom of K50 and T50 columns: Although the general particle sizes ranged between 1 to 100 µm, the particles from the bottom of K50 and T50 showed overall smaller particle sizes ranging between 1 and 20 µm. Moreover, the K50 showed particle sizes predominantly ranging between 1 to 10 µm in diameter with some particles measured between 10 and 20 µm in diameter. The T50 columns however, exhibited particles greater than 10 µm and but less than 20 µm in diameter. Minimal larger agglomerated and irregular shaped particles observed in the

UNIVERSITY of the WESTERN CAPE
https://etd.uwc.ac.za

K50 and T50 columns. Furthermore, the bottom of the column fly ash samples, exhibited minerals latched onto the spheres and it is believed to be iron-rich mineral phases. The accumulation of Fe at the bottom of all columns is also physically observed in FIGURE 3.6.

Middle and Top of K50 and T50 columns: The particle sizes of the fly ash from the middle and top of the columns, showed larger particles ranging up to 40 µm in diameter for K50 and 60 µm in diameter for T50 respectively. Furthermore, larger agglomerated and irregular amorphous particles were significantly more in abundance in the middle and top parts of the columns.

K60b and T60b columns: The fly ash from the longer columns exhibited particle sizes ranging between 1 to 100 µm in diameter. The columns also showed large particles measuring up to size 70 µm in diameter which is larger than what was observed from the shorter (K50 and T50) columns. Some calcium minerals were observed in the fly ash from the T60b column and are consistent with the high Ca concentration presented in the external elemental composition of the T60b column (FIGURE 4.3 and FIGURE 4.8). Overall the abundance of agglomerated and irregular shaped particles was much more prevailing in the K60b and T60b columns (FIGURE 4.4).

UNIVERSITY of the
WESTERN CAPE

https://etd.uwc.ac.za

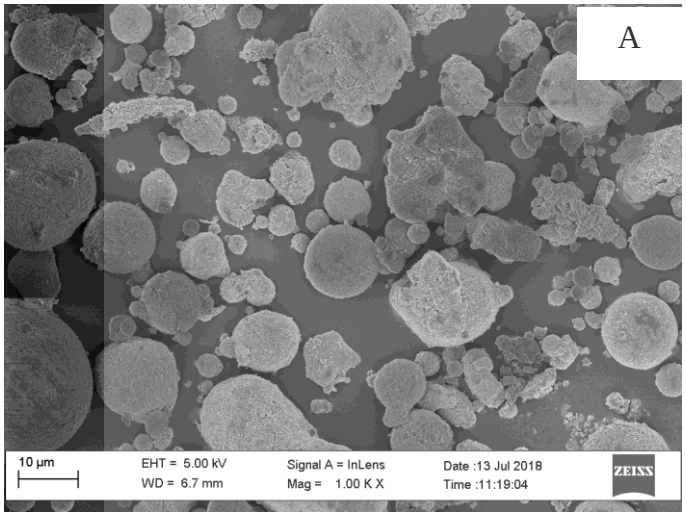

FIGURE 4.1. *SEM images of (A) fly ash spheres and sizes*

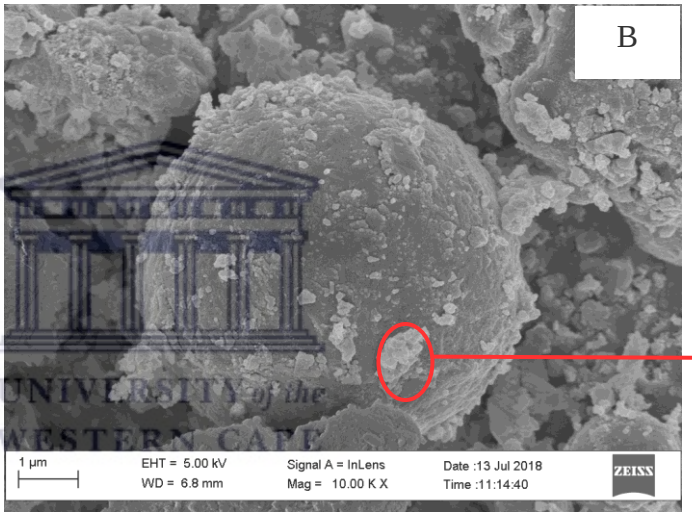

FIGURE 4.2*. SEM images of (B) Iron-rich material*

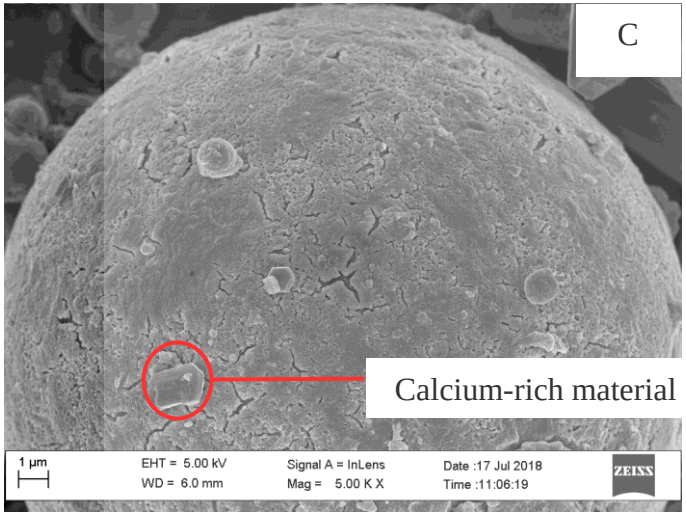

FIGURE 4.3. *SEM images of (C) calcium-rich material*

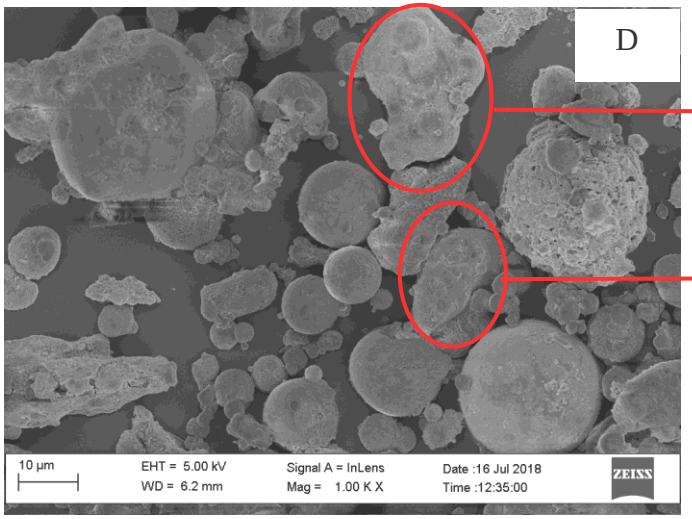

FIGURE 4.4. *SEM images of (E) agglomerated particles and irregular shaped amorphous particles*

https://etd.uwc.ac.za

4.1.4 Qualitative external elemental composition

The external elemental composition of the fly ash from the K50, T50, K60b and T60b columns is presented in FIGURE 4.5, FIGURE 4.6, FIGURE 4.7 and FIGURE 4.8 respectively. The fly ash predominantly consists of alumina-silicate spheres with lesser amounts of iron and calcium. Furthermore, lesser amounts of alumina-silica and calcium spheres are present at the inflow of the columns and increased towards the middle and top in K50 and T50, suggesting that the AMD dissolves these elements and transports them upward through the column. K60b and T60b however, did not show a similar trend as the alumina-silica concentrations remained similar through the entire columns. Furthermore, there is a slight increase in Ca observed toward the top of the columns, suggesting that $Ca(OH)_2$ minerals dissolves at the bottom of the columns due to the continuous percolation of AMD but also drive the secondary mineralization of $CaSO4.2H_2O$ towards the middle and top of the column (FIGURE 4.5, FIGURE 4.6, FIGURE 4.7 and FIGURE 4.8).

The accumulation of Fe at the inflow of the columns was visually observed in the laboratory during and after testing (FIGURE 3.6). In correspondence to the visual observations, the Fe concentrations in the external elemental composition from the SEM data, confirms that Fe accumulates at the contact phase of AMD and fly ash. The Fe concentrations are more abundant at the bottom of the columns compared to the middle and top (FIGURE 4.5, FIGURE 4.6, FIGURE 4.7 and FIGURE 4.8). That abundance of Fe at the inflow of the columns suggests that jarosite ($KFe_3(SO_4)_2(OH)_6 + 6H^+$) clogs up void spaces in between fly ash particles. Therefore, it is considered to have the most significant influence on the decreasing hydraulic conductivity of the fly ash columns.

https://etd.uwc.ac.za

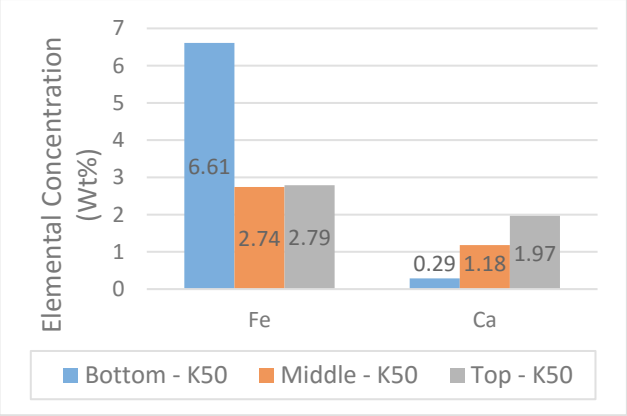

FIGURE 4.5. *External elemental composition of Fe and Ca minerals by weight percentage on Fly Ash particles from the K50 column.*

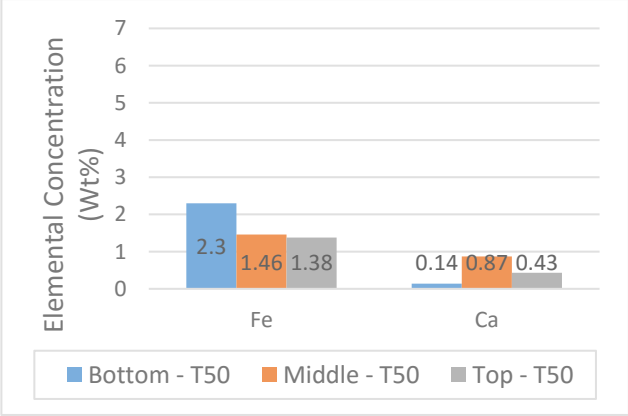

FIGURE 4.6. *External elemental composition of Fe and Ca minerals by weight percentage on Fly Ash particles from the T50 column.*

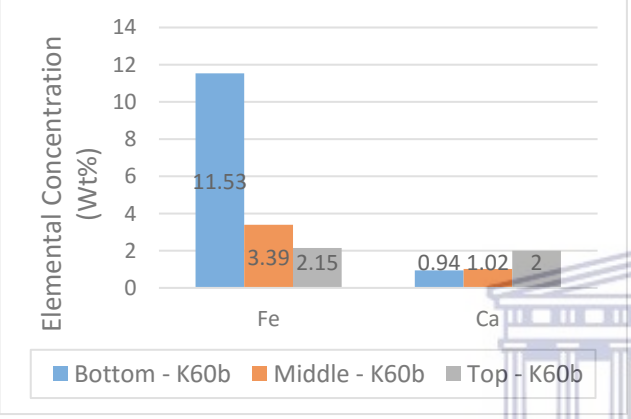

FIGURE 4.7*. External elemental composition of Fe and Ca minerals by weight percentage on Fly Ash particles from the K60b column.*

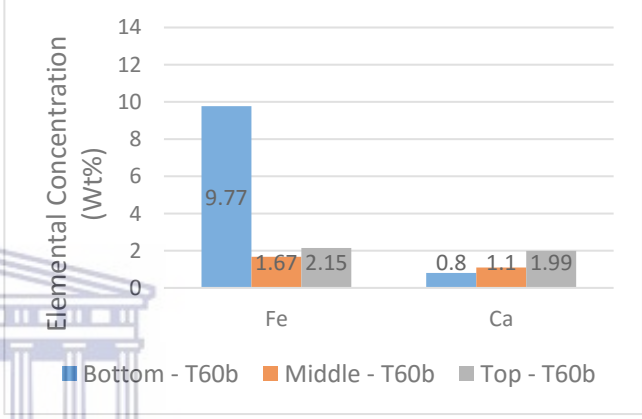

FIGURE 4.8. *External elemental composition of Fe and Ca minerals by weight percentage on Fly Ash particles from the T60b column.*

UNIVERSITY of the
WESTERN CAPE

https://etd.uwc.ac.za

4.2 AMD Water Chemistry

As expected, the sulphate concentration is significantly high, confirming what McCarthy (2011) reported on the impact of acid mine drainage in South Africa. The pH, EC and most of the elemental concentrations of Driefontein Pit Lake are consistent with the general water quality of AMD in the Witbank area. The water quality parameters that were targeted for this study are listed in TABLE 4.3.

***TABLE 4.3**. Composition of the chemical concentrations of Acid Mine Drainage used as influent.*

Chemical parameter	AMD					
	Unit	15-09-17	03-10-17	23-10-17	30-10-17	15-11-17
pH	-	2.5 – 2.7				
EC	mS/m	535	545	535	530	540
Si	mg/l	4.87	3.87	4.51	4.61	4.88
Al		83.6	67.2	83.4	91.1	90.5
Ca		353	294	410	406	406
Fe		190	138	178	177	182
K		2.74	3.44	3.14	3.05	3.30
Mg		169	165	212	200	215
Mn		53.2	44.1	50.3	49.5	52.9
Na		34.3	30.0	35.4	40.0	38.6
S as SO4		2 893	2 507	3 094	3 170	3 260
Cr		0.054	0.048	0.054	0.048	0.064

UNIVERSITY of the
WESTERN CAPE

4.3 Field Hydraulic Conductivity of Ash

Falling head infiltration tests were conducted on existing ash dumps to determine the change in hydraulic conductivity relative to the age of the ash.

4.3.1 Kendal power station (K-Ash)

Freshly dumped ash (K-Fresh): The hydraulic conductivity for the freshly dumped ash exhibited values ranging between 0.49 m/d – 0.79 m/d on three of the five tested holes. The other two holes showed K-value outliers of 0.37 m/d and 0.98 m/d respectively. FIGURE 4.9 depicts the hydraulic conductivity for one the 5 holes that was tested in the freshly dumped ash. A hydraulic conductivity of 0.49 m/d was measured for KF-H4 (Refer to APPENDIX B for data from the other tested holes).

https://etd.uwc.ac.za

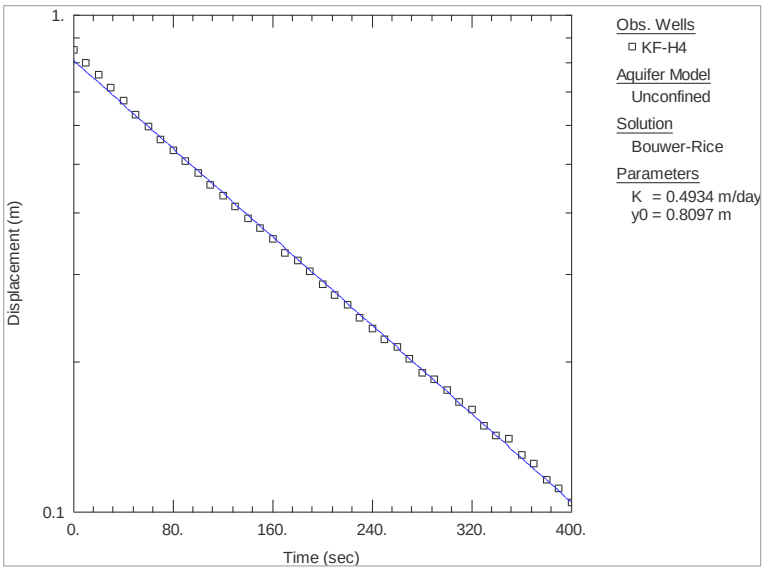

FIGURE 4.9. The hydraulic conductivity determined for KF-H4 using the Bouwer and Rice solution.

5 Year old ash (K5): Ash that has been dumped 5 years prior to the hydraulic conductivity testing, showed K-values ranging between 0.36 m/d – 0.57 m/d. FIGURE 4.10 depicts the hydraulic conductivity for K5-H5 using the Bouwer and Rice solution, K was measured at 0.57 m/d (Refer to APPENDIX B for data from the other tested holes).

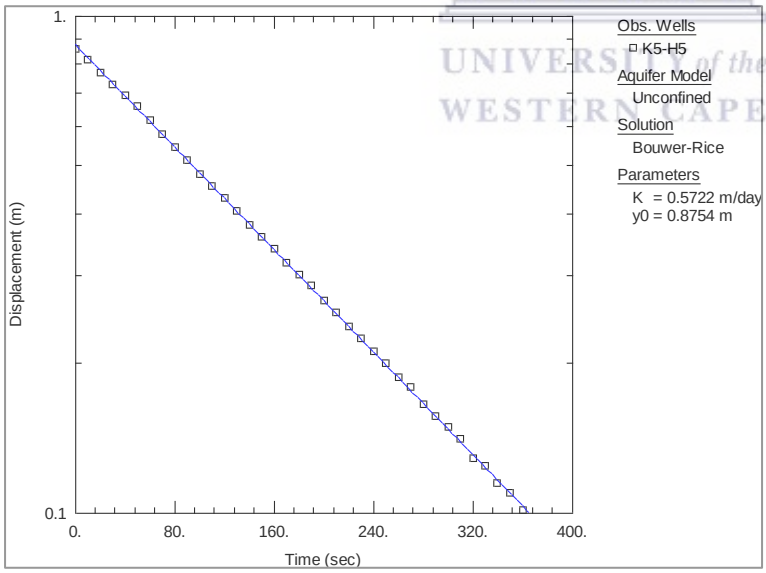

UNIVERSITY of the
WESTERN CAPE

FIGURE 4.10. The hydraulic conductivity determined for K5-H4 using the Bouwer and Rice solution.

10 Year old ash (K10): Ash that has been dumped 10 years prior to the hydraulic conductivity testing, showed K-values ranging between 0.29 m/d – 0.53 m/d. FIGURE 4.11 exhibits the

https://etd.uwc.ac.za

hydraulic conductivity for K10-H3 which was determined through the Bouwer and Rice solution. The K was measured at 0.29 m/d for this specific hole. (Refer to APPENDIX B for data from the other tested holes).

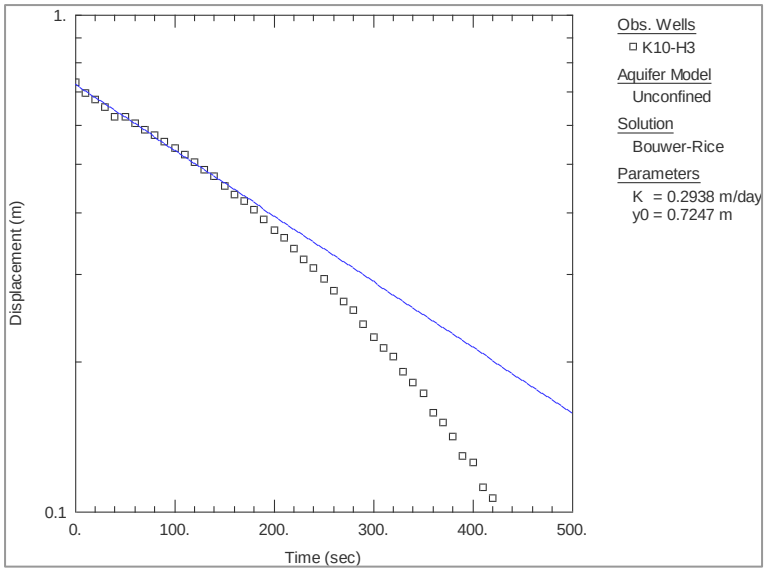

***FIGURE 4.11**. The hydraulic conductivity determined for K10-H3 using the Bouwer and Rice solution.*

15 Year old ash (K15): Ash that has been dumped 15 years prior to the hydraulic conductivity testing, showed K-values ranging between 0.25 m/d – 0.53 m/d. One of the holes exhibited an outlier with a K-value of 0.75 m/d. FIGURE 4.12 exhibits the hydraulic conductivity of K15-H1 that was determined through the Bouwer and Rice solution. The K was measured at 0.40 m/d (Refer to APPENDIX B for data from the other tested holes).

UNIVERSITY of the WESTERN CAPE

https://etd.uwc.ac.za

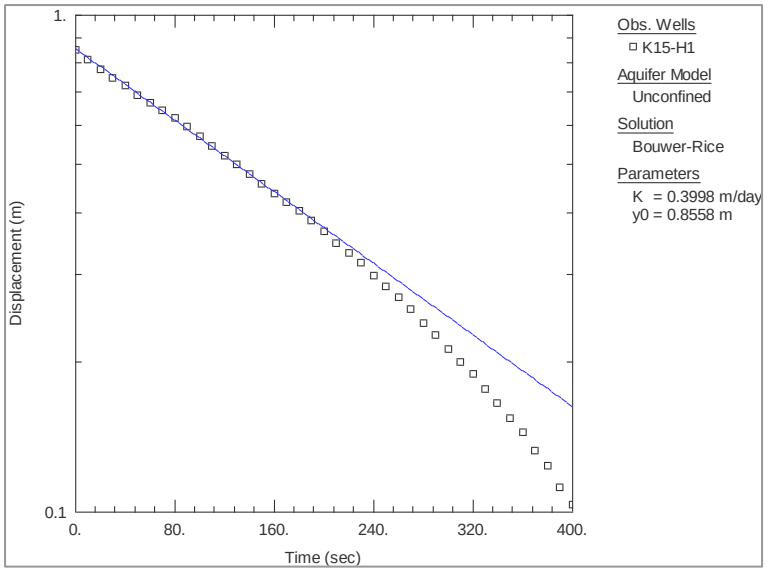

FIGURE 4.12. *The hydraulic conductivity determined for K15-H1 using the Bouwer and Rice solution.*

20 Year old ash (K20): Ash that has been dumped 20 years prior to the hydraulic conductivity testing, showed K-values ranging between 0.20 m/d – 0.29 m/d. FIGURE 4.13 exhibits the hydraulic conductivity of K20-H3 that was determined through the Bouwer and Rice solution. The K was measured at 0.27 m/d (Refer to APPENDIX B for data from the other tested holes).

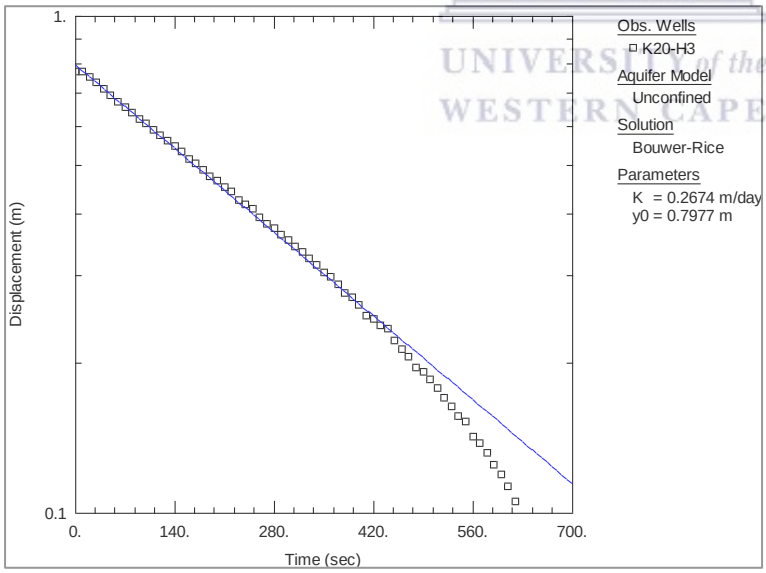

FIGURE 4.13. *The hydraulic conductivity determined for K20-H3 using the Bouwer and Rice solution.*

https://etd.uwc.ac.za

4.3.1.1 Combined field hydraulic conductivity for Kendal

Overall, the data derived from the hydraulic conductivity testing on the Kendal ash dump, showed a decreasing trend in the hydraulic conductivity relative to increasing age of the ash. FIGURE 4.14 depicts the hydraulic conductivity data for all the holes tested at various ages. The whiskers on the plot represents the minimum and maximum hydraulic conductivity measurements at each respective age. The x marks represents the average of all the data points from the respective ages and the horizontal line within the boxes is a representation of the median. The median for the 10 years old (K10) tested ash are not very visible on the plot, which is due to the fact that the median and the 25th percentile data the same K-values are at 0.29 m/d. The freshly dumped ash is loosely dumped, non-compacted and unconsolidated material and therefore it exhibits the highest K-values on the Kendal ash dump. The pozzolanic nature of the Kendal ash plays a role in the hardening of ash over time. Water from precipitation and irrigation reacts with the CaO minerals in the ash, causing the ash to set and solidify. The pozzolanic nature, together with compaction and the mineralization of calcium rich minerals over time, has an impact on the decreasing hydraulic conductivity of the ash over time. In the field, it was also experienced that it was harder to drill auger holes into the ash of older age in comparison to the freshly dumped ash, and that hardening effect increased with increasing age (FIGURE 4.14).

UNIVERSITY of the
WESTERN CAPE

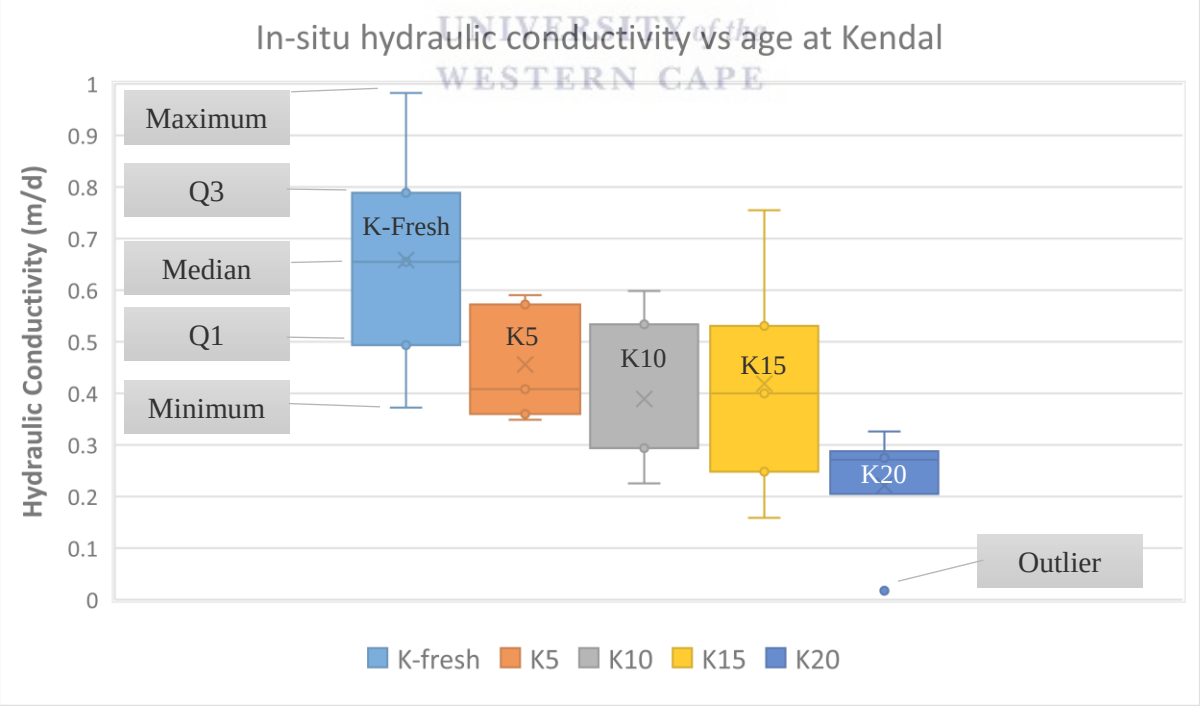

FIGURE 4.14. *In-situ hydraulic conductivity of ash of different age at Kendal Power Station ash dump.*

https://etd.uwc.ac.za

4.3.2 Tutuka power station (T-Ash)

Freshly dumped ash (T-Fresh): The hydraulic conductivity for the freshly dumped ash exhibited K-values ranging between 0.33 m/d – 0.46 m/d. FIGURE 4.15 exhibits the hydraulic conductivity of TF-H2 that was determined through the Bouwer and Rice solution. The K was measured at 0.46 m/d (Refer to APPENDIX B for data from the other tested holes).

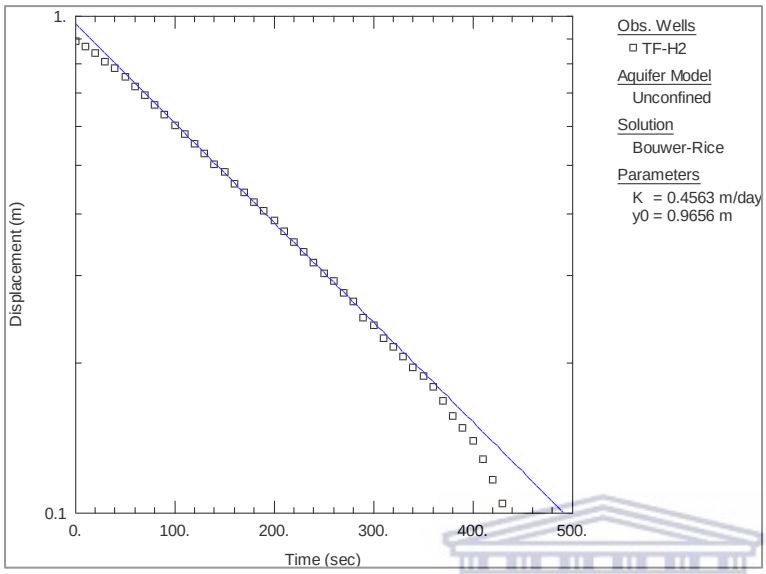

FIGURE 4.15. *The hydraulic conductivity determined for TF-H2 using the Bouwer and Rice solution.*

UNIVERSITY of the
WESTERN CAPE

1 Year old ash (T1): Ash that has been dumped 1 year prior to the hydraulic conductivity testing, showed K-values ranging between 0.33 m/d – 0.46 m/d. FIGURE 4.16 exhibits the hydraulic conductivity of T1-H2 that was determined through the Bouwer and Rice solution. The K was measured at 0.33 m/d (Refer to APPENDIX B for data from the other tested holes).

https://etd.uwc.ac.za

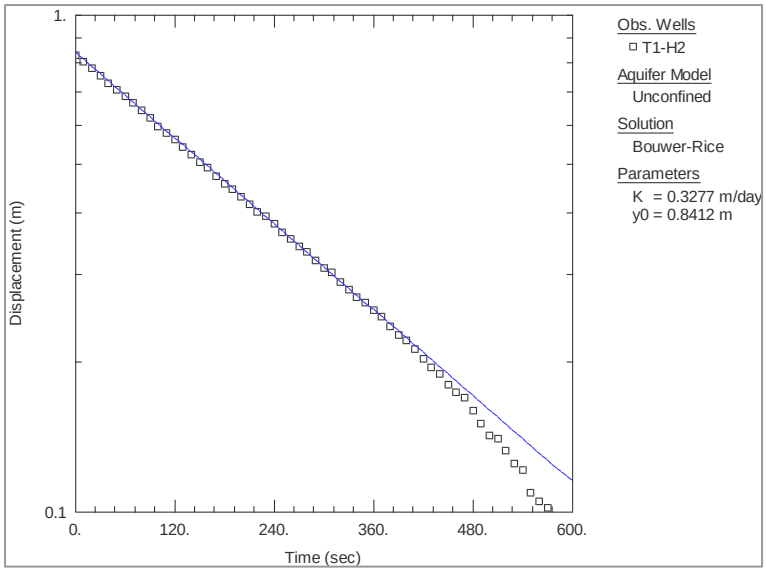

FIGURE 4.16. The hydraulic conductivity determined for T1-H2 using the Bouwer and Rice solution.

5 Year old ash (T5): Ash that has been dumped 5 years prior to the hydraulic conductivity testing, showed K-values ranging between 0.08 m/d – 0.14 m/d. FIGURE 4.17 exhibits the hydraulic conductivity of T5-H3 that was determined through the Bouwer and Rice solution. The K was measured at 0.14 m/d (Refer to APPENDIX B for data from the other tested holes).

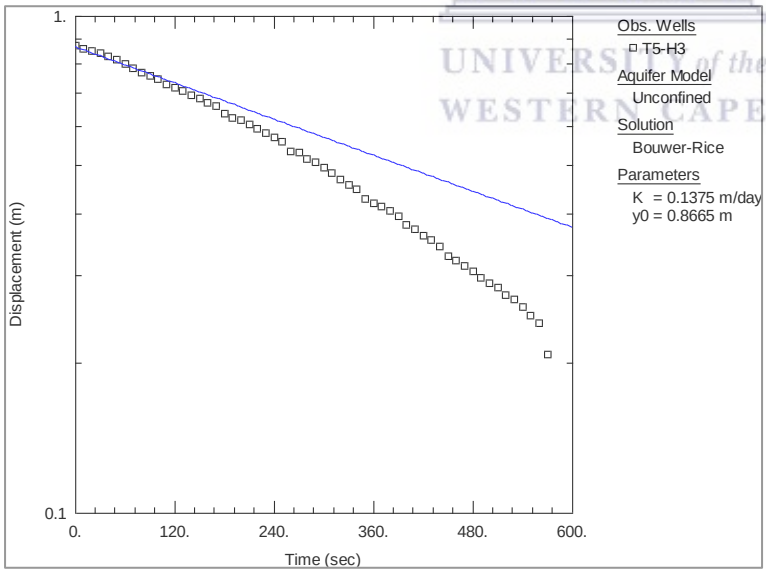

UNIVERSITY of the
WESTERN CAPE

FIGURE 4.17. The hydraulic conductivity determined for T5-H3 using the Bouwer and Rice solution.

20 Year old ash (T20): Ash that has been dumped 20 years prior to the hydraulic conductivity testing, showed K-values ranging between 0.20 m/d – 0.33 m/d. One of the 4 tested holes

https://etd.uwc.ac.za

exhibited an outlier with a K-value of 0.58 m/d. FIGURE 4.18 exhibits the hydraulic conductivity of T20-H3 that was determined through the Bouwer and Rice solution. The K was measured at 0.23 m/d (Refer to APPENDIX B for data from the other tested holes).

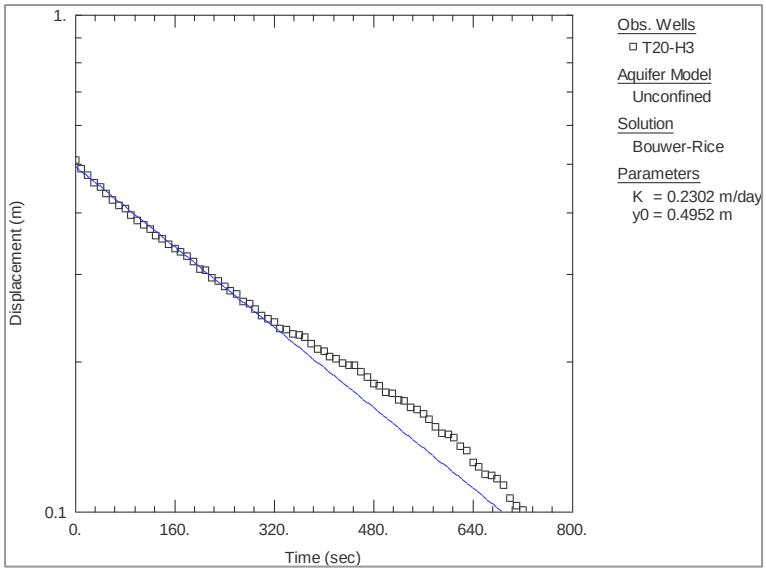

FIGURE 4.18. *The hydraulic conductivity determined for T20-H3 using the Bouwer and Rice solution.*

30 Year old ash (T30): Ash that has been dumped 30 years prior to the hydraulic conductivity testing, showed K-values ranging between 0.25 m/d – 0.28 m/d. One of the 5 tested holes exhibited an outlier with a K-value of 0.41 m/d. FIGURE 4.19 exhibits the hydraulic conductivity of T30-H2 that was determined through the Bouwer and Rice solution. The K was measured at 0.26 m/d (Refer to APPENDIX B for data from the other tested holes).

UNIVERSITY of the
WESTERN CAPE

https://etd.uwc.ac.za

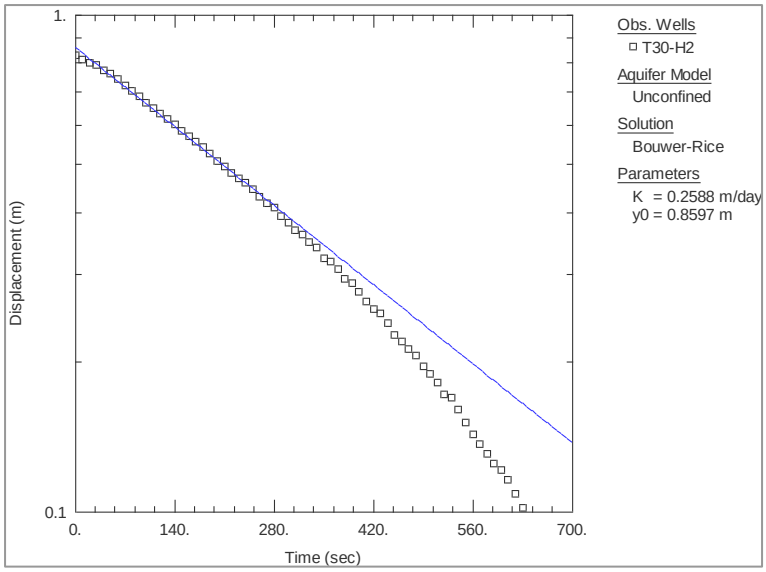

FIGURE 4.19. *The hydraulic conductivity determined for T30-H2 using the Bouwer and Rice solution.*

4.3.2.1 Combined field hydraulic conductivity for Tutuka

Similar to the Kendal ash dump, the hydraulic conductivity data for the Tutuka ash dump showed an overall decreasing trend in K-values relative to increasing age (FIGURE 4.20). October (2011) tested and determined the hydraulic conductivity of Tutuka ash and found results similar to the measured hydraulic conductivity of the fresh ash. Moreover, the overall hydraulic conductivity of the Tutuka ash dump is comparatively lower than the K-values from the Kendal ash dump. Furthermore, the 5-year old ash exhibited irregularly low hydraulic conductivity values compared to the K-values of the rest of the ash dump. This could be caused by the excessive irrigation of brine water at the time the ash was dumped. The excess brine water together with the pozzolanic nature of the ash caused the ash to set more than usual. Moreover, it was significantly harder to drill auger holes into the 5-year old ash when compared to the other ages.

https://etd.uwc.ac.za

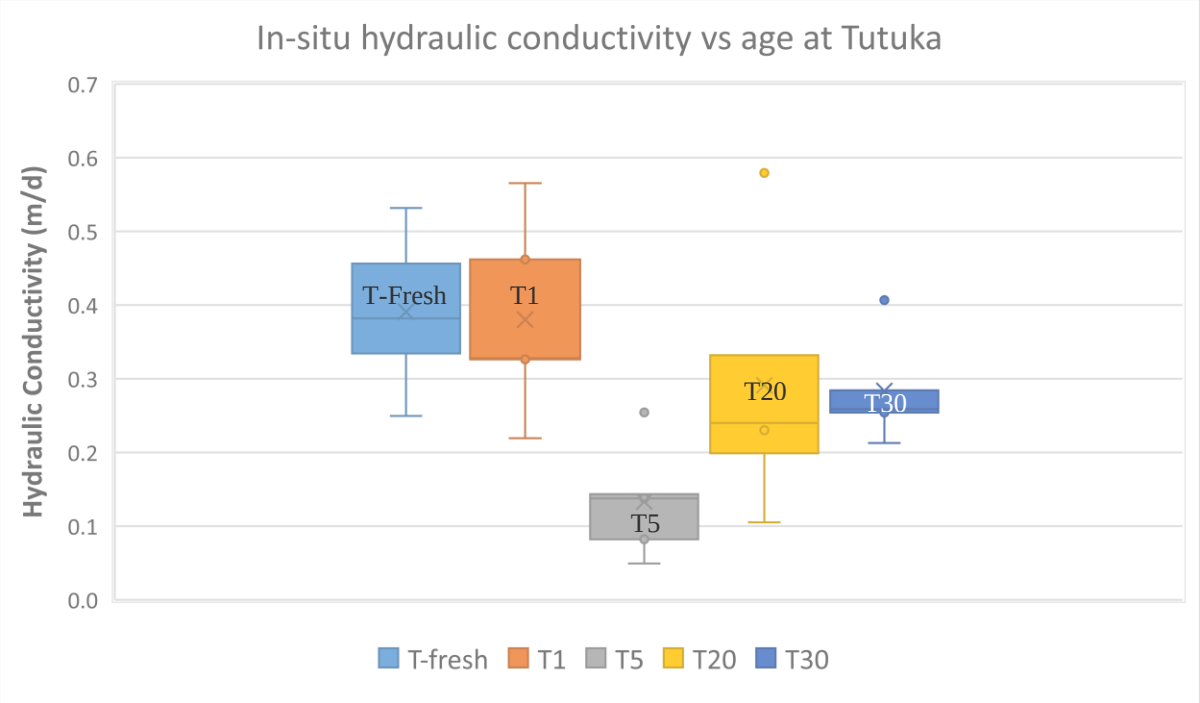

FIGURE 4.20. In-situ hydraulic conductivity of ash of different age at Tutuka Power Station ash dump.

UNIVERSITY of the
WESTERN CAPE

4.4 Laboratory Hydraulic Conductivity of Fly Ash

The initial hydraulic conductivity of fly ash pre-cured to 3 days and 28 days respectively was compared to evaluate the effect of the cured waiting period. The results are presented in TABLE 4.4 and as expected, no significant differences in hydraulic conductivity was observed for the Kendal ash. Although all the hydraulic conductivity values for the columns were measured at 10^{-1} m/d during the initial stages (first 4 days) of testing, the Tutuka ash showed relatively higher K-values for the 3 day cured fly ash compared to the 28 days cured fly ash.

TABLE 4.4. A comparison in hydraulic conductivity of fly ash cured for 3 and 28 days respectively.

Column Name	Cured Moisture Content (%)	Cured waiting time (days)	Initial K (m/d)
Kash50	50	3	0.16
Kash60	60	3	0.16
K50	50	28	0.17
K60	60	28	0.29
Tash50	50	3	0.81
Tash60	60	3	0.44
T50	50	28	0.21
T60	60	28	0.31

https://etd.uwc.ac.za

The hydraulic conductivity of K-Ash and T-Ash columns was measured and the changes over time were monitored routinely throughout the duration of the experimental procedure. In addition to the hydraulic conductivity testing, the pH of inflow AMD and the discharge was measured to determine the influence of ash on AMD flowing through it. The fly ash in all the columns was mixed to slurries at various moisture content respectively and cured for 28 days before hydraulic conductivity testing commenced. It is also important to note that columns K40, K50, K60, T40, T50 and T60 was 0.2 m in length, whereas, columns K60b and T60b was 0.5m in length, indicating that the 0.5 m columns consisted of significantly larger volumes of fly ash.

4.4.1 Hydraulic conductivity of K-Ash and T-Ash at 40% moisture content

Hydraulic conductivity values for Kendal ash (K40), pre-cured to 40% moisture, started at 0.1 m/d and increased slightly towards 0.2 m/d after approximately 12 000 mL of AMD was leached through the 20 cm column. Thereafter the hydraulic conductivity decreased until the column eventually clogged up after 25 000 mL of AMD and flow-through was completely restricted (FIGURE 4.21).

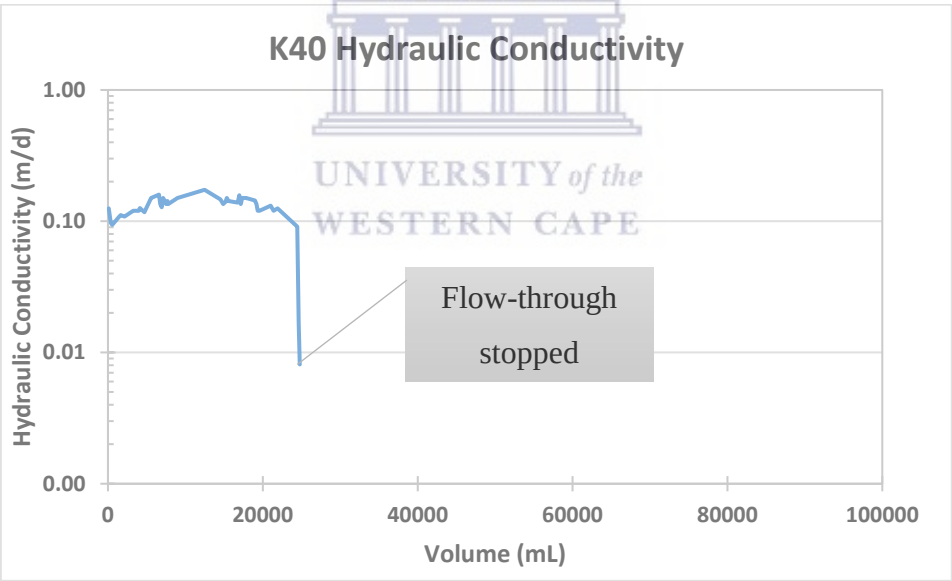

FIGURE 4.21. The hydraulic conductivity of the K40 column pre-cured to 40% moisture content.

Tutuka ash (T40), pre-cured to 40% moisture, showed a relatively higher initial hydraulic conductivity value at approximately 0.2 m/d. The hydraulic conductivity increased rapidly to 0.6 m/d due to the dissolving of the portlandite mineral (pozzolanic material) and thereafter decreased over time due to the secondary mineralization of Gypsum. The hydraulic

https://etd.uwc.ac.za

conductivity decreased to three orders of magnitude from 10^{-1} m/d to 10^{-3} m/d after approximately 60 000 mL of AMD had leached through the column (FIGURE 4.22).

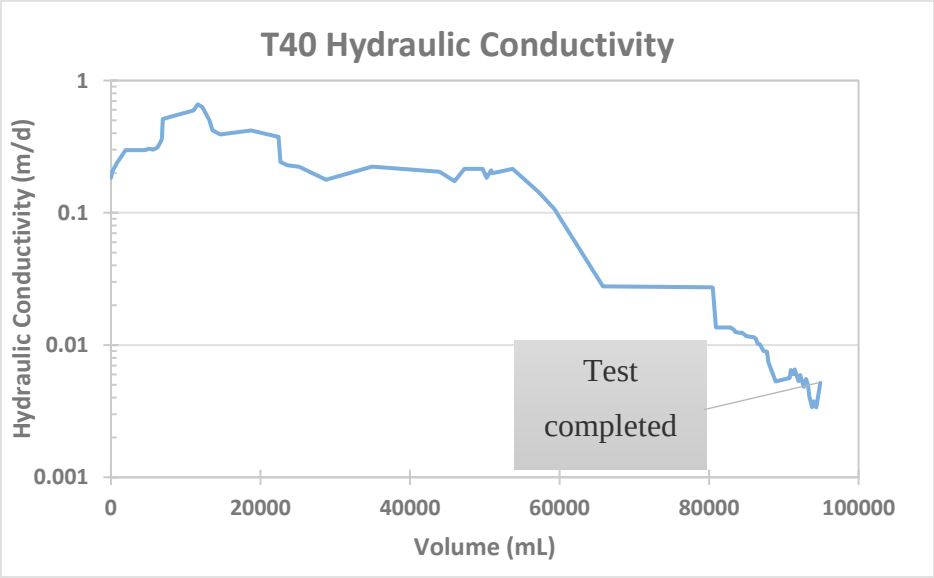

***FIGURE 4.22**. The hydraulic conductivity of the T40 column pre-cured to 40% moisture content.*

UNIVERSITY of the WESTERN CAPE

The pH measurements of both K40 and T40 showed similar trends as the ash initially buffers the AMD from an inflow pH of 2.5 to a discharge pH of 12. The K40 however, shows a slightly stronger buffering potential than the T40. The general trend of the pH shows some acidification over time as the pH decreased from 12 towards a pH of 4 where it stabilized, due to large volumes of AMD flowing through short ash columns (FIGURE 4.23).

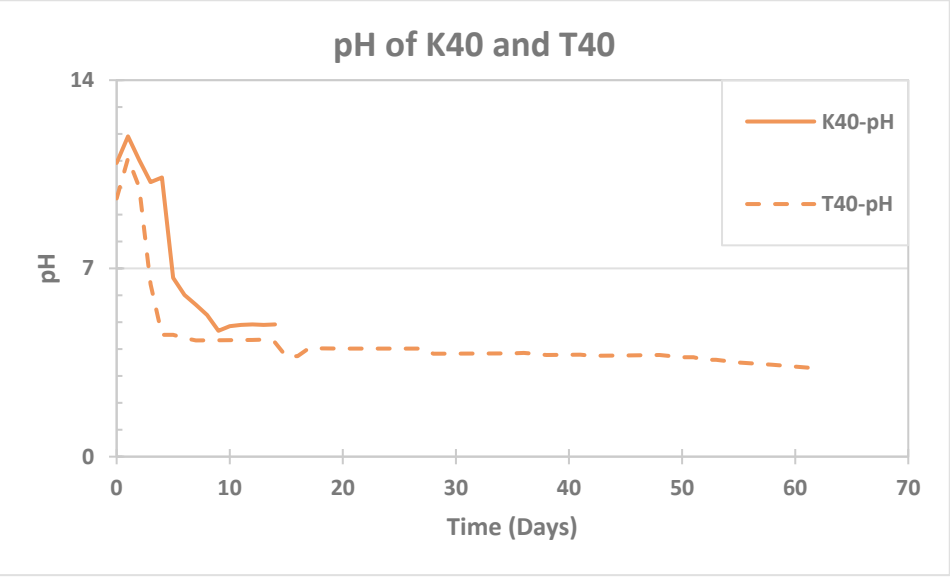

***FIGURE 4.23**. The pH of the K40 and T40 leachate over time.*

https://etd.uwc.ac.za

The curing moisture in the ash during placement, allows for pozzolanic reactions (portlandite) to solidify the ash and lowers the K by an order of magnitude, relative to fresh ash. Thereafter, the AMD dissolves these pozzolanic gels and causes the K to increase slightly. The secondary mineralization of calcium rich minerals (gypsum) in the ash contributes to a further lowering in the K by an order of magnitude. The hydraulic conductivity decreased 3 orders of magnitude, from an initial 10^{-1} m/d to 10^{-3} m/d, with the AMD iron (jarosite) concentration above 170 mg/l playing the dominant role in reducing the hydraulic conductivity as it clogs void spaces at low pH conditions (FIGURE 4.24). The chemical analysis of the leachate are discussed in chapter 4.5.

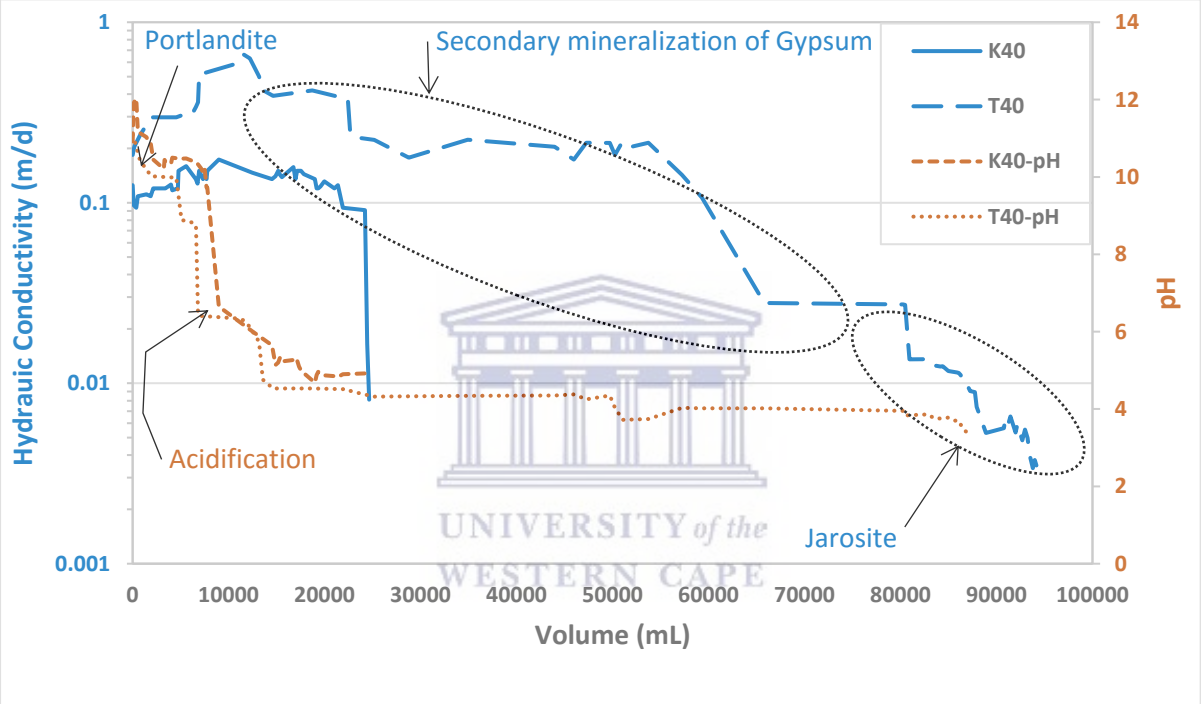

FIGURE 4.24. The change in hydraulic conductivity of fly ash over time plotted with the change in pH of the discharge of fly ash pre-cured to 40% moisture content.

4.4.2 Hydraulic conductivity of K-Ash and T-Ash at 50% moisture content

K50 and T50 showed very similar initial hydraulic conductivity values starting at 0.1 m/d. The hydraulic conductivity increased gradually towards 0.2 m/d, due to the dissolution of the portlandite minerals (pozzolanic material) which had formed during the curing phase. Ultimately, the hydraulic conductivity started too decrease due to the secondary mineralization of Gypsum and after 12 000 mL of AMD had leached through the columns. The K-values from the K50 column however, decreased more rapidly over time compared to the T50.

https://etd.uwc.ac.za

Subsequently, the K-values from both columns decreased to three orders of magnitude from 10^{-1} m/d to 10^{-3} m/d (FIGURE 4.25).

The initial buffering potential of both K50 and T50 showed similar pH values at approximately 12 and stabilized at pH = 4 after some acidification occurred. Initially the K50 buffering potential was slightly stronger than the buffering potential of T50. However, after 40 000 mL AMD had leached through the columns, the late time pH of K50 decreased towards the same pH of the influent AMD water at a pH of 2.5 and the pH of the T40 column remained above a pH of 4 for longer until it also decreased to a pH of 2.5 (FIGURE 4.25).

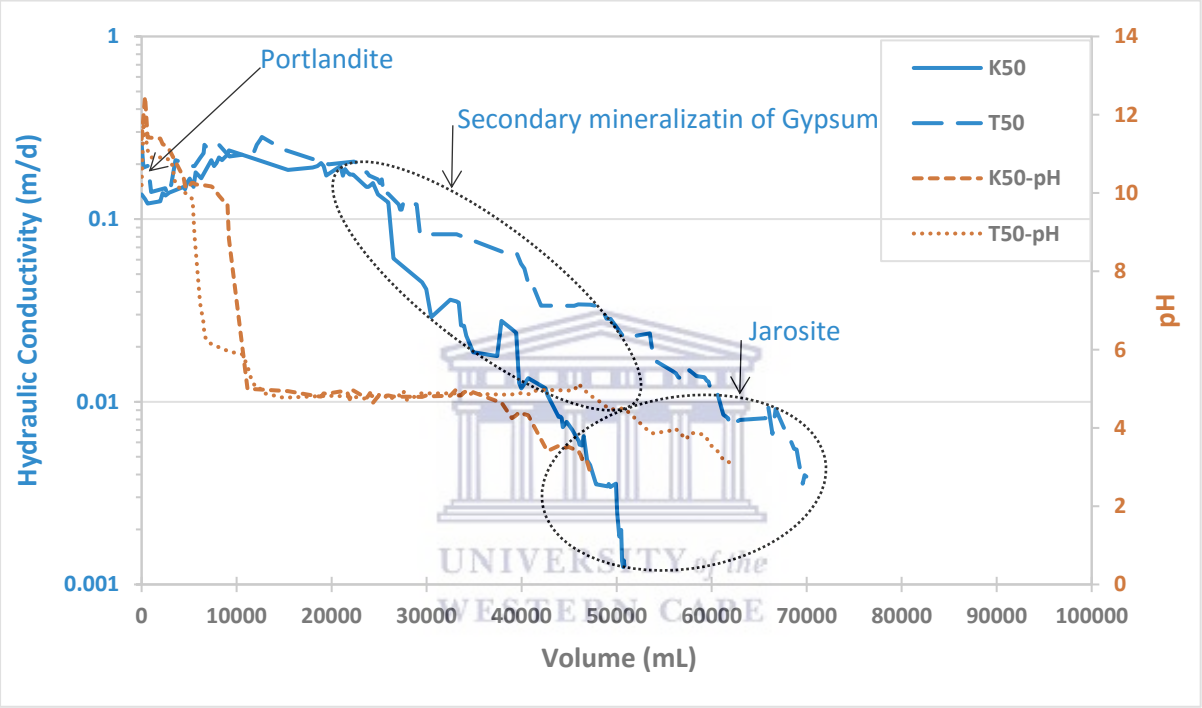

FIGURE 4.25. The change in hydraulic conductivity of fly ash over time plotted with the change in pH of the discharge of fly ash pre-cured to 50% moisture content.

4.4.3 Hydraulic conductivity of K-Ash and T-Ash at 60% moisture content

4.4.3.1 K60 and T60 columns

K60 and T60 showed very similar initial hydraulic conductivity values starting at 0.11 m/d. The hydraulic conductivity increased slightly until it ultimately started too decreased after 12 000 mL AMD leached through the columns. The hydraulic conductivity of the K60 column started to decrease again just like the K40 and K50 columns showed. The hydraulic conductivity further decreased by an order of magnitude from 10^{-1} m/d to 10^{-2} m/d after 40 500

https://etd.uwc.ac.za

mL of AMD had leached through. The hydraulic conductivity only decreased to the 3rd order of magnitude after 78 600 mL of AMD had leached through the column.

The T60 column however, decreased more rapidly over time than the K60 until both decreased to two orders of magnitude. The initial hydraulic conductivity was measured at 0.25 m/d and increased towards 0.45 m/d after 13 260 mL of AMD had leached through the column. The hydraulic conductivity decreased gradually from 10^{-1} m/d to 10^{-2} m/d after 24 600 mL of AMD had leached through. The K decreased from 10^{-2} m/d to 10^{-3} m/d and after 60 640 *mL* of AMD had leached through, the last K measured was at 0.006 m/d. (FIGURE 4.26).

The pH measurements of both K60 and T60 showed similar trends as the ash initially buffers the AMD from an inflow pH of 2.5 to an outflow pH of 12. The K60 however, shows a slightly stronger buffering potential than the T60. The general trend that the pH shows some acidification over time as the outflow pH decreased from 12 towards a pH of 4 where it stabilized (FIGURE 4.26).

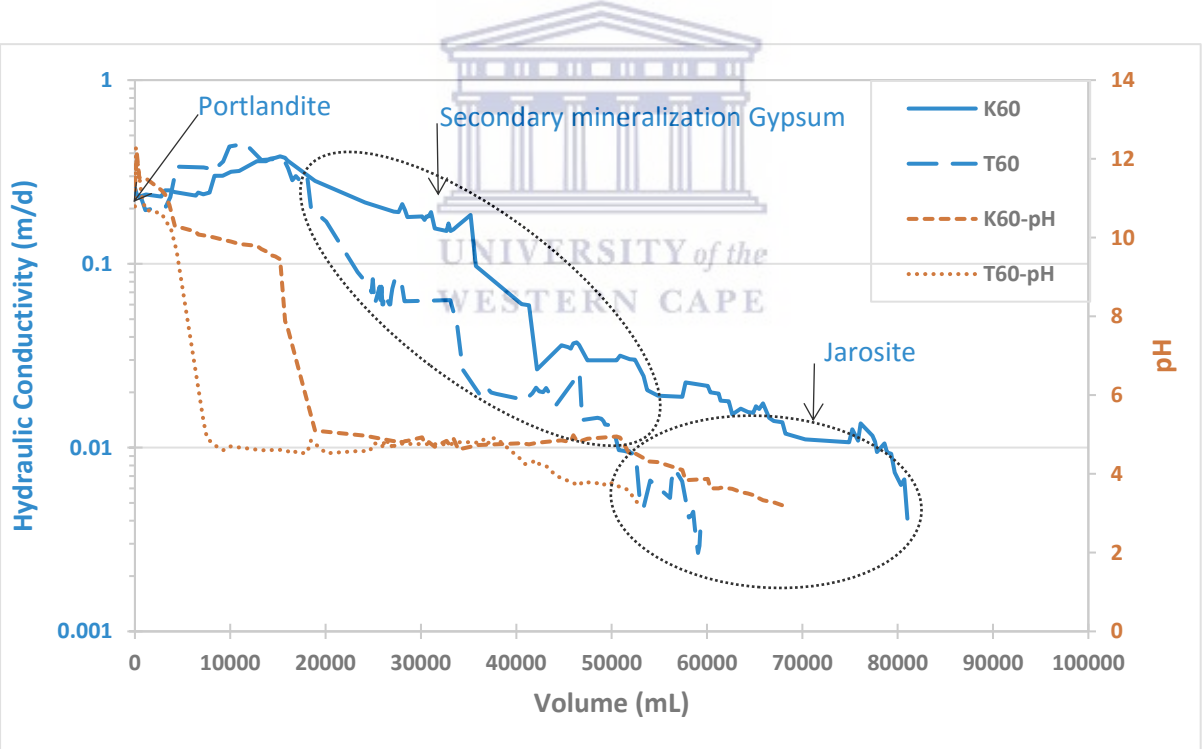

FIGURE 4.26. *The change in hydraulic conductivity of fly ash over time plotted with the change in pH of the discharge of fly ash pre-cured to 60% moisture content.*

https://etd.uwc.ac.za

4.4.3.2 K60b and T60b columns

The fly ash in the K60b column was mixed to 60% moisture content before curing. The early time hydraulic conductivity measured for K60b showed similar results compared to K60. Although there was a general decreasing trend in hydraulic conductivity over time, the K60b column exhibited relatively higher K-values compared to the shorter columns. The hydraulic conductivity decreased by an order of magnitude from 10^{-1} m/d to 10^{-2} m/d after 42 600 mL of AMD had leached through the column. Moreover, the hydraulic conductivity decreased from 0.07 m/d towards 0.03 m/d on the last day of testing. The hydraulic conductivity of K60b did not decrease by 3 orders of magnitude, whereas, the hydraulic conductivity of the shorter columns did.

The fly ash in the T60b column was mixed to 60% moisture content before curing. The early time hydraulic conductivity measured for T60b was slightly higher at 0.34 m/d. Although, there was a general decreasing trend in hydraulic conductivity over time, the T60b column exhibited relatively higher K-values compared to the shorter columns. The hydraulic conductivity decreased by an order of magnitude from 10^{-1} m/d to 10^{-2} m/d after 38 712 mL of AMD had leached through the column. Moreover, the hydraulic conductivity decreased from 0.09 m/d towards 0.05 m/d on the last day of testing. The hydraulic conductivity of T60b did not decrease to 3 orders of magnitude, whereas, the hydraulic conductivity of the shorter columns did.

UNIVERSITY of the
WESTERN CAPE

https://etd.uwc.ac.za

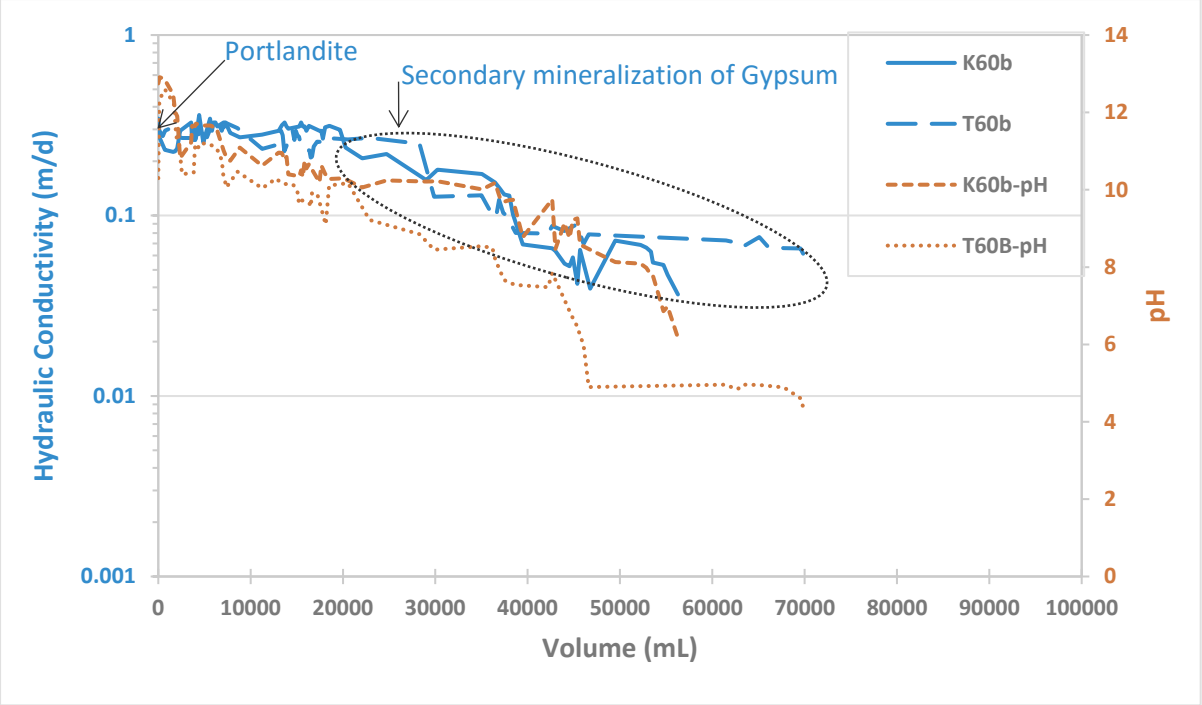

***FIGURE 4.27**. The change in hydraulic conductivity of fly ash over time plotted with the change in pH of the discharge of fly ash pre-cured to 60% moisture content*

In retrospect, there are pozzolanic gels formed during the curing phase of fly ash with AMD water. These pozzolanic gels (portlandite ($Ca(OH)_2$) fill up pore spaces and causes the fly ash to set and harden during the 28 day waiting period, resulting in that initial low hydraulic conductivity values observed in all the columns. However, due to the low calcium oxide content in Class F fly ash, the fly ash doesn't have the self-cementing properties like the Class C fly ash do. Therefore, the AMD water dissolves these pozzolanic bindings during the initial stages of the hydraulic conductivity testing which causes that gradual increase in K. Thereafter, the secondary mineralization of gypsum causes the K to decrease again. Eventually, the jarosite minerals in the AMD accumulate at the contact face with fly ash and over time cause that final decrease in K.

Overall, the pH concentrations of leachate for all the columns remained above the influent AMD pH of 2.5 throughout the entire testing period. According to Nhan et al., (1996), the initial pH of the effluent are controlled by the dissolution of $Ca(OH)_2$ and $Mg(OH)_2$. Moreover, the K-Ash columns exhibited a stronger buffering behaviour through time in comparison to the buffering behaviour of the T-Ash columns. The K-Ash also consists of slightly higher concentrations of CaO and MgO (TABLE 4.1) compared to the T-Ash, hence the stronger buffering behaviour. Even though the pH concentration of the leachate eventually drops below

https://etd.uwc.ac.za

pH = 4.5, it was also observed that the hydraulic conductivity had decreased to three orders of magnitude decreasing from 10^{-1} m/d to 10^{-3} m/d. This suggests that by the time the fly ash has reached its capacity to buffer AMD, the volumes of leachate percolating through the fly ash are minimal.

4.4.4 The relationship between hydraulic conductivity and moisture content for K-Ash and T-ash columns

K-Ash shows a consistent relationship between curing moisture content and hydraulic conductivity. The lower curing moisture content results in a lower hydraulic conductivity during the entire test period (FIGURE 4.28).

T-Ash however, showed more inconsistent results in the relationship between moisture content and the change in hydraulic conductivity over time. This may be due to lesser volumes of the silt sized particles materials in the Tutuka ash when compared the silt sized ratio in the Kendal ash, resulting in the inconsistency of flow through (FIGURE 4.29).

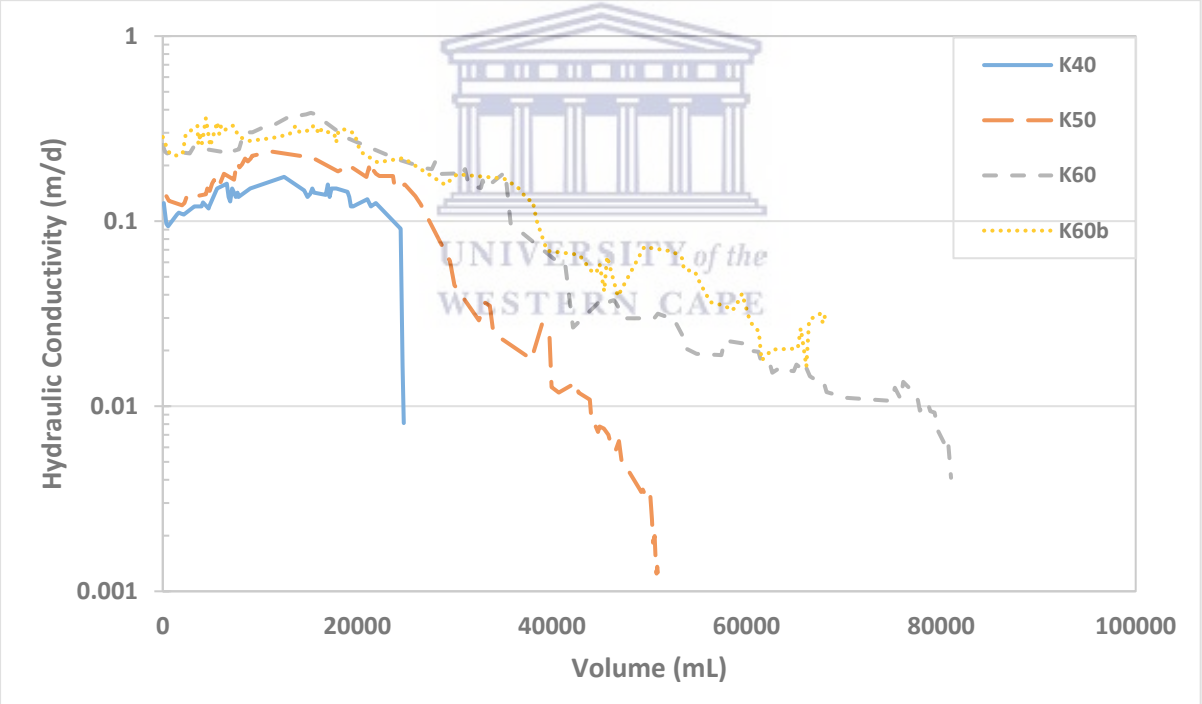

***FIGURE 4.28**. The relationship between the hydraulic conductivity vs the various moisture content of K-Ash columns.*

https://etd.uwc.ac.za

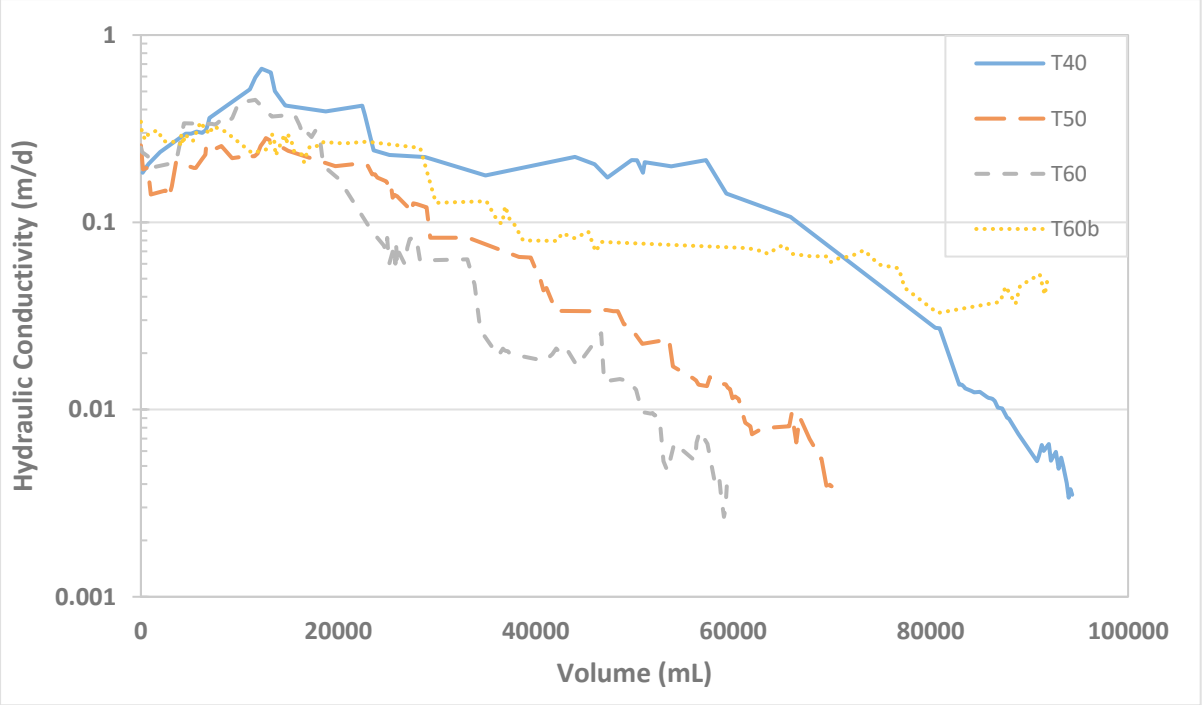

***FIGURE 4.29**. The relationship between the hydraulic conductivity vs the various moisture content of the T-Ash columns.*

It appeared that the moisture content had a significant influence on the hydraulic conductivity behaviour of the ash from Kendal power station. The ash with lowest moisture content showed the lowest hydraulic conductivity and further decreased faster over time in comparison to the ash with higher moisture content. The Tutuka ash however, showed an inconsistent relationship between the hydraulic conductivity and the moisture content. Therefore, it can by concluded that the moisture content played major role in the decreasing hydraulic conductivity over time in the Kendal ash, and not so much in the Tutuka ash.

4.5 Laboratory Geochemistry

The temporal change in electrical conductivity (EC) from the leachate was measured and observed routinely throughout the hydraulic conductivity testing period. The results are presented in FIGURE 4.34 and FIGURE 4.35 showing a comparison of EC of the influent AMD against the leachate EC. Furthermore, the chemical concentrations of Si, Al, Fe, S, Ca, Mg, Na, K, Mn and Cr in the AMD and leachate were measured to evaluate the leaching properties of fly ash once it is exposed to AMD. FIGURE 4.36 to FIGURE 4.45 depicts the elemental concentrations of the influent AMD compared to the leachate concentrations over time.

https://etd.uwc.ac.za

4.5.1 Acid Mine Drainage

The following relate to the geochemical reactions in mine material:

- The mine material will consist of a solid, water and gas phase. Without one of these phases, no acid-mine drainage (AMD) production and drainage are possible. The waste rock material (solid phase) are the reactive part of the three phases and contains sulphide minerals that reacts spontaneously with oxygen and water.

- Upon oxidation, pyrite will react with the infiltrating oxygen and water to produce Fe^{3+}, SO_4^{2-} and acidity:

$$\text{pyrite} + 3.5H_2O + 3.75O_{2(aq)} \Rightarrow Fe(OH)_{3(ppd)} + 2SO_4^{2-} + 4H^+ \qquad \text{Reaction (8)}$$

- Water serves as the transport medium for the products of AMD as it percolates through the waste material. The water phase also serves as the medium in which dissolution of neutralizing minerals can take place. The acid produced by the pyrite will be consumed by calcite (and/or dolomite) if present in the rock:

$$\text{calcite} + 2H^+ \Rightarrow Ca^{2+} + CO_{2(g)} + H_2O \qquad \text{Reaction (9)}$$

- The Ca^{2+} and SO_4 produced will form gypsum and the above equations could be rewritten as follows:

$$\text{pyrite} + 2\text{calcite} + 5.5H_2O + 3.75O_{2(aq)} \Rightarrow Fe(OH)_{3(ppd)} + 2\text{gypsum} + 2CO_{2(g)} \qquad \text{Reaction (10)}$$

- If all the carbonate minerals (generally, calcite and dolomite) are depleted, then the seepage from the dumped material becomes acidic. Silicate minerals can also consume some of the acidity. However, silicate minerals react too slowly to prevent acidification in material with a significant potential to generate acidic drainage.

- In acidic seepage, metals will also be leached out at elevated concentrations and the final stage of AMD would have been reached.

An important aspect in environmental geochemistry of a mine is therefore to determine whether enough neutralization minerals exists or not, and when it will become depleted. It is not possible to determine the time scale for these mineral reactions from the laboratory tests. Even with leach tests neutralization minerals are often not depleted and more important, the tests also do not have exactly the same rock/water/gas ratio as the backfilled material in the mining pit.

UNIVERSITY of the WESTERN CAPE
https://etd.uwc.ac.za

4.5.2 Fly ash environmental geochemistry

The following relate to the geochemical reactions that can be associated with fly ash:

- Quartz (SiO_2) and mullite ($3Al_2O_3.2SiO_2$ or $2Al_2O_3.SiO_2$) are usually present as major minerals in the fly ash. The amorphous phase in fly ash is however dominant and is comprised mostly of SiO_2 (am) and Al-silicates like $Al_2Si_2O_7$ (am). $Al_2Si_2O_7$ (am) can form from kaolinite at temperatures above 500ºC. Above 1000 ºC the $Al_2Si_2O_7$ (am) starts to crystalise into mullite.

- Aluminium (Al) behaves as an amphoteric metal with both acid and base properties. Weathering of ash can result in the release of Al as observed in the column leach tests, e.g.

$$Al_2Si_2O_7(am) + 2OH^- + 3H_2O \Rightarrow + 2Al(OH)_4^- + 2SiO_2(aq) \qquad \text{Reaction (11)}$$

At alkaline conditions, Al forms the stable complex $Al(OH)_4^-$ as indicated in FIGURE 4.30. Aluminium will become less soluble under neutral conditions as was seen in the coal ash columns in contact with AMD.

- Ca in the coal ash is present mostly as lime (CaO), portlandite ($Ca(OH)_2$) and calcite ($CaCO_3$). The lime results in a high paste pH of 11-12 and reacts according to reaction 12 and reaction 13 below:

UNIVERSITY of the
WESTERN CAPE

$$CaO + H^+ \Rightarrow CaOH \qquad \text{Reaction (12)}$$

$$CaOH + H^+ \Rightarrow H_2O + Ca^{2+} \qquad \text{Reaction (13)}$$

- Traces of Cr, V, B and Mo leached from the fly ash under a fairly wide pH range. All these elements forms fairly stable and soluble oxyanions over a wide pH range. The stability of the Cr-H_2O system is depicted in FIGURE 4.31. Under oxidising conditions Cr is fairly soluble and forms the stable Cr(VI) oxyanion CrO_4^{2-}. V is fairly soluble and stable over a wide pH range as depicted in FIGURE 4.32 and forms the oxyanion VO_3OH^{2-}. B forms the stable BO_2^- (FIGURE 4.33) and Mo the stable and fairly soluble molybdate ion MoO_4^{2-}.

- The reaction between coal ash and AMD will therefore result in high Ca and sulphate that is generated. Metals introduced with the AMD (like Fe, Mn, Co, Ni) will mostly precipitate as they are fairly insoluble under neutral to alkaline conditions. Trace metal(loid)s from the ash like Cr, V, B and Mo is stable over a wide pH range and will

https://etd.uwc.ac.za

not be highly affected by the AMD. Cr(III) is however more likely to be present at neutral conditions than Cr(VI).

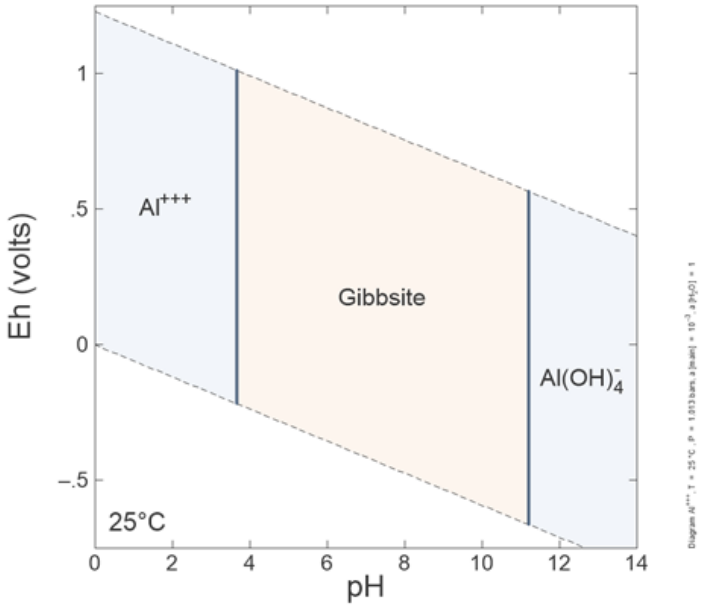

FIGURE 4.30. *Stability diagram for the Al-H2O system at standard conditions (activity Al = 1e^{-3}).*

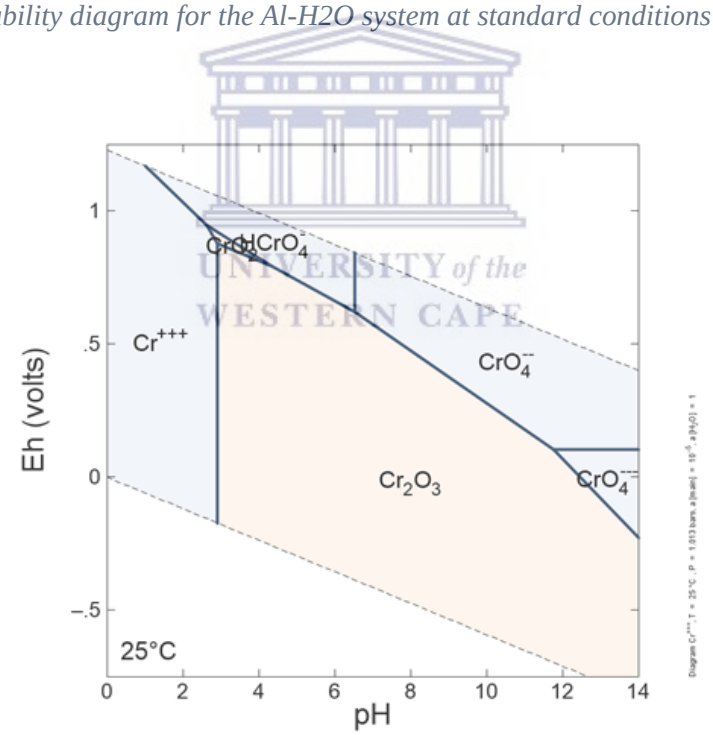

FIGURE 4.31. *Stability diagram for the Cr-H2O system at standard conditions (activity Cr = 1e^{-5}).*

UNIVERSITY of the WESTERN CAPE

https://etd.uwc.ac.za

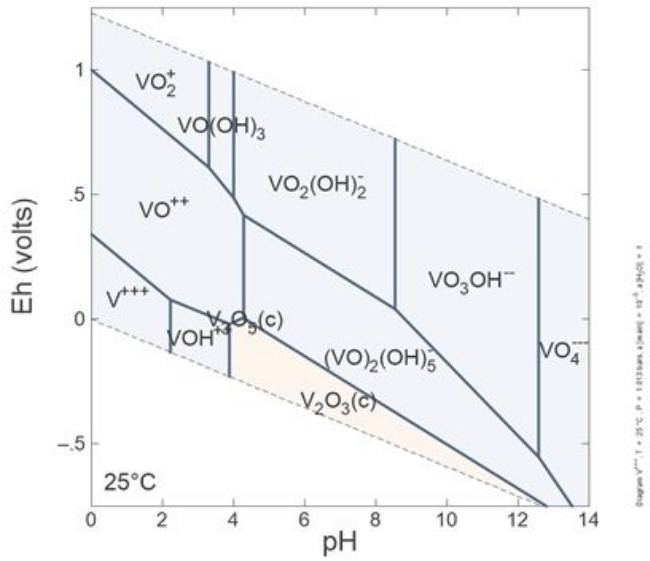

FIGURE 4.32. *Stability diagram for V at standard conditions (activity Al = 1e^{-5}).*

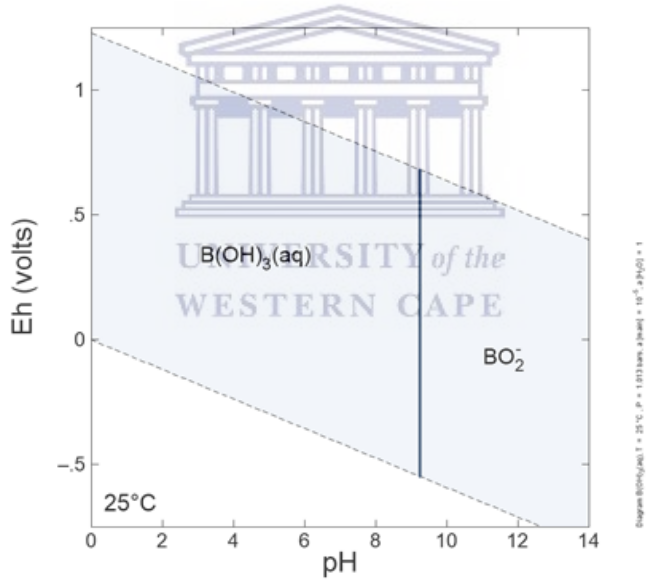

FIGURE 4.33*. Stability diagram for the B-H2O system at standard conditions (activity Al = 1e^{-5}).*

https://etd.uwc.ac.za

4.5.3 Leachate chemistry analysis

4.5.3.1 EC of AMD compared to EC of leachate

The temporal trend in EC concentrations leaching from the hydraulic conductivity testing are shown in FIGURE 4.34 and FIGURE 4.35. The EC concentrations of the leachate were routinely measured throughout the duration of the testing period and, were compared to the EC of the influent AMD. It was observed that the EC concentrations of the leachate remained lower than the EC of the AMD. The overall EC peak of the leachate measured during the testing period, was 490 mS/m for all the columns. The general EC concentration in the leachate ranged between 350 mS/m and 490 mS/m. In contrast, the T40 column exhibited higher EC values, with a peak value of 525 mS/m measured. The T40 column also exhibited the highest initial hydraulic conductivity peaking at 0.6 m/d, suggesting that the Fly Ash had limited impact on the AMD quality due to the higher flow rates during the initial stages of testing. Overall, the EC concentrations from all the columns were lower than the EC of influent AMD.

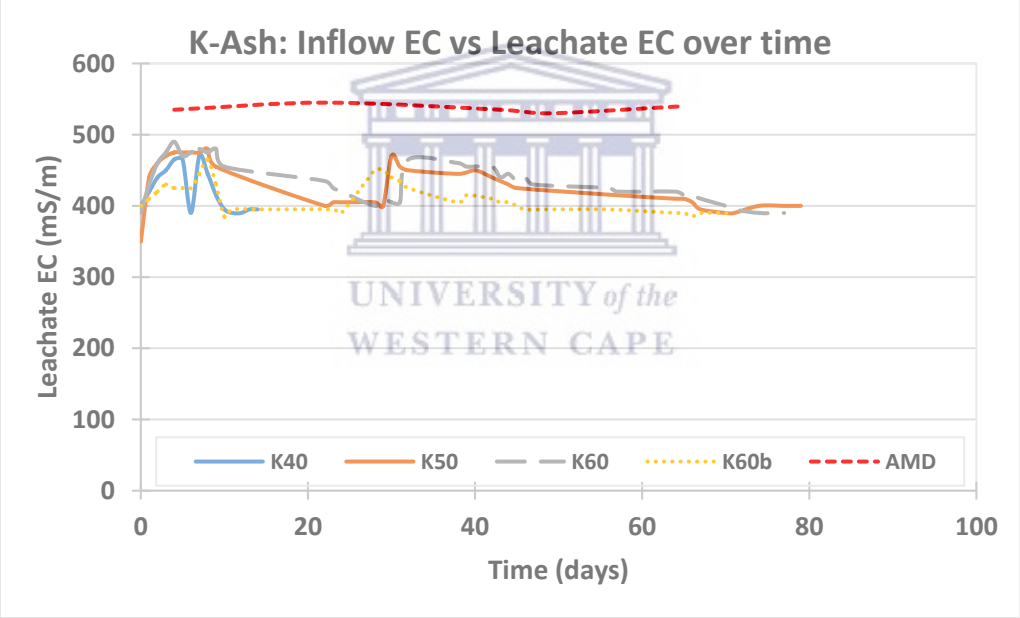

***FIGURE 4.34**. The EC concentration of influent AMD compared to the temporal trend in EC of the effluent for K-Ash.*

https://etd.uwc.ac.za

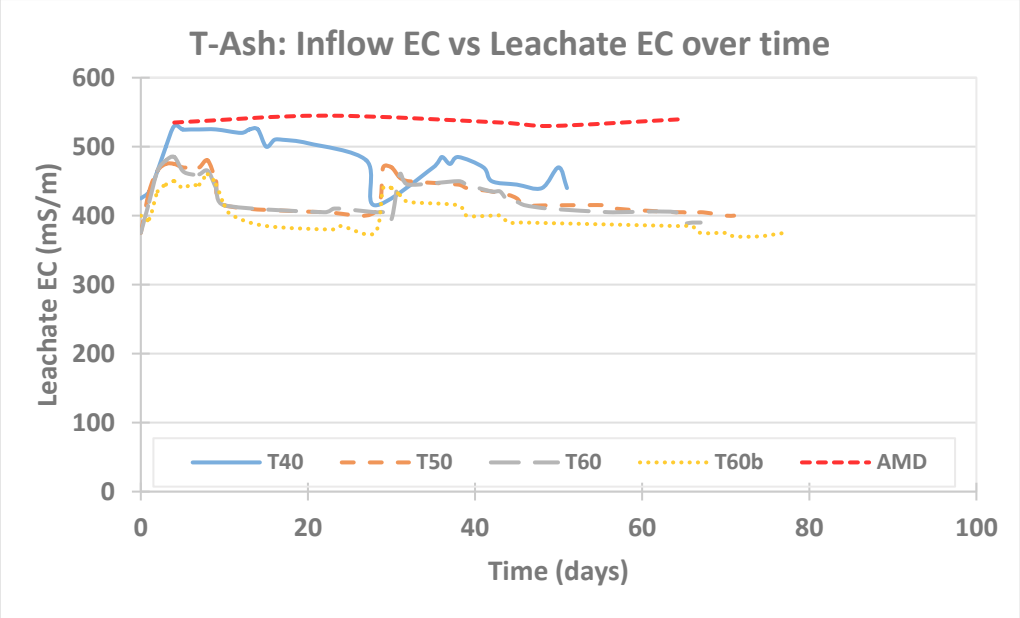

FIGURE 4.35. *The EC concentration of influent AMD compared to the temporal trend in EC of the effluent for T-Ash.*

UNIVERSITY of the
WESTERN CAPE

4.5.3.2 Comparison of AMD and Leachate Water Quality

The elemental composition of leachate water quality was compared to the AMD water quality. The target elements in the evaluation were the concentrations of Si, Al, Fe, S, Ca, Mg, Na, K, Mn and Cr. The results exhibit the change in elemental concentrations of the leachate plotted against the elemental concentrations in the influent AMD water. The leachate samples were collected and analysed routinely until the 65th day of hydraulic conductivity testing.

Si: The Si concentration in the AMD ranged between 3.87 mg/L and 4.88 mg/L throughout the duration of the leaching period. The initial leachate concentrations of Si in the effluent from the K50 and T50 columns, were measured at 0.51 mg/L and 1.68 mg/L respectively after 4 days of leaching. The Si concentration in the effluent increased and by day 8 of testing, and thereafter the Si concentration in the leachate was similar to the AMD and remained like that until testing was concluded. In contrast to the short columns, the longer K60b and T60b columns exhibited dissimilar results. The initial Si concentration in K60b and T60b leachate was 0.56 mg/L and 1.04 mg/L respectively. Thereafter, the concentrations remained significantly lower compared to the AMD concentrations. The K60b column exhibited concentrations of 10^{-1} mg/L throughout the entire leaching period, whereas, the T60b column showed concentrations of 10^{-1} mg/L until day 53 of leaching and increased to 10^{0} mg/L.

https://etd.uwc.ac.za

Overall, the longer columns exhibited Si concentrations of the leachate to remain lower compared to the AMD water Si concentrations (FIGURE 4.36).

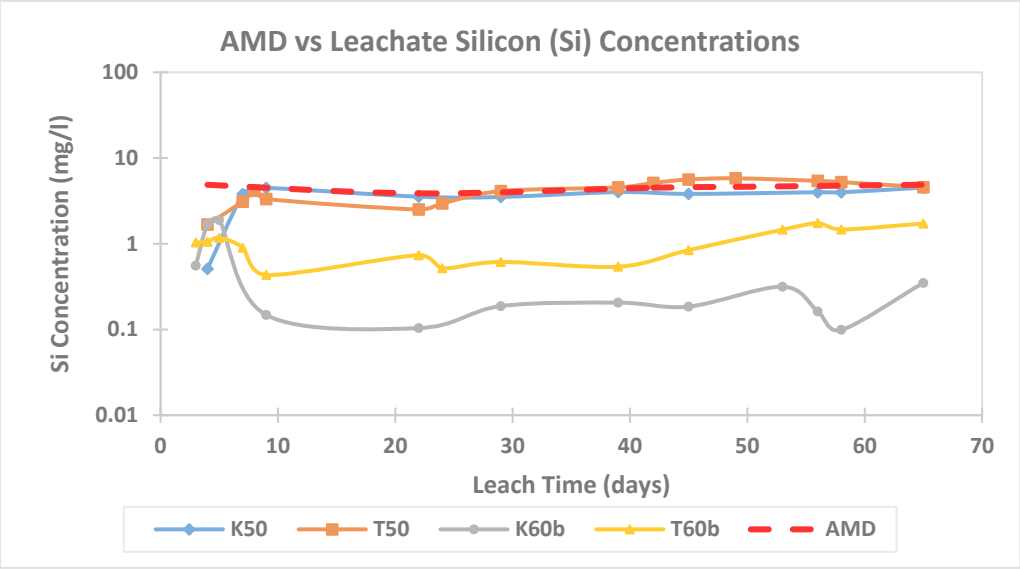

FIGURE 4.36. A comparison between influent AMD and leachate Si concentrations.

UNIVERSITY of the WESTERN CAPE

Al: The Al concentrations in the AMD ranged between 67.2 mg/l and 91.1 mg/L throughout the leaching period. The initial Al concentrations in the leachate of K50 and T50 were measured at 2.74 mg/L and 0.547 mg/L respectively. The leachate concentrations increased to 10^{+2} mg/l and remained similar to the Al concentrations in the AMD water. The leachate from the longer K60b and T60b columns showed initial Al concentrations of 1.41 mg/L and 0.76 mg/L respectively. The leachate concentrations initially decreased in K60b discharge and fluctuated between 10^{-1} mg/L and 10^{-2} mg/L until the end of testing, but, the Al concentrations in the T60b leachate decreased slightly and increased back to 10^{0} mg/L at the 45th day of leaching. Overall, the Al concentrations in the AMD were measured at 10^{+2} mg/L and the Al concentrations in the leachate remained below that throughout the leaching procedure (FIGURE 4.37).

https://etd.uwc.ac.za

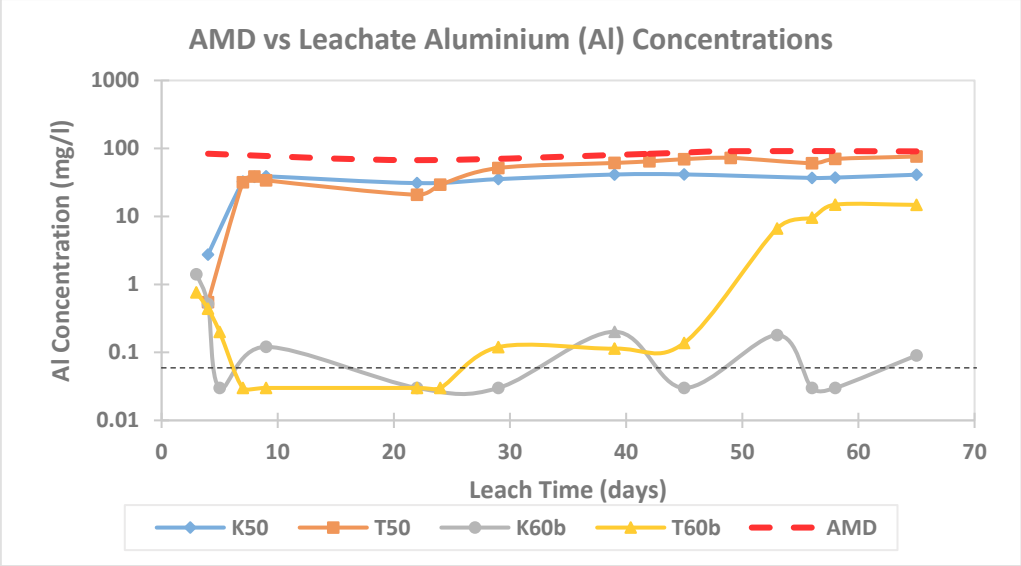

FIGURE 4.37. *A comparison between influent AMD and leachate Al concentrations.*

Fe: The Fe concentrations in the AMD ranged between 138 mg/L and 190 mg/L throughout the leaching period. The early time of Fe concentrations in the leachate of all the columns were measured at 10^{-2} mg/L. Leachate concentrations from the K60b and T60b columns persisted at 10^{-2} mg/L throughout the entire testing period. The Fe concentrations from the K50 and T50 leachates increased after 22 days of leaching, with the K50 leachate concentrations increasing to 10^{+1} mg/L and the T50 leachate concentration to 10^{0} mg/L until the testing was concluded. Overall, the Fe concentrations of the leachate from all the columns remained lower in comparison to the Fe concentrations in the influent AMD water (FIGURE 4.38). The low concentrations of Fe measured in the effluent is controlled by the fact that jarosite minerals do not flow through the fly ash and rather fill up void spaces as visually observed in FIGURE 3.6.

https://etd.uwc.ac.za

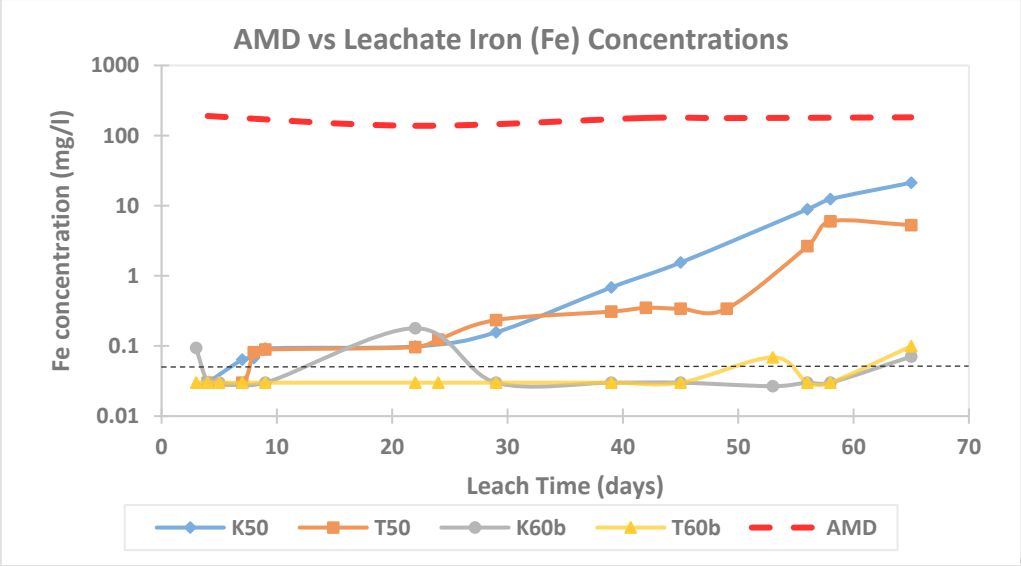

FIGURE 4.38. A comparison between influent AMD and leachate Fe concentrations.

S as SO_4: The S concentrations in the AMD and the leachate of the K50 and T50 columns, showed very similar results throughout the duration of the leaching period. The leachate concentrations from the K60b and T60b columns showed S concentrations of about 1000 mg/L less than the AMD S concentrations. The S concentrations in the K60b and T60b did increase by day 22 of leaching, however, it remained below the S concentration in the AMD for the remainder of the leaching period (FIGURE 4.39).

UNIVERSITY of the
WESTERN CAPE

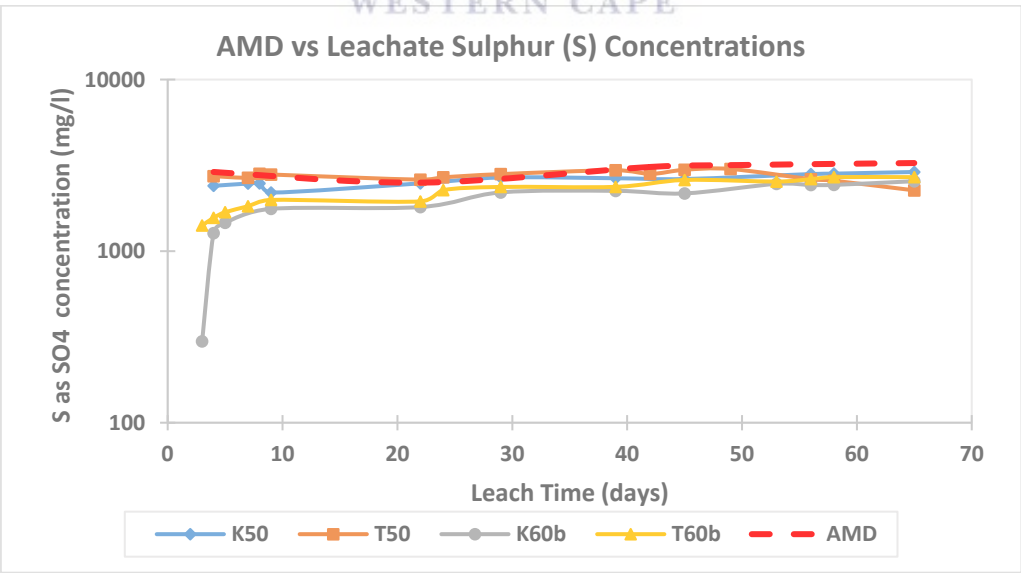

FIGURE 4.39. A comparison between influent AMD and leachate S as SO_4 concentrations.

https://etd.uwc.ac.za

Ca: The Ca concentrations in the leachate from all the columns were about 200-300 mg/L higher than the Ca concentration in the AMD water until day 35 of leaching. Thereafter, the Ca concentrations in the leachate exhibited similar concentration compared to the AMD water (FIGURE 4.40). Those initial high calcium concentrations in the effluent are due to the dissolution of $Ca(OH)_2$ that was formed during the curing phase pre-hydraulic testing. Subsequently, the AMD reacts continuously with CaO minerals of the fly ash during percolation and thus the Ca concentrations remained higher in the effluent than in the influent AMD.

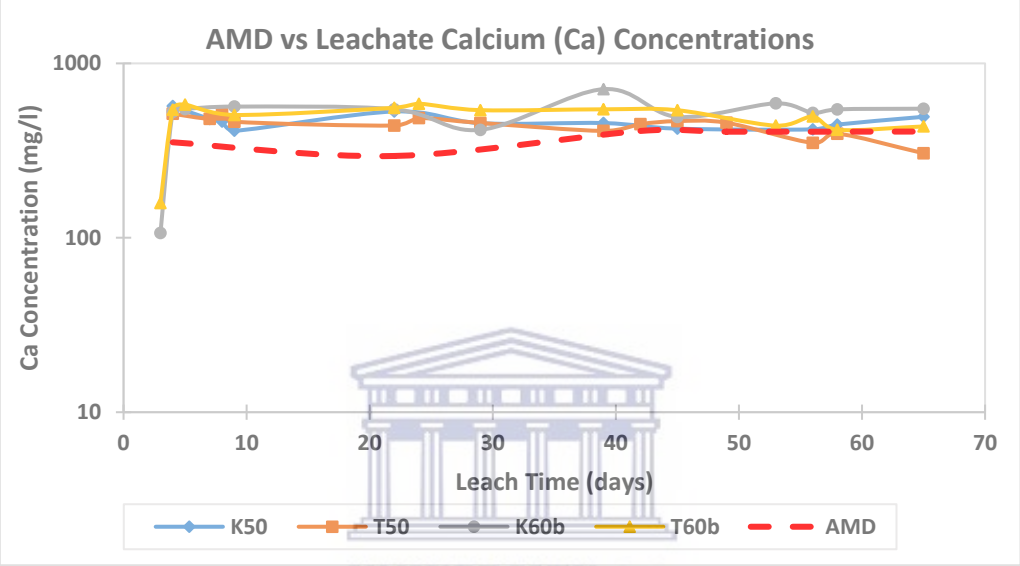

UNIVERSITY of the
WESTERN CAPE

FIGURE 4.40. A comparison between influent AMD and leachate Ca concentrations.

Mg: The early time Mg concentrations from the K60b and T60b columns were 10^0 mg/L compared to the 10^{+2} mg/L measured in the AMD water. By day 9 of testing, the leachate concentrations increased to 10^{+2} mg/L and thereafter the Mg concentrations in leachate and AMD water remained at 10^{+2} mg/L throughout the remainder of the leaching period. The Mg concentrations in the leachate were slightly higher than the AMD concentrations (FIGURE 4.41). The higher Mg concentrations in the effluent samples are a result of $Mg(OH)_2$ dissolution.

https://etd.uwc.ac.za

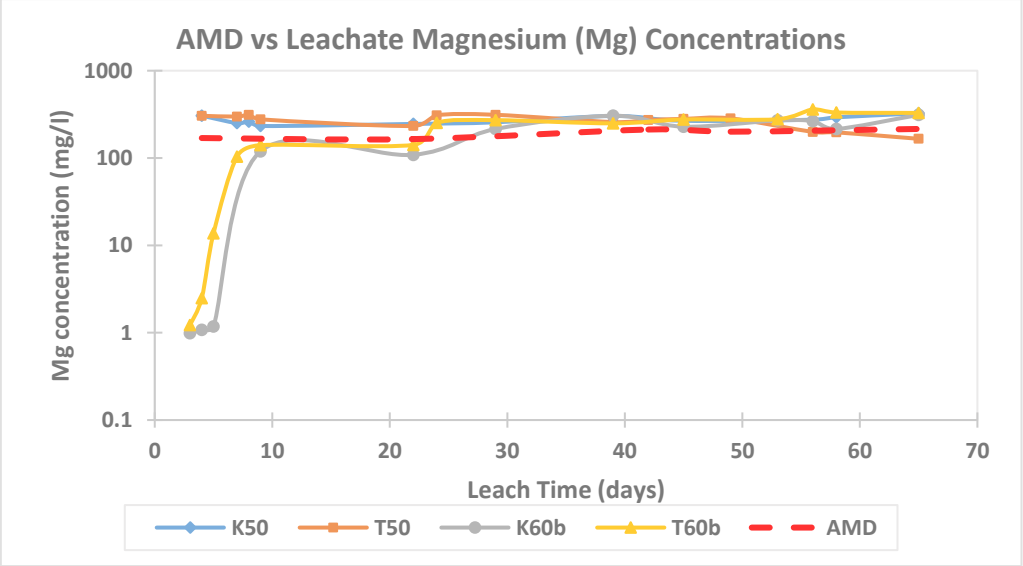

FIGURE 4.41. A comparison between influent AMD and leachate Mg concentrations.

Na: The Na concentrations from both the AMD and the leachate were measured at 10^{+1} mg/L throughout the duration of the leaching period with leachate concentrations being slightly higher than the AMD. The T60b leachate, however, exhibited an initial Na concentration of 10^{+2} mg/L but decreased and followed the same trend as the other leachates (FIGURE 4.42).

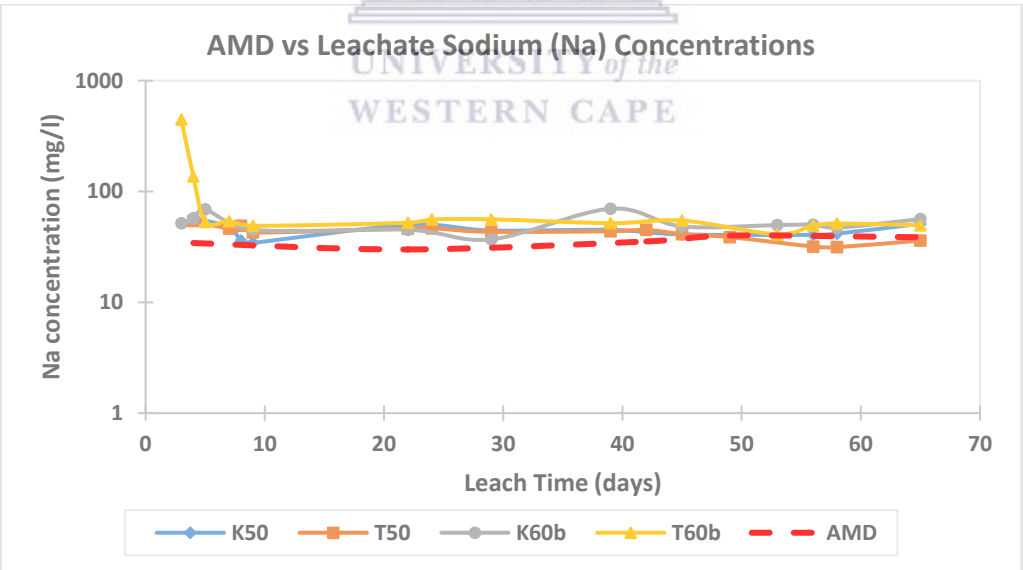

FIGURE 4.42. A comparison between influent AMD and leachate Na concentrations.

K: The K concentrations in the leachate were higher than the K concentrations in the influent AMD water, due to high K concentrations in the fly ash (FIGURE 4.43).

https://etd.uwc.ac.za

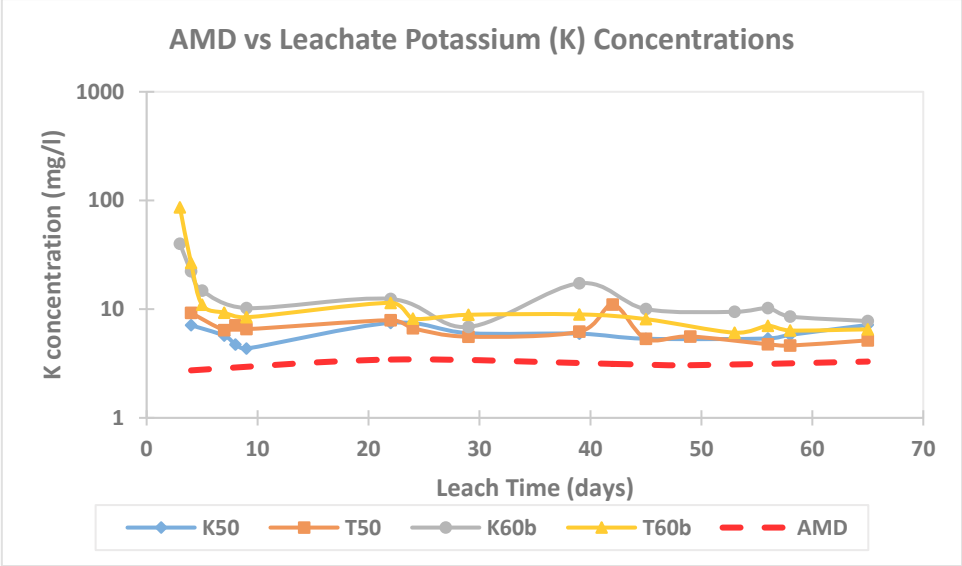

FIGURE 4.43. A comparison between influent AMD and leachate K concentrations.

Mn: The early time Mn concentrations from the K60b and T60b leachates were 10^{-1} mg/L and decreased to 10^{-2} mg/L. The T60b leachate concentrations increased to 10^{+1} mg/L by day 24 of leaching, whereas, the K60b leachate only increased to 10^{+1} mg/L by day 45 of leaching. Moreover, the K50 and T50 leachate concentrations were similar to the AMD concentration throughout the duration of the leaching period (FIGURE 4.44).

UNIVERSITY of the
WESTERN CAPE

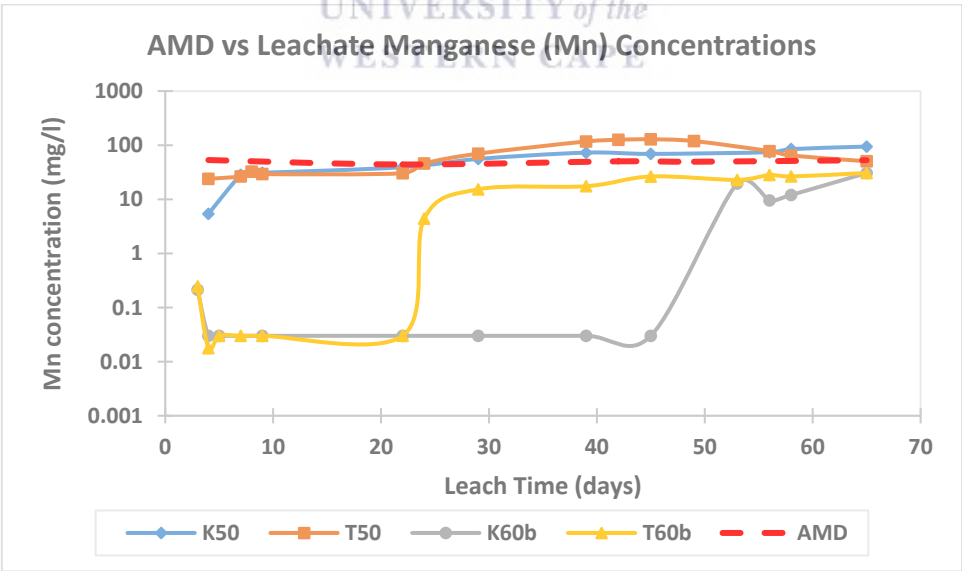

FIGURE 4.44. A comparison between influent AMD and leachate Mn concentrations.

https://etd.uwc.ac.za

Cr: The early time Cr concentrations from all the leachates were higher than the Cr concentrations of the influent AMD water. About 0.2 mg/L Cr leached through the K50 and T50 columns, whereas, 1.95 mg/L and 4.95 mg/L Cr leached from the K60b and T60b columns respectively. Though these initial high leaching concentrations of Cr occurred during the initial stages of testing, the Cr concentrations decreased in all the leachates and became negligible eventually (below detection limit of 0.01 mg/L). It appears that decreasing K provides for favourable conditions for fly ash to absorb Cr and prevent it from leaching (FIGURE 4.45).

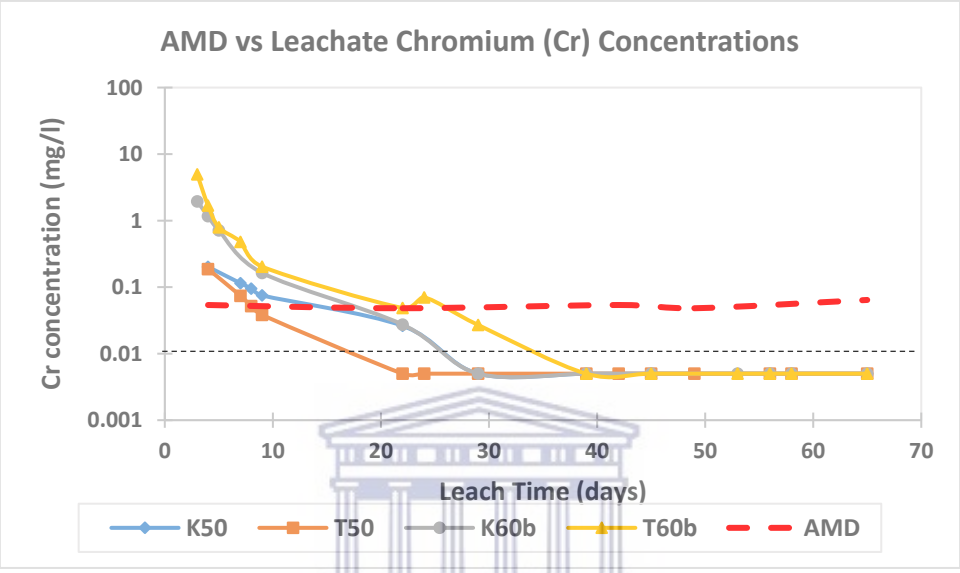

FIGURE 4.45. A comparison between influent AMD and leachate Cr concentrations.

UNIVERSITY of the
WESTERN CAPE

In retrospect, the moisture in the ash during placement, allows pozzolanic reactions to solidify the ash and lowers the K by an order of magnitude, relative to fresh ash. During leaching, the secondary mineralization of calcium rich minerals in the ash contributes to a further lowering in the K by an order of magnitude. Sulphate and Iron minerals from the AMD also played a major role in the decreasing K as it accumulates in void spaces and having a clogging effect (FIGURE 4.46). From the chemical analysis of the leachate samples, it was observed that Fe and Cr does not leach (FIGURE 4.38 and FIGURE 4.45). The alkaline nature of the ash initially neutralizes the acidic levels of AMD from inflow pH = 2.5 to an outflow pH = 11. Acidification of the outflow from pH = 11 towards a pH = 4 is observed during testing. Overall the K decreased 3 orders of magnitude from an initial 10^{-1} m/d to 10^{-3} m/d, with the Fe concentration of above 170 mg/L playing the dominating role in reducing the hydraulic conductivity under the lower pH conditions.

https://etd.uwc.ac.za

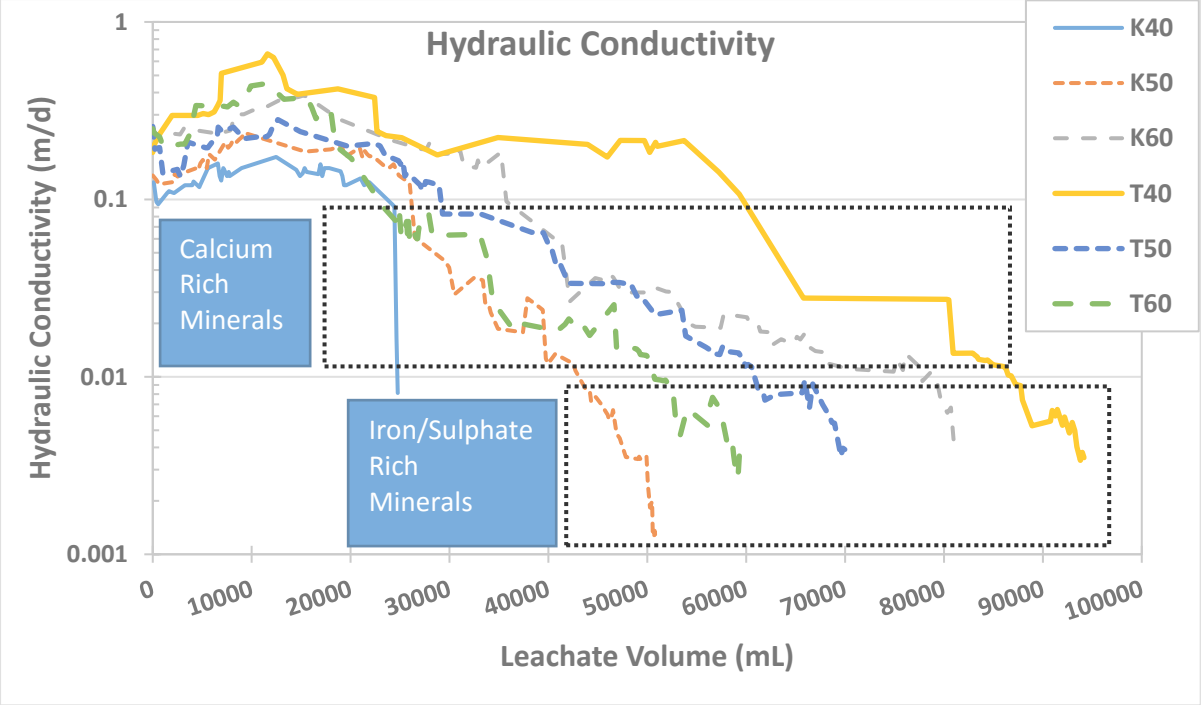

FIGURE 4.46. *The hydraulic conductivity of K-Ash and T-Ash columns*

UNIVERSITY of the WESTERN CAPE

In all columns leached with AMD solutions, Ca was the dominant cation that leached out, with sulphate being the dominant anion. The sulphate was much higher in the leachate of the AMD columns because of the higher sulphate in the inlet fluid. The Ca originates from both the lime in the ash (that neutralise the acid) and the inlet fluid. The high mineral content AMD and especially the high concentration Fe in the AMD plays an important role in the hydraulic conductivity changes over time. The $Fe(OH)_3$ in the ash dissolves at the reaction front and jarosite forms which is a stable Fe-sulphate in acidic conditions.

4.6 Conclusion

The results and discussion chapter provided knowledge and a general understanding of what might happen to the hydro-geochemical properties of fly ash once backfilled into opencast acidic mine environments.

https://etd.uwc.ac.za

5 EXPECTED MINE BACKFILL CHANGES UNDER DIFFERENT FLY ASH DISPOSAL SCENARIOS

5.1 Topographic

Historical coal mines in the Witbank area discharge AMD water to neighbouring water bodies such as pit lakes, rivers, streams and dams. This phenomenon is primarily due to the collapse of underground historical mining pillars, resulting in the formation of void spaces through which the AMD is generated and discharged into the environment. The disposal of fly ash as a monolith into old and future coal mines may aid in the stabilization of the topography of a decommissioned coal mine.

Also, when opencast coal mines are backfilled, there are usually not enough spoils to backfill the entire mining void. Therefore, pit lakes are formed due to the lack of backfill materials. It is also assumed that some settling occurs after the mine is backfilled, which may lead into some depressions forming on the surface that alters the runoff patterns of a backfilled mine. Fly ash has strengthening properties through its pozzolanic nature. Therefore, fly ash may be used to shape the topography of a mining void to alleviate negative long-term impacts (i.e. runoff) after mine closure.

5.2 Hydraulic conductivity (K) in backfill

UNIVERSITY of the
WESTERN CAPE

The backfill of opencast coal mines consists of a mixture of unmined coal spoils and loosely unconsolidated host rocks. The loosely unconsolidated host rocks consist of pyrite-rich rock types such as Shales, Sandstones and Mudstones. Due to the loosely unconsolidated materials in the backfill, voids in between the aforementioned rocks are expected to be greater than the voids between consolidated unmined host rocks. Furthermore, the large boulders of the mining spoils are backfilled in such a way that it’s dumped over the pit sides and rolls to the bottom of the pit. This means that there is no compaction of these boulders because the bulldozers doesn’t rework the bottom of the pit. Hodsgson and Krantz (1998) investigated the characteristics of opencast coal mine spoils and found that the permeability was so high that it was impossible to measure a dewatering cone of depression. The study concluded that it might have been due to the large boulders at the bottom of the pit that caused the hydraulic conductivity to be so high.

Disposing fly ash as a monolith with the backfill spoils, may be used to alter the hydraulics of specific areas of the backfill. The decreasing hydraulic conductivity properties of a fly ash

https://etd.uwc.ac.za

monolith may act as a barrier to groundwater discharge from the backfill pit into the surrounding environment. Also, the fly ash can be placed as a capping layer above the backfilled spoils, which may cause lesser amounts of infiltration into the backfill due to the pozzolanic nature of the fly ash. A capping layer may also result in the oxygen ingress into the backfill to be limited, which may cause favourable conditions for limiting AMD generation.

5.3 Water table in backfill

The water table within the backfill of opencast coalmines are generally subjected to the inflow of groundwater from the neighbouring aquifers around the backfilled area. Water from precipitation and natural runoff will also add to the water table through recharge and downward percolation processes. During the operational phase of a mine, the water table within the backfill is at the pit floor due to dewatering processes and high hydraulic conductivities (FIGURE 2.3). However, post-mine closure, the water table will recover to approximately the same height as the lowest decanting position within the backfill. The decanted water accumulates in a pit lake as shown in FIGURE 5.1 and ultimately interacts with surrounding water bodies. Naturally the water table remains at the decanting elevation and water will flow either into the pit lake or vice versa depending on the water balance between the pit lake and the surrounding water bodies (aquifers, rivers and streams). The water balance between the backfill and pit lake will cause a fluctuation in water levels and flow direction, for example, during periods of drought it is expected that the water level of the pit lake will drop below the groundwater table due to excessive evaporation, resulting in backfill discharge towards the pit lake. During the rainy season, the expected water level of the pit lake could rise higher than the backfill water table, resulting in groundwater recharge from the pit lake and potentially water discharging to nearby rivers and streams (Mpetle and Johnstone, 2018). As aforementioned and especially in the Witbank area, with a pH of 2.5, some pit lakes are highly acidic and negatively impacts on the nearby streams and rivers.

A fly ash monolith deposited at the decanting position within the backfill, may have a significant influence on how the water table in the backfill will behave. Initially, the backfill water table are expected to be at the lowest decanting position and will rise over time as a result of the decreasing hydraulic conductivity of the ash monolith. As a result, the rising water table will result in the backfilled spoils to become more saturated, and thus limiting the spoils to oxygen exposure. With limited oxygen within the backfill spoils, it will limit the generation of AMD.

https://etd.uwc.ac.za

5.4 Post Closure Coal Mine Scenarios

A few coal mining scenarios will be illustrated below and the impact it has on the environment. The scenarios that will be illustrated are:

1. A base case of the current coal mining impacts after the mine has been decommissioned
2. A scenario where fly ash are placed in the form of a monolith above the water table within the backfill of the mine
3. A scenario where a fly ash monolith are placed at the decanting point in the backfill where it intersects the water table

These scenarios illustrate how coal mines impacts on the environment and also depicts how fly ash can be used in an attempt to alleviate some of these negative impacts.

5.4.1 Base Case: Coal mine backfill without fly ash

A schematic scenario of the current post-closure coal mining activities is depicted in FIGURE 5.1. AMD is generated in coal mines due to oxidizing conditions in the unsaturated pyrite rich backfill spoils. Moreover, the backfill spoils consists of unconsolidated host rocks and are characterised with heterogeneous rock sizes, causing large void spaces between these rocks. These void spaces cause the hydraulic conductivity to be relatively high and consequently recharge from precipitation and surface runoff, together with the recharge from neighbouring aquifers flushes through the backfill and discharges at the lowest point which is the pit lake as shown in FIGURE 5.1. This current mining practice causes AMD to discharge from these mining voids and impacts negatively on the neighbouring water bodies due to the abundance of sulphates (above 2000 mg/L) and Fe (above 150 mg/L) concentration in AMD water and also the acidic nature with pH concentrations measured at pH = 2.5.

https://etd.uwc.ac.za

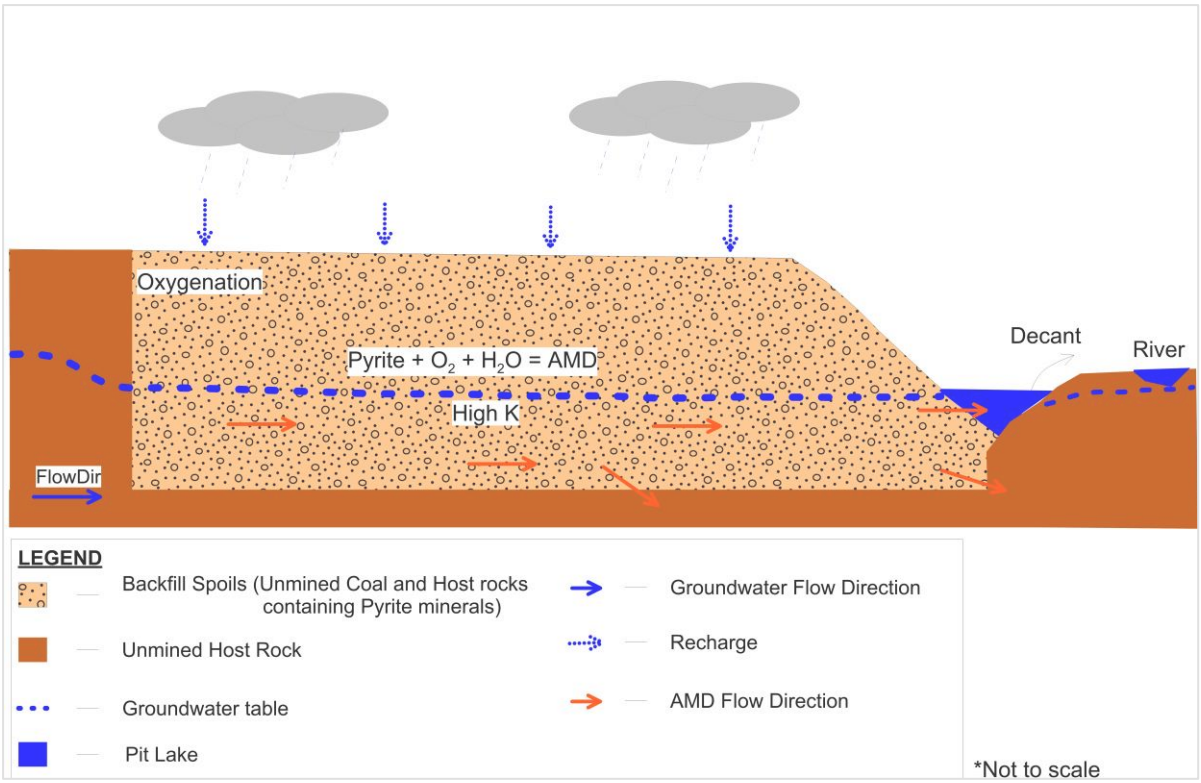

FIGURE 5.1. Conceptual depiction of an opencast coal mine backfilled without fly ash.

5.4.2 Fly ash monolith above water table

The hydraulic properties of a fly ash monolith deposited above the water table will potentially behave similarly to the hydraulic behaviour of ash on the existing fly ash dumps. The monolith will be subjected to natural recharge from rainfall and it is not expected to come into contact with the water table. The water from recharge will leach through the monolithic fly ash and add to the water table and therefore mix with AMD in the backfill pit. Thus, the water percolating through the fly ash monolith are expected to have a very alkaline nature and therefor have a buffering impact on the acidic nature of the AMD.

The hydraulic conductivity of the fly ash monolith is expected to decrease over time as the fly ash will set and harden due to its pozzolanic nature and the secondary mineralization of gypsum. Initial hydraulic conductivity ranges are expected to be between 0.3 m/d - 0.9 m/d and they will decrease over time towards 0.02 m/d – 0.33 m/d after 20 – 30 years (FIGURE 5.2). Therefore, the fly ash monolith may cause less water to flow through the backfill and eventually result in reduced volumes of discharge into the pit lake.

https://etd.uwc.ac.za

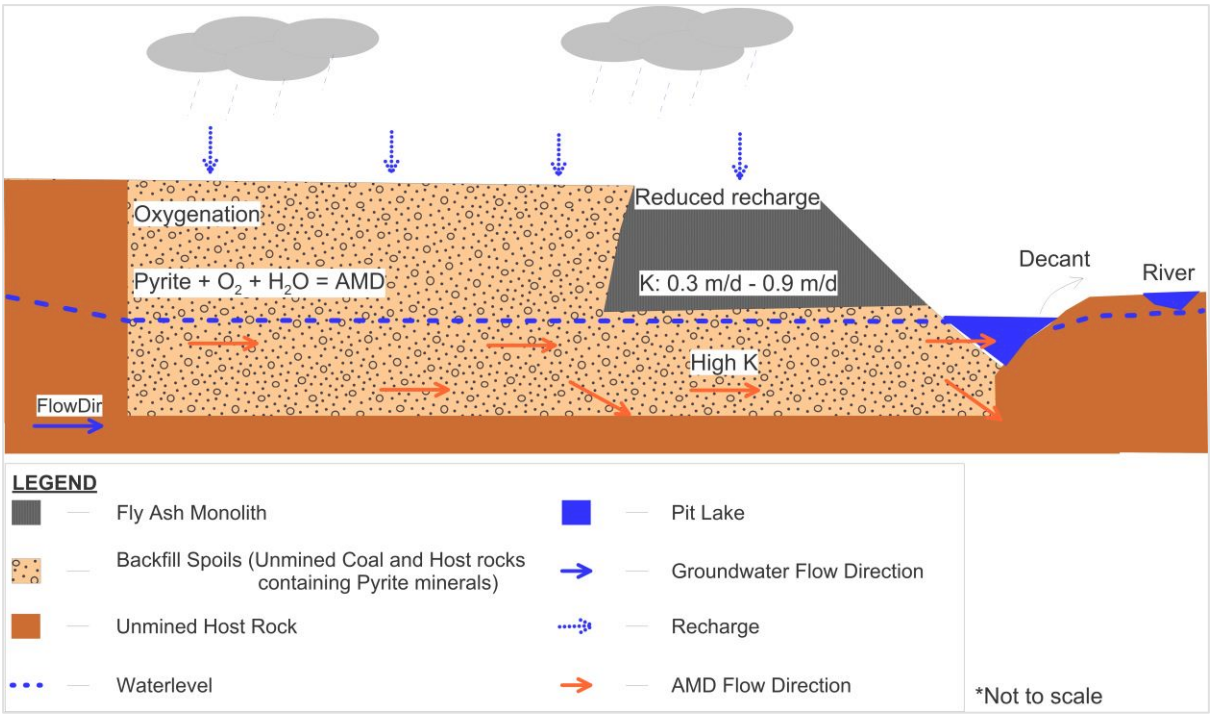

FIGURE 5.2. *Conceptual depiction of an opencast coal mine backfilled with fly ash above the water table.*

UNIVERSITY of the
WESTERN CAPE

5.4.3 Fly ash monolith below water table

The hydraulic properties of fly ash deposited below the water table and in contact with AMD are expected to behave similarly to the hydraulic conductivity measured in the laboratory column experiments. The chemical elements in the AMD will react with the fly ash and as a result will influence the hydraulic conductivity of fly ash to decrease over time. However, the rate at which the hydraulic conductivity of fly ash will decrease over time is predominantly dependent on the chemical composition of AMD, as well as the mineral composition of the fly ash. For example, high concentrations of Fe in the AMD will cause the fly ash to become nearly impermeable due to the chemical evidence that Fe does not flow through fly ash but rather has a clogging effect on it.

The water table in the backfill will be significantly influenced by a fly ash monolith as shown in FIGURE 5.3. Initially the water table will be expected to be at the lowest decant elevation in the backfill area, however, with the decreasing hydraulic properties of fly ash over time it is expected that flow through will be limited and cause the water table to rise instead. If the water table rise over time, it means that the pyrite minerals from the back fill spoils will be limited to oxygen exposure.

https://etd.uwc.ac.za

In retrospect, the geochemistry data showed that the initial water quality of the leachate proved to be better than the influent AMD water quality. By the time that some of the chemical elements begin to leach out, the hydraulic conductivity is so low that the volumes of the discharge are almost negligible and highly manageable. It is expected that a fly ash monolith below the water table would hydraulically and geochemically behave and show similar results to the laboratory column testing.

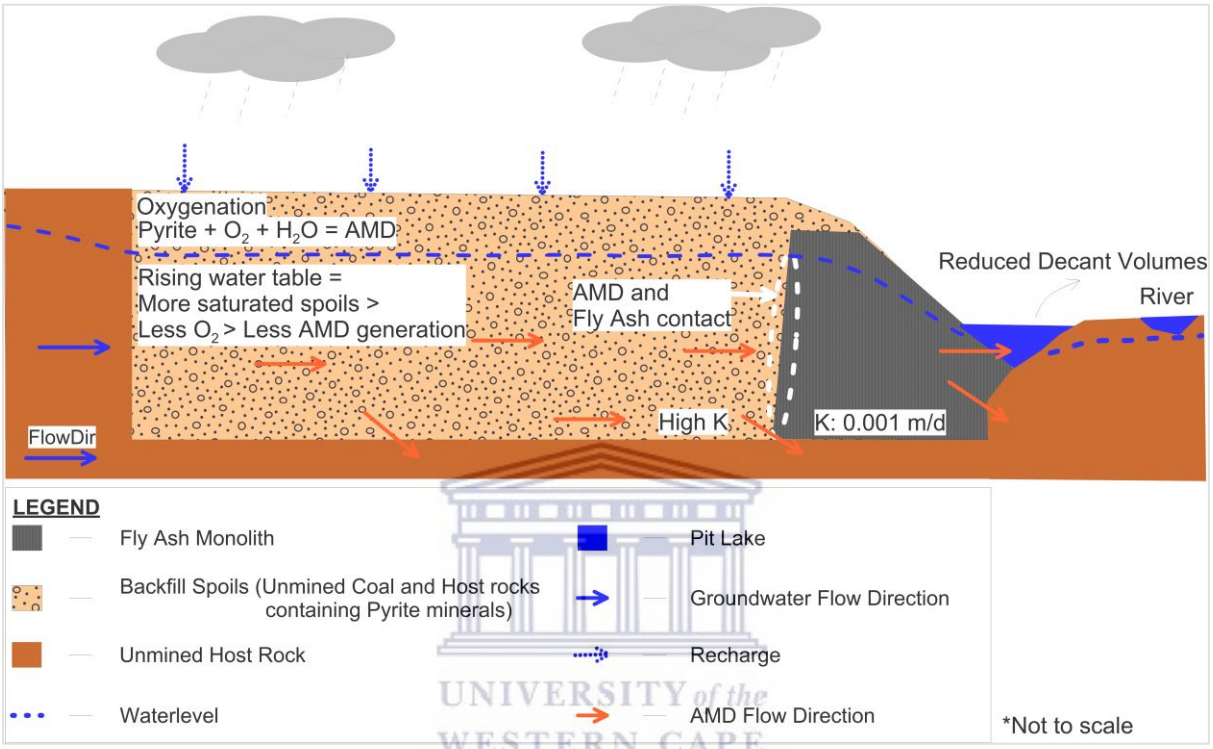

UNIVERSITY of the
WESTERN CAPE

FIGURE 5.3. Conceptual depiction of an opencast coal mine backfilled with fly ash below the water table.

5.5 Conclusion

Chapter 5 provided both a conceptual and visual understanding of what is generally expected to happen if fly ash is backfilled as a monolith into opencast coal mines.

https://etd.uwc.ac.za

6 CONCLUSIONS AND RECOMMENDATIONS

6.1 Conclusion

The field test results showed that the hydraulic conductivity of ash decreases over time, due to the natural pozzolanic properties of the ash together with the secondary mineralisation of calcium rich minerals. Water from precipitation and irrigation reacts with the CaO minerals in the ash, causing the ash to set and solidify. The hydraulic conductivity at the Kendal power station ash dump ranged from 0.49 m/d – 0.79 m/d (freshly dumped ash) towards 0.20 m/d – 0.29 m/d (20 year old ash). The ash at the Tutuka power station ash dump exhibited hydraulic conductivity ranging from 0.33 m/d – 0.46 m/d (freshly dumped ash) towards 0.25 m/d – 0.28 m/d (30 year old ash).

The laboratory hydraulic conductivity of fly ash also showed decreasing trends over time. The hydraulic conductivity overall decreased from initial K values of 10^{-1} m/d towards 10^{-3} m/d. These hydraulic conductivity changes over time, are initially subjected to the pozzolanic bindings that formed during the curing phase of the experiment. During the experiment, the secondary mineralization of calcium rich minerals causes these minerals to deposit in the flow paths. Lastly, the Fe (>150 mg/L) and SO_4 (>2000 mg/L) concentrations in the AMD together with the low pH = 2.5 causes a clogging effect at the front face of the fly ash, which ultimately causes the hydraulic conductivity to decrease towards 10^{-3} m/d. One of the columns completely clogged up while flow through in the other columns was restricted, which indicates a possibility of the fly ash to become an impermeable hydraulic barrier.

UNIVERSITY of the
WESTERN CAPE

From the geochemical leach test results, it was observed that most of the leachate water was of a better quality than the influent AMD water quality. The outflow pH was higher than the pH of the outflow AMD. Overall, the discharge EC reduced compared to EC of inflow AMD, although Na and K in the leachate exhibited higher concentrations compared to the AMD inflow concentrations. However, most of the other chemical elements such as Fe, Si, Al, Mn, Cr and SO_4 showed significantly lower concentrations in the discharge when compared to the inflow AMD concentrations.

Based on this research, an ash monolith deposited at the decanting position of an opencast mine void, may have a positive influence, including:

https://etd.uwc.ac.za

1. The water table in the backfill is expected to rise to the top of the monolith over time, due to decreasing hydraulic conductivity of the ash, reducing AMD generation because of reduced oxygen exposure of the waste rocks in the backfill.
2. Increased pH and the associated reduction in concentrations of Fe, Si, Al, Mn, Cr and SO_4 of the AMD water that do percolate through the ash monolith.
3. The topography, hydraulic conductivity and the water table within the backfill can be altered to manage the decant position, elevation and improve water quality from the ash monolith backfilled coal mines.

6.2 Recommendations

A field scale case study using ash backfilling into an opencast coal mine void on a controlled field site is required. The fly ash should be disposed of as a monolith into the backfill of the opencast mining void. In accordance to the hydraulic conductivity and chemical leachate results, it is recommended that the monolith should be sufficiently thick to allow for the following processes:

- Allow adequate travel time for the AMD through the monolith to allow for neutralization of the acidic water when the mine starts decanting. The water and salt balances must be determined to evaluate the role of any preferential flow paths and blinding effects of ash backfill at field scale.
- To allow for the secondary mineralization and deposition of calcium rich minerals within the ash monolith. It was evident that its effect is more pronounced in the longer laboratory columns compared to the shorter ones. The secondary mineralization will reduce the flow by one order of magnitude, reducing flow through the ash monolith and potentially prevent ash from reaching its full neutralization capacity.
- To allow for the jarosite ($KFe^{3+}_3(OH)_6(SO_4)_2$) minerals to accumulate at the front face of the monolith to effectively reduce flow-through, while allowing for the neutralisation of AMD through the monolith. The Fe (>150 mg/L) and SO_4 (>2000 mg/l) concentrations in the AMD with low pH (pH = 2.5) at the front face is important for jarosite deposition. The jarosite deposition will reduce the hydraulic conductivity by two orders of magnitude, thus reducing flow volumes further. Sufficient thickness is expected to make acidification of entire monolith impossible.

The thickness of the ash monolith would have to be determined based on measured or predicted decant volumes and expected decant water quality at a trial site. Monitoring must

UNIVERSITY of the WESTERN CAPE
https://etd.uwc.ac.za

be included to investigate the probability of potential impacts after ash monolith backfilling.

…….

7 REFERENCES

Akinyemi S, Akinlua A, Gitari W, Akinyeye, RO and Petrik LF (2013) Chemical Partitioning and Mobility of Trace Elements in Dry Disposed Weathered Ash Conditioned with high-Saline Effluents. Coal Combust Gasiffication Products 5:57–72. doi: 10.4177/CCGP-D-13-00002.1

Alhomair SA, Gorakhki MH and Bareither CA (2017) Hydraulic Conductivity of Fly Ash-Amended Mine Tailings. Colorado State University. doi:10.1007/s10706-016-0101-z

AQUAREAD Water Monitoring Instruments (2019). In: https://www.aquaread.com/need-help/what-are-you-measuring/ec/ Accessed: 05 June 2019.

ASTM D5084-16a (2016) Standard Test Methods for Measurement of Hydraulic Conductivity of Saturated Porous Materials Using a Flexible Wall Permeameter. West Conshohocken, PA

Bell FG, Bullock SET, Hälbich TFJ and Lindsay P (2001) Environmental impacts associated with an abandoned mine in the Witbank Coalfield, South Africa. *International Journal Coal Geology* 45:195–216. doi: 10.1016/S0166-5162(00)00033-1

Bowden LI, Jarvis A, Orme P, Moustafa M and Younger PL (2000) Construction of a novel Permeable Reactive Barrier (PRB) at Shilbottle , Northumberland , UK : engineering design considerations and preliminary performance assessment. In: 9th INTERNATIONAL MINE WATER CONGRESS.

BS EN 197-1 (2011) Cement Part 1: Composition, Specifications and Conformity Criteria for Common Cements. Br Stand 50. doi: doi:10.3403/30205527U

Campbell AE (1999) Chemical, physical and mineralogical properties associated with the hardening of some South African fly ashes. University of Cape Town. doi: 10.1088/1751-8113/44/8/085201

Chelin MJ (2000) An assessment of water management issues facing the coal minning industry

UNIVERSITY of the WESTERN CAPE

https://etd.uwc.ac.za

of the Witbank and Middelburg Dam catchments. University of Pretoria

Cogho VE and van Niekerk AM (2009) Optimum Coal Mine Water Reclamation Project. In: International Mine Water Conference. pp 130–140

Daniels W, Stewart B, Haering K and Zipper C (2002) The potential for beneficial reuse of coal fly ash in southwest Virginia mining environments. Virginia Coop Ext

DEA (Department of Environmental Affairs) (2009) Development of a Revised Waste Classification System for South Africa

Ecology (2003) An Assessment of Laboratory Leaching Tests for Predicting the Impacts of Fill Material on Ground Water and Surface Water Quality --*A Report to the Legislature,* Washington Sate, Department of Ecology

Eskom (2017) Ash management in eskom. In: www.eskom.co.za. June 2018

Fetter CW (2001) Applied Hydrogeology, 4th Edition. University of Wisconsin - Oshkosh

Fisher GL, Prentice BA, Sllberman D, Ondov JM, Bierman AH, Ragainl RC and McFarland R (1978) Physical and Morphological Studies of Size-Classified Coal Fly Ash. *Environment Sciience Technology 12:447–45*1. doi: 10.1021/es60140a008

Fox JM (2017) Fly Ash Classification – Old and New Ideas. In: *World of Coal Ash (WOCA) Conference in Lexington*, KY - May 9-11, 2017. pp 1–19

Geldenhuis S and Bell FG (1998) Acid mine drainage at a coal mine in the eastern Transvaal, South Africa. *Environmental Geology 34:234–242*. doi: 10.1007/s002540050275

Hodgson FDI and Krantz RM (1998) Groundwater Quality Deterioration in the Olifants River Catchment Above the Loskop Dam With Specialised Investigation in the Witbank

Hung PA and Hai NX (2014) Mineral composition and properties of modified fly ash. *ARPN Journal of Agriculture and Biological Science 9:51–54*

Kostas K, Georgios B and Ioannis P (2000) Hydraulic performance of laboratory PRBs for the decontamination of acidic mine waters. *9th International Mine Water Congress 347–354*

Kruseman GP, and de Ridder NA (1994) Analysis and evaluation of pumping test data

Kutchko BG and Kim AG (2006) Fly ash characterization by SEM-EDS. *Fuel 85:2537–2544*. doi: 10.1016/j.fuel.2006.05.016

UNIVERSITY of the WESTERN CAPE

https://etd.uwc.ac.za

Lupankwa K, Naicker K, Bezuidenhout N and Ochieng L (2008) Contaminant Source-Term Model Development for a Backfilled Opencast Coal Mine in the Karoo Basin

Mahlaba JS, Kearsley EP and Kruger RA (2011) Effect of fly ash characteristics on the behaviour of pastes prepared under varied brine conditions. *Minerals Engineering 24:923–929*. doi: 10.1016/j.mineng.2011.04.009

McCarthy TS (2011) The impact of acid mine drainage in South Africa. *South African Journal of Science* 107:1–7. doi: 10.4102/sajs.v107i5/6.712

Minerals Council South Africa (2018) Facts and Figures 2017 Contents

Moghal AAB (2013) Geotechnical and physico-chemical characterization of low lime fly ashes. *Advances in Materials Science and Engineering 2013:11*. doi: 10.1155/2013/674306

Mpetle M and Johnstone A (2018) The Water Balance of South African Coal Mines Pit Lakes. In: *11th ICARD | IMWA | MWD Conference* – "Risk to Opportunity" water. pp 679–684

Muchingami I (2013) Non-invasive Characterization of Unsaturated Zone Transport in Dry Coal Ash Dumps: A Case Study of Tutuka, South Africa. A Thesis Submitted in fulfillment of the requirements for the degree of Master of Science. The University of the Western Cape

UNIVERSITY of the
WESTERN CAPE

Murray J, Kirschbaum A, Dold B, Guimaraes EM and Miner EP (2014) Jarosite versus Soluble Iron-Sulfate Formation and Their Role in Acid Mine Drainage Formation at the Pan de Azúcar Mine Tailings (Zn-Pb-Ag), NW Argentina. *Minerals 4:477–502*. doi: 10.3390/min4020477

Nhan CT, Graydon JW and Kirk DW (1996) Utilizing coal fly ash as a landfill barrier material. *Waste Management 16:587–595*. doi: 10.1016/S0956-053X(96)00108-0

Norton PJ and Associates PJN (1995) The Impact of Mine Closures on Ground Water and the Environment : A UK Lesson for all Countries. 85–91

October GA (2011) Development of a Conceptual Model for Ash Dump System Using Hydraulic and Tracer Test Techniques. A Thesis Submitted in fulfillment of the requirements for the degree of Master of Science. The University of the Western Cape

Prasad B and Mondal KK (2008) Heavy metals leaching in Indian fly ash. *Journal of*

https://etd.uwc.ac.za

Environmental Science and Engineering 50:127–132

Reynolds-Clausen K and Singh N (2016) Eskom's revised coal ash strategy and implementation progress

Sivapullaiah PV and Lakshmikantha H (2004) Properties of fly ash as hydraulic barrier. *Soil Sediment Contamination 13:489–504*. doi: 10.1080/10588330490500437

Stats SA (2008) South Africa Energy Statistics. United Nations Off Stat South Africa 1–16

Tastan EO, Edil TB, Benson CH and Aydilek AH (2011) Stabilization of Organic Soils Using Fly Ash. *Journal of Geotechnical and Geoenvironmental Engineering 137:819–833*. doi: 10.1061/(ASCE)GT.1943-5606.0000502.

USEPA (2012) Constituents in Solid Materials Using an Up-Flow Percolation Column. pp 1–28

USEPA (2014) Leaching Test Relationships, Laboratory-to-Field Comparisons and Recommendations for Leaching Evaluation using the Leaching Environmental Assessment Framework

Vadapalli VRK, Petrik LF, Fester V, Slatter P and Sery G (2007) Effect of fly ash particle size on its capacity to neutralize acid mine drainage and influence on the rheological behavior of the residual solids. *World of Coal Ash (WOCA), May 7-10, 2007*, Northern Kentucky, USA

Younger PL (2007) Groundwater in the Environment: An Introduction. HSBC Chair in Environmental Technologies. Institute for Research on Environment and Sustainability. University of Newcastle Newcastle, Upon Tyne United, United Kingdom

Younger PL and Wolkersdorfer C (2003) Mining Impacts on the Fresh Water Environment : Technical and Managerial Guidelines for Catchment Scale Management

Zarga Y, Ben Boubaker H, Ghaffour N and Elfil H (2013) Study of calcium carbonate and sulfate co-precipitation. *Chemical Engineering Science 96:33–41*. doi: 10.1016/j.ces.2013.03.028

Zhang X (2014) Management of coal combustion wastes. IEA Clean Coal Centre

UNIVERSITY of the
WESTERN CAPE

https://etd.uwc.ac.za

APPENDIX A: Darcy column test data.

Column Name	**K40**				
Length	20				
Cross-sectional Area (m2)	0.006362				
Hydraulic Gradient	2.5				
Time (Days)	**Total Volume (mL)**	**Q (m3/d)**	**K (m/d)**	**pH**	**EC (mS/m)**
1	100	0.001991	0.125164	10.92	400
	370	0.001541	0.096902	11.91	420
	550	0.001493	0.093873	12.03	415
2	1450	0.001727	0.108576	11.17	445
	1650	0.00177	0.111257	11.03	440
	1870	0.001748	0.109901	10.9	440
	2150	0.001727	0.108576	10.88	440
3	3250	0.001911	0.120158	10.45	440
	3330	0.001911	0.120158	10.21	450
	3410	0.001911	0.120158	10.44	455
	3990	0.001911	0.120158	10.4	450
	4130	0.002007	0.126166	10.34	460
	4708	0.001863	0.117154	10.5	445
	4780	0.001911	0.120158	10.48	460
	5580	0.002389	0.150197	10.47	455
4	6580	0.002537	0.159502	10.48	460
	6760	0.00215	0.135178	10.38	465
	6930	0.002031	0.127668	10.34	475
	7130	0.002389	0.150197	10.29	470
	7320	0.002269	0.142687	10.22	465
	7500	0.00215	0.135178	10.12	455
	7690	0.002269	0.142687	10.23	445
	7780	0.00215	0.135178	9.73	470
5	8980	0.002389	0.150197	9.72	460
6	12470	0.00276	0.173504	6.65	465
7	14520	0.002332	0.146621	6.01	390
	14880	0.00215	0.135178	5.65	470
	15160	0.00223	0.140184	5.14	465
	15360	0.002389	0.150197	5.2	455
	15550	0.002269	0.142687	5.34	450
8	16750	0.002205	0.138644	5.23	450
	16960	0.002508	0.157707	5.27	445
	17140	0.00215	0.135178	5.2	440
	17340	0.002389	0.150197	5.26	435
	17540	0.002389	0.150197	5.1	430
	17840	0.002389	0.150197	5	425
9	18990	0.002289	0.143939	4.93	420

https://etd.uwc.ac.za

	19170	0.00215	0.135178	4.68	415
	19330	0.001911	0.120158	4.88	410
	19560	0.001911	0.120158	4.96	410
	19970	0.001959	0.123162	4.92	405
10	21020	0.00209	0.131423	4.87	400
	21380	0.001911	0.120158	4.85	395
11	21900	0.001991	0.125164	4.83	390
12	24200	0.001493	0.093873	4.9	390
13	24440	0.001448	0.091029	4.92	390
14	24640	0.000263	0.016535	4.9	395
15	24770	0.000129	0.008111	4.92	395

Column Name	**K50**				
Length (m)	0.2				
Cross-sectional Area (m2)	0.006362				
Hydraulic Gradient	2.5				
Time (days)	**Total Volume (mL)**	**Q (m3/d)**	**K (m/d)**	**pH**	**EC (mS/m)**
1	370	0.002172	0.136543	11.38	350
	630	0.002048	0.128741	12.47	440
	1970	0.001937	0.121782	11.42	450
2	2220	0.001991	0.125164	11.39	450
	2520	0.002205	0.138644	11.25	460
	2900	0.002139	0.134505	11.21	455
	4420	0.002222	0.139684	11.11	455
3	4570	0.002389	0.150197	10.4	460
	4820	0.002317	0.145691	10.18	470
	5070	0.002542	0.15981	10.11	465
	5274	0.002652	0.166719	10.19	465
	5474	0.002508	0.157707	10.26	470
	5679	0.002389	0.150197	10.26	465
	6279	0.002867	0.180237	10.22	470
	7329	0.002664	0.167477	10.21	470
4	7619	0.003344	0.210276	10.17	480
	7879	0.003106	0.195257	10.12	475
	8149	0.003225	0.202766	10.02	485
	8459	0.003464	0.217786	9.93	465
	8739	0.003344	0.210276	9.84	470
	9039	0.003464	0.217786	9.75	470
	9189	0.003583	0.225296	9.72	475
	11149	0.003782	0.237812	8.83	480
5	15399	0.003501	0.220117	5	480
6	17999	0.002958	0.185959	4.94	475
7	18509	0.003046	0.191502	4.83	475

UNIVERSITY of the
WESTERN CAPE

https://etd.uwc.ac.za

	18899	0.003106	0.195257	4.81	475
	19169	0.003225	0.202766	4.8	475
	19429	0.003106	0.195257	4.88	480
	20929	0.002756	0.173305	4.87	480
8	21189	0.003106	0.195257	4.93	475
	21419	0.002747	0.172727	4.88	480
	21669	0.002986	0.187747	4.9	475
	21909	0.002867	0.180237	4.89	470
	22259	0.002787	0.17523	4.73	475
	23659	0.002787	0.17523	4.96	465
9	23859	0.002389	0.150197	4.76	460
	24049	0.002389	0.150197	4.82	455
	24354	0.002429	0.152701	4.89	445
	24879	0.002508	0.157707	4.64	440
	25969	0.00217	0.136429	4.8	435
	26509	0.001964	0.123496	4.83	425
22	29519	0.000968	0.060891	4.8	420
23	29969	0.000717	0.045059	4.79	400
24	30489	0.000657	0.041339	4.83	405
28	32489	0.000462	0.02907	4.81	405
29	33129	0.000576	0.036192	4.82	405
	33379	0.000564	0.03548	4.99	400
30	33609	0.000556	0.03493	4.83	385
	33929	0.000417	0.026197	4.83	470
31	34169	0.000414	0.026046	4.91	460
32	34899	0.000366	0.022989	4.93	455
38	37429	0.000297	0.018658	4.91	450
40	37879	0.000283	0.01781	4.68	445
42	38979	0.000441	0.027729	4.65	450
43	39429	0.000397	0.024964	4.25	440
44	39739	0.000379	0.023841	4.32	435
45	39959	0.000202	0.012693	4.4	430
	40699	0.000188	0.011842	4.37	425
	42519	0.000214	0.013471	4.32	420
57	42729	0.000189	0.011858	3.49	415
64	43899	0.000173	0.010858	3.41	415
65	44079	0.000131	0.008268	3.54	410
66	44209	0.000132	0.008306	3.51	410
67	44329	0.00013	0.008156	3.5	405
70	44729	0.000116	0.007268	3.49	395
71	44894	0.000124	0.007769	3.5	390
74	45339	0.00012	0.007573	3.52	390
77	45809	0.000111	0.007008	3.47	400
79	46009	0.000101	0.006346	3.41	400

UNIVERSITY of the
WESTERN CAPE

https://etd.uwc.ac.za

80	46099	9.7E-05	0.006097	3.41	400
81	46199	9.25E-05	0.005818	3.35	
82	46349	9.24E-05	0.005807	3.31	
84	46539	9.16E-05	0.005758	3.2	
87	46889	0.000103	0.006488	3.25	
91	47219	7.62E-05	0.004794	3.14	
101	47839	7.16E-05	0.004504	2.86	
121	49059	5.62E-05	0.003534		
123	49169	5.47E-05	0.003442		
126	49339	5.64E-05	0.003546		
128	49469	5.43E-05	0.003414		
133	49919	5.49E-05	0.003451		
135	50059	5.67E-05	0.003564		
140	50269	3.91E-05	0.002458		
144	50389	2.91E-05	0.001832		
147	50479	3.05E-05	0.001917		
149	50559	3.17E-05	0.00199		
154	50679	2.14E-05	0.001346		
156	50749	1.98E-05	0.001247		
158	50814	2.16E-05	0.001357		
160	50879	2.01E-05	0.001265		
170	51079	1.99E-05	0.00125		
173	51169	2.96E-05	0.001863		

UNIVERSITY of the
WESTERN CAPE

Column Name	**K60**				
Length (m)	0.2				
Cross-sectional Area (m2)	0.006362				
Hydraulic Gradient	2.5				
Time (days)	**Total Volume (mL)**	**Q (m3/d)**	**K (m/d)**	**pH**	**EC (mS/m)**
1	200	0.004114	0.258679	11.33	390
	450	0.003789	0.238257	12.13	430
	1160	0.003692	0.232148	11.52	460
2	2760	0.003789	0.238257	11.5	465
	3160	0.003692	0.232148	11.21	460
	3610	0.004	0.251493	11.1	465
	4190	0.004	0.251493	10.83	460
3	6390	0.003912	0.24596	10.3	470
	6640	0.003744	0.235398	10.15	475
	7180	0.003888	0.244451	10.08	470
	7830	0.003802	0.239019	10.06	470
	8350	0.003888	0.244451	10.03	480
	9210	0.0048	0.301792	10	480
	10070	0.0048	0.301792	9.95	475

https://etd.uwc.ac.za

	10940	0.00504	0.316881	9.9	480
4	12790	0.005097	0.320487	9.84	490
	13270	0.00576	0.36215	9.79	490
	13750	0.00576	0.36215	9.71	495
	14230	0.00576	0.36215	9.65	480
	14725	0.00594	0.373467	9.56	500
	15225	0.006	0.37724	9.52	495
	15745	0.00612	0.384785	9.45	485
	15995	0.006	0.37724	7.88	480
5	18895	0.0058	0.364665	7.72	475
6	24145	0.004494	0.28254	5.1	470
7	27145	0.003429	0.215566	4.97	475
	27655	0.00306	0.192392	4.83	480
	28035	0.00304	0.191135	4.86	485
	28315	0.00336	0.211254	4.8	480
	28575	0.00312	0.196165	4.83	475
8	30125	0.002862	0.179914	4.84	470
	30365	0.00288	0.181075	4.93	475
	30575	0.00276	0.17353	4.79	480
	30815	0.00288	0.181075	4.8	485
	31055	0.00288	0.181075	4.81	485
	31445	0.00304	0.191135	4.76	485
9	32685	0.00248	0.155926	4.69	485
	32885	0.0024	0.150896	4.84	480
	33105	0.00264	0.165986	4.77	480
	33405	0.0024	0.150896	4.85	475
	33915	0.002448	0.153914	4.9	465
10	35205	0.00258	0.162213	4.62	460
	35755	0.002933	0.184428	4.69	455
22	40565	0.001548	0.097352	4.73	445
23	41335	0.00096	0.060358	4.78	435
24	42165	0.000947	0.059564	4.75	425
28	44735	0.000424	0.026629	4.79	420
29	45445	0.000574	0.036071	4.85	400
30	45711	0.00056	0.035229	4.82	410
	45979	0.00055	0.034556	4.82	405
31	46339	0.000588	0.036954	4.98	405
	46579	0.000595	0.037412	4.84	405
32	47459	0.000576	0.036215	4.82	400
38	50514	0.000475	0.02988	4.89	465
39	50884	0.000475	0.02988	4.95	460
42	51894	0.000503	0.031656	4.92	455
43	52444	0.000482	0.03028	4.5	455
44	52854	0.000478	0.030079	4.52	440

UNIVERSITY of the
WESTERN CAPE

https://etd.uwc.ac.za

45	53344	0.000436	0.027436	4.47	445
46	53714	0.000389	0.02447	4.4	435
47	54864	0.000327	0.020577	4.32	440
56	57414	0.000305	0.019182	4.3	430
57	57744	0.000301	0.018901	4.1	425
64	60079	0.00036	0.022634	3.84	420
65	60344	0.000344	0.02166	3.87	420
66	61224	0.000318	0.019986	3.63	415
67	61434	0.000313	0.019682	3.63	415
70	62284	0.000286	0.018	3.65	410
71	62649	0.000284	0.017858	3.63	400
74	63549	0.000241	0.015165	3.62	395
77	64299	0.000259	0.016284	3.54	390
79	64859	0.000248	0.01561	3.5	390
80	65129	0.000246	0.015477	3.46	
81	65469	0.000267	0.016797	3.39	
82	65869	0.000258	0.016225	3.38	
84	66519	0.000277	0.017411	3.33	
87	66999	0.000231	0.014533	3.3	
91	67899	0.000222	0.013972	3.28	
92	68219	0.000219	0.013739	3.2	
101	70309	0.000189	0.011913	3.1	
121	74909	0.000176	0.011095		
123	75249	0.00017	0.010688		
126	75849	0.0002	0.012575		
127	76109	0.000173	0.010908		
133	77359	0.000215	0.013542		
134	77619	0.000185	0.011607		
135	77819	0.000171	0.010778		
140	78609	0.000151	0.009465		
144	78889	0.000168	0.010541		
147	79329	0.00015	0.009415		
149	79699	0.000147	0.009249		
154	80349	0.000117	0.007326		
156	80699	9.96E-05	0.006262		
158	81019	0.000107	0.00671		
160	81229	6.53E-05	0.004106		
170	82409	0.000118	0.007412		
173	82809	0.000132	0.008318		

Column Name	**K60b**
Length (m)	0.5
Cross-sectional Area (m2)	0.006362

https://etd.uwc.ac.za

Hydraulic Gradient	2.5				
Time (days)	**Total Volume (mL)**	**Q (m3/d)**	**K (m/d)**	**pH**	**EC (mS/m)**
1	140	0.002076	0.284822	12.75	400
	480	0.00197	0.270209	12.91	410
	720	0.001799	0.246806	12.88	415
2	1620	0.001684	0.231003	12.84	420
	1820	0.001641	0.22514	12.46	420
	2060	0.001655	0.227002	12.01	420
	2360	0.001717	0.235475	11.9	400
3	3560	0.00215	0.294933	10.82	425
	3660	0.002389	0.327703	11.22	430
	3740	0.001911	0.262163	11.65	435
	3840	0.001911	0.262163	11.64	420
	3993	0.002193	0.300832	11.66	435
	4073	0.001911	0.262163	11.65	420
	4423	0.001959	0.268717	11.71	430
	4873	0.002628	0.360474	11.68	435
4	5603	0.001852	0.254043	11.66	435
	5813	0.002508	0.344088	11.66	425
	5993	0.00215	0.294933	11.65	440
	6193	0.002389	0.327703	11.59	435
	6393	0.002389	0.327703	11.52	435
	7083	0.002269	0.311318	11.53	440
	7283	0.002389	0.327703	11.01	440
	7783	0.002389	0.327703	10.89	435
5	8833	0.00209	0.28674	10.75	425
6	11233	0.001977	0.271203	11.09	425
7	13033	0.002048	0.280889	10.62	425
	13393	0.00215	0.294933	10.96	445
	13683	0.002309	0.31678	10.95	455
	13883	0.002389	0.327703	10.77	460
	14073	0.002269	0.311318	10.85	450
8	15273	0.002205	0.302495	10.4	465
	15463	0.002269	0.311318	10.35	465
	15663	0.002389	0.327703	10.5	460
	15853	0.002269	0.311318	10.33	455
	16043	0.002269	0.311318	10.76	450
	16313	0.00215	0.294933	10.55	445
9	17463	0.002289	0.314049	10.66	435
	17643	0.00215	0.294933	10.19	430
	17823	0.00215	0.294933	10.63	430
	18067	0.001943	0.266532	10.54	420
	18537	0.002246	0.308041	10.41	405
10	19687	0.002289	0.314049	10.28	410

UNIVERSITY of the
WESTERN CAPE

https://etd.uwc.ac.za

	20287	0.002177	0.298574	10.29	385
11	22087	0.001734	0.237801	10.27	400
15	24727	0.001514	0.207626	10.06	395
23	29027	0.001597	0.219077	10.24	395
24	30237	0.001145	0.157109	10.21	395
28	35057	0.001307	0.179345	10.22	390
29	36477	0.001239	0.169941	10.01	450
30	37027	0.001111	0.15246	10.18	450
	37467	0.001023	0.140294	9.77	440
31	38017	0.000953	0.130762	9.69	435
	38407	0.000939	0.128778	9.73	435
32	39477	0.000738	0.101265	9.74	430
38	42657	0.000504	0.069136	8.77	425
39	43007	0.00048	0.065907	9.75	405
42	43997	0.000464	0.063601	8.47	415
43	44527	0.000395	0.054124	9.14	410
44	44897	0.000382	0.052384	8.75	405
45	45377	0.000427	0.058629	9.22	405
46	45677	0.000305	0.041834	9.26	400
49	46767	0.00047	0.064466	8.58	395
56	49487	0.000287	0.039324	8.45	395
64	52237	0.000529	0.072554	8.13	395
65	52847	0.000501	0.068749	8.09	390
66	53362	0.000484	0.066426	7.98	390
67	53562	0.000459	0.06302	7.8	385
70	54702	0.0004	0.054922	7.78	390
71	55157	0.000388	0.053285	6.86	390
74	56277	0.000342	0.046926	6.98	390
77	57567	0.000266	0.036547	6.17	
79	57822	0.000256	0.035111	6.23	
80	58102	0.000251	0.034435	6.29	
81	58392	0.000249	0.034136	6.27	
82	58792	0.00024	0.03288	6.28	
84	59542	0.000247	0.0339	6.31	
87	60372	0.000296	0.040541	6.32	
91	61272	0.000208	0.028496	6.15	
92	61552	0.000184	0.025305	5.97	
101	62627	0.000129	0.017682	5.92	
121	65267	0.000148	0.02024		
123	65567	0.000149	0.020481		
126	66147	0.000192	0.026398		
127	66427	0.000119	0.016385		
133	67537	0.000213	0.029284		
134	67857	0.00023	0.031544		

UNIVERSITY of the
WESTERN CAPE

https://etd.uwc.ac.za

135	68097	0.000205	0.028089		
140	69247	0.000228	0.031281		

Column Name	**T40**				
Length (m)	0.2				
Cross-sectional Area (m2)	0.006362				
Hydraulic Gradient	2.5				
Time (days)	**Total Volume (mL)**	**Q (m3/d)**	**K (m/d)**	**pH**	**EC (mS/m)**
1	170	0.002925	0.183915	9.6	425
	770	0.003258	0.204815	11.09	435
	1950	0.003772	0.237154	10.97	445
2	4540	0.00473	0.297391	10.42	465
	5090	0.00473	0.297391	10.02	465
	5640	0.004849	0.304901	9.98	455
	6210	0.004778	0.300395	8.88	470
	6590	0.004945	0.310909	8.87	465
	6816	0.005399	0.339446	8.82	465
	6936	0.005733	0.360474	8.76	485
3	11036	0.008162	0.513174	6.45	525
	11596	0.009443	0.593721	6.41	500
	12216	0.010511	0.660868	6.34	510
	13166	0.010033	0.630829	6.29	510
	13566	0.007975	0.501428	6.12	530
	14624	0.006689	0.420553	5.74	535
4	18724	0.006219	0.39099	4.76	525
5	22424	0.006671	0.419419	4.53	530
	22674	0.005972	0.375493	4.53	525
	23574	0.003851	0.242109	4.51	530
6	25174	0.00364	0.228872	4.47	520
7	28774	0.003546	0.222973	4.41	525
9	34909	0.002829	0.177865	4.32	525
12	43959	0.003551	0.223278	4.33	525
13	45959	0.003247	0.204119	4.34	520
	47259	0.002756	0.173305	4.35	525
14	49709	0.003419	0.214985	4.38	520
	50249	0.003413	0.214568	4.25	525
	50849	0.002925	0.183915	4.35	525
	51029	0.003333	0.209578	4.03	515
15	53729	0.003166	0.199035	3.8	495
16	57239	0.003416	0.214772	3.72	500
17	59299	0.002266	0.142459	3.74	510
20	65799	0.001701	0.106916	4.03	510
27	80283	0.000442	0.027814	4.02	505

UNIVERSITY of the WESTERN CAPE

https://etd.uwc.ac.za

	80483	0.000434	0.027309	4.02	480
28	80923	0.000432	0.027144	3.95	455
35	82898	0.000216	0.013572	3.83	415
36	83148	0.000216	0.013593	3.84	470
37	83358	0.000211	0.013253	3.86	485
38	83498	0.000206	0.012967	3.82	475
41	84158	0.0002	0.012551	3.78	485
42	84398	0.000197	0.012362	3.79	470
45	84978	0.000198	0.01243	3.75	450
48	85678	0.000186	0.011689	3.76	445
50	85878	0.000183	0.011524	3.78	440
51	86068	0.000183	0.01148	3.7	470
52	86268	0.000181	0.011407	3.7	440
53	86488	0.000177	0.011112	3.6	
55	86808	0.000163	0.010241	3.6	
58	87248	0.000161	0.010126	3.5	
62	87748	0.000144	0.009048	3.42	
63	87938	0.000142	0.008923	3.28	
72	88898	0.000118	0.007399		
92	90768	8.43E-05	0.005301		
94	90948	8.96E-05	0.005632		
97	91258	0.000103	0.006467		
99	91458	9.56E-05	0.006008		
104	91978	0.000104	0.006547		
106	92188	8.48E-05	0.005331		
111	92678	9.45E-05	0.00594		
115	92968	7.68E-05	0.00483		
118	93228	8.81E-05	0.005538		
120	93428	7.91E-05	0.004976		
125	93788	6.42E-05	0.004039		
127	93978	5.38E-05	0.003384		
129	94158	5.97E-05	0.003757		
131	94338	5.57E-05	0.003504		
141	94878	5.37E-05	0.003376		
144	95128	8.23E-05	0.005174		

UNIVERSITY of the
WESTERN CAPE

Column Name	**T50**				
Length (m)	0.2				
Cross-sectional Area (m2)	0.006362				
Hydraulic Gradient	2.5				
Time (days)	**Total Volume (mL)**	**Q (m3/d)**	**K (m/d)**	**pH**	**EC (mS/m)**
1	200	0.004095	0.257481	10.2	375
	690	0.00305	0.191741	11.8	435

https://etd.uwc.ac.za

	1010	0.003116	0.19591	11.04	470
2	2490	0.00224	0.14081	10.91	460
	2790	0.00235	0.147735	10.91	465
	3130	0.002139	0.134505	10.86	470
	3560	0.002471	0.155377	10.84	440
3	5360	0.003344	0.210276	10.22	465
	5560	0.003106	0.195257	9.84	475
	6160	0.003106	0.195257	8.91	470
	6530	0.00344	0.216284	7.18	475
	6620	0.003655	0.229802	6.67	480
	7050	0.004061	0.255335	6.35	470
	8150	0.003822	0.240316	6.18	480
	9240	0.004061	0.255335	6.06	475
4	10620	0.003501	0.220112	5.95	485
	10920	0.003583	0.225296	5.88	475
	11210	0.003464	0.217786	5.7	485
	11510	0.003583	0.225296	5.52	475
	11810	0.003583	0.225296	5.27	485
	12120	0.003703	0.232806	5.12	490
	12460	0.004061	0.255335	5.01	485
	12660	0.0043	0.270355	5.01	485
5	14910	0.004479	0.28162	4.9	475
6	19700	0.00383	0.240834	4.77	470
7	22350	0.003174	0.199548	4.82	470
	22980	0.003285	0.206521	4.8	470
	23430	0.003185	0.200263	4.76	480
	23710	0.002867	0.180237	4.75	485
	23950	0.002867	0.180237	4.77	485
8	24850	0.002756	0.173305	4.78	480
	25070	0.002628	0.165217	4.88	480
	25280	0.002508	0.157707	4.81	475
	25500	0.002628	0.165217	4.82	475
	25680	0.00215	0.135178	4.84	470
	25960	0.00223	0.140184	4.8	465
9	27060	0.00219	0.137681	4.72	460
	27220	0.001911	0.120158	4.85	450
	27370	0.001792	0.112648	4.79	440
	27595	0.001792	0.112648	4.88	430
	27945	0.002007	0.126166	4.92	420
10	28945	0.001991	0.125164	4.71	415
	29305	0.001911	0.120158	4.82	415
22	33155	0.001315	0.082677	4.88	410
28	38295	0.001315	0.082677	4.88	405
29	39495	0.001039	0.065303	4.85	405

UNIVERSITY of the
WESTERN CAPE

https://etd.uwc.ac.za

30	39935	0.001031	0.064833	4.86	470
	40285	0.000907	0.057037	4.89	470
31	40765	0.000853	0.053642	4.89	460
	41085	0.000689	0.043326	4.86	455
32	42045	0.00071	0.044613	4.93	455
38	45525	0.000535	0.033626	4.97	450
39	45965	0.000533	0.033501	4.95	445
42	47215	0.000543	0.034136	5.13	440
43	47835	0.000541	0.034007	4.82	435
44	48315	0.000533	0.033501	4.75	430
45	48935	0.000533	0.033501	4.65	430
46	49375	0.000454	0.028518	4.54	425
49	50795	0.000452	0.028429	4.47	415
56	53495	0.000357	0.022418	4.5	415
57	53885	0.000377	0.023715	3.89	415
64	55925	0.00027	0.017003	3.86	410
65	56245	0.000233	0.014677	3.94	405
66	56490	0.000228	0.014305	3.98	405
67	56640	0.000216	0.013593	3.89	400
70	57340	0.000215	0.013531	3.88	405
71	57640	0.000212	0.013351	3.7	400
74	58390	0.000237	0.014896	3.86	400
77	59240	0.00022	0.013822	3.87	
79	59470	0.000217	0.013634	3.82	
80	59670	0.000208	0.013061	3.74	
81	59920	0.000205	0.012874	3.64	
82	60200	0.000183	0.01148	3.55	
84	60560	0.000187	0.011734	3.52	
87	61220	0.000181	0.011379	3.43	
91	61730	0.000135	0.008502	3.18	
92	61900	0.000129	0.008133	3.15	
101	62960	0.000117	0.007381	3.1	
121	65670	0.000126	0.007952		
123	65930	0.000129	0.008136		
126	66390	0.000153	0.009596		
128	66730	0.000106	0.006675		
135	67730	0.000145	0.009119		
140	68310	0.000111	0.006964		
144	68680	9.8E-05	0.006162		
147	68940	8.81E-05	0.005538		
149	69160	8.71E-05	0.005474		
154	69580	7.49E-05	0.004712		
156	69780	5.67E-05	0.003562		
158	69970	6.31E-05	0.003965		

UNIVERSITY of the
WESTERN CAPE

https://etd.uwc.ac.za

160	70170	6.19E-05	0.003893		
170	70770	5.97E-05	0.003751		
173	70980	6.91E-05	0.004347		

Column Name	**T60**				
Length (m)	0.2				
Cross-sectional Area (m2)	0.006362				
Hydraulic Gradient	2.5				
Time (days)	**Total Volume (mL)**	**Q (m3/d)**	**K (m/d)**	**pH**	**EC (mS/m)**
1	110	0.003981	0.250329	10.79	375
	690	0.003772	0.237154	12.27	420
	1090	0.003583	0.225296	11.09	480
2	2820	0.003116	0.19591	10.71	470
	3240	0.003258	0.204815	10.61	465
	3720	0.003258	0.204815	10.4	465
	4360	0.003675	0.231073	10.28	455
3	7210	0.005375	0.337944	9.67	475
	7560	0.005327	0.33494	5.32	480
	8160	0.005279	0.331936	4.91	475
	8660	0.005619	0.353264	4.77	470
	9260	0.005375	0.337944	4.68	475
	9910	0.005733	0.360474	4.6	485
	11586	0.006928	0.435572	4.7	475
	13262	0.007167	0.450592	4.65	475
4	15562	0.005835	0.366854	4.6	485
	16062	0.005972	0.375493	4.61	485
	16502	0.005256	0.330434	4.57	480
	16882	0.004539	0.285375	4.61	470
	17282	0.004778	0.300395	4.55	480
	17662	0.004539	0.285375	4.51	480
	18062	0.004897	0.307905	4.53	475
	18472	0.004778	0.300395	4.54	470
5	20072	0.003185	0.200263	4.85	470
6	23352	0.002702	0.169878	4.52	465
7	24612	0.001433	0.090118	4.58	460
	24812	0.001194	0.075099	4.58	460
	24952	0.001115	0.070092	4.66	465
	25062	0.001314	0.082609	4.67	465
	25152	0.001075	0.067589	4.71	465
8	25672	0.000956	0.060079	4.78	465
	25772	0.001194	0.075099	4.72	465
	25852	0.000956	0.060079	4.71	465
	25952	0.001194	0.075099	4.73	465

UNIVERSITY of the WESTERN CAPE

https://etd.uwc.ac.za

	26032	0.000956	0.060079	4.71	460
	26152	0.000956	0.060079	4.64	455
9	26702	0.001095	0.06884	4.88	455
	26782	0.000956	0.060079	4.77	440
	26862	0.000956	0.060079	4.77	435
	26994	0.001051	0.066087	4.8	420
	27238	0.001166	0.073296	4.61	415
10	27888	0.001294	0.081357	4.72	415
	28268	0.001327	0.083443	4.77	415
22	33078	0.000995	0.062582	4.76	415
23	33798	0.001009	0.063464	4.75	405
24	34378	0.000739	0.046453	4.8	410
28	36198	0.000423	0.026584	4.81	410
29	36668	0.000308	0.019339	4.79	405
30	36818	0.000336	0.021155	4.89	405
	36968	0.00033	0.020717	4.8	395
31	37168	0.000327	0.020575	4.78	460
	37348	0.000326	0.020481	4.8	460
32	37933	0.000317	0.019938	4.91	445
38	40623	0.000312	0.019591	4.9	445
39	40923	0.000291	0.018317	4.34	450
42	41683	0.00029	0.018206	4.25	445
43	42073	0.000314	0.019763	4.3	435
44	42403	0.000337	0.021204	4.35	435
45	42803	0.000322	0.020251	4.25	420
46	43123	0.000319	0.020026	4.22	420
49	44183	0.000336	0.021105	4.2	415
56	46633	0.000272	0.0171	3.95	410
57	46913	0.000406	0.025529	3.7	405
64	48523	0.000225	0.014125	3.8	405
65	48913	0.000231	0.014535	3.76	405
66	49158	0.000229	0.014373	3.72	390
67	49308	0.000221	0.013907	3.71	390
70	49908	0.000212	0.013351	3.76	390
71	50158	0.00021	0.013214	3.78	
74	50758	0.000203	0.012747	3.71	
77	51308	0.000154	0.009701	3.68	
79	51648	0.000152	0.009587	3.64	
80	51828	0.000151	0.009506	3.6	
81	52028	0.000152	0.009587	3.56	
82	52248	0.000148	0.0093	3.5	
84	52558	0.000149	0.009339	3.4	
87	52933	0.000141	0.008844	3.3	
91	53343	8.44E-05	0.005304	3.25	

UNIVERSITY of the
WESTERN CAPE

https://etd.uwc.ac.za

101	54038	7.47E-05	0.004694	3.2
121	56118	0.000105	0.006626	
123	56288	8.46E-05	0.005319	
126	56608	0.000106	0.006675	
133	57398	0.000122	0.00767	
140	58108	0.000104	0.006554	
144	58358	6.62E-05	0.004164	
147	58558	6.78E-05	0.00426	
149	58738	7.12E-05	0.004479	
154	59058	5.71E-05	0.00359	
156	59208	4.25E-05	0.002671	
158	59348	4.65E-05	0.002922	
160	59548	6.19E-05	0.003893	
170	60348	7.96E-05	0.005002	
173	60648	9.88E-05	0.006209	

Column Name	**T60b**				
Length (m)	0.5				
Cross-sectional Area (m2)	0.006362				
Hydraulic Gradient	2.5				
Time (days)	**Total Volume (mL)**	**Q (m3/d)**	**K (m/d)**	**pH**	**EC (mS/m)**
1	110	0.002511	0.344447	10.3	400
	490	0.002153	0.295302	12.3	395
	740	0.002007	0.275252	12.51	430
2	1690	0.002154	0.295524	12.59	430
	1940	0.002263	0.310374	12.23	435
	2220	0.002138	0.29332	11.37	435
	2580	0.001994	0.273529	11.25	405
3	3830	0.001959	0.268717	10.4	440
	3912	0.001959	0.268717	10.45	445
	3992	0.001911	0.262163	10.82	445
	4092	0.001911	0.262163	11.13	440
	4242	0.00215	0.294933	11.07	450
	4322	0.001911	0.262163	11.11	440
	4402	0.001911	0.262163	11.08	445
	5272	0.00215	0.294933	11.19	445
4	6052	0.001979	0.271443	11.2	450
	6282	0.002508	0.344088	11.12	450
	6482	0.002389	0.327703	11.05	450
	6672	0.002269	0.311318	11	450
	6862	0.002269	0.311318	10.86	460
	7042	0.00215	0.294933	10.78	460

UNIVERSITY of the
WESTERN CAPE

https://etd.uwc.ac.za

	7232	0.002269	0.311318	10.37	455
	7372	0.002269	0.311318	10.21	455
5	8562	0.002369	0.324972	10.06	445
6	11262	0.002224	0.305103	10.47	440
7	12762	0.001706	0.234074	10.04	445
	13062	0.001792	0.245777	10.29	445
	13302	0.001911	0.262163	10.23	455
	13482	0.00215	0.294933	10.2	460
	13652	0.002031	0.278548	10.18	465
8	14552	0.001654	0.226872	10.15	465
	14732	0.00215	0.294933	10.14	460
	14892	0.001911	0.262163	10.09	460
	15072	0.00215	0.294933	10.02	460
	15242	0.002031	0.278548	9.95	460
	15492	0.001991	0.273086	9.64	455
9	16372	0.001752	0.240316	9.73	450
	16512	0.001672	0.229392	9.65	445
	16640	0.001529	0.20973	9.56	440
	16834	0.001545	0.211915	9.91	430
	17202	0.001758	0.24119	9.92	420
10	18142	0.001871	0.256701	9.9	420
	18492	0.001858	0.25488	9.1	415
11	20542	0.001957	0.268426	10.11	395
15	22892	0.001923	0.263804	10.17	400
23	28292	0.001964	0.269468	9.22	385
24	29872	0.001819	0.249573	8.85	380
28	35002	0.000926	0.127058	8.45	385
29	36172	0.000944	0.129555	8.54	375
30	36582	0.000733	0.100617	8.5	440
	36902	0.000716	0.098164	8.12	440
31	37362	0.00089	0.122151	7.98	430
	37702	0.000754	0.103376	7.7	430
32	38712	0.000728	0.099842	7.62	425
38	42207	0.000583	0.080042	7.54	420
39	42657	0.00058	0.079497	7.48	415
42	43967	0.000638	0.08755	7.85	400
43	44717	0.000598	0.082085	7.17	400
44	45317	0.000628	0.086112	6.76	400
45	46067	0.000651	0.089245	6.49	390
46	46617	0.000508	0.069724	5.98	390
64	61477	0.000573	0.078649	4.9	390
65	62587	0.000531	0.072823	4.96	385
66	63212	0.000516	0.070727	4.84	385
67	63432	0.000508	0.069724	4.9	385

UNIVERSITY of the
WESTERN CAPE

https://etd.uwc.ac.za

70	65082	0.000494	0.067801	4.96	375
71	65962	0.000553	0.075916	4.95	375
74	67737	0.000494	0.067801	4.93	370
77	69537	0.000481	0.065981	4.89	370
	69837	0.000479	0.06576	4.61	375
79	70137	0.000448	0.061444	4.58	
80	70717	0.000448	0.061444	4.57	
81	71307	0.00047	0.064466	4.58	
82	71957	0.000475	0.065107	4.51	
84	73247	0.000481	0.065981	4.49	
87	74767	0.000517	0.070983	4.48	
91	76767	0.000433	0.059402	4.48	
92	77367	0.000414	0.056827	4.46	
101	80707	0.000326	0.044687	4.47	
121	87047	0.000239	0.03277		
123	87597	0.000274	0.037549		
126	88597	0.000332	0.045514		
127	89047	0.000267	0.036615		
133	91047	0.000333	0.045726		
134	91547	0.000385	0.052855		
135	91897	0.000299	0.040963		
140	93837	0.000375	0.05139		

UNIVERSITY of the
WESTERN CAPE

https://etd.uwc.ac.za

APPENDIX B: Falling head hydraulic test data.

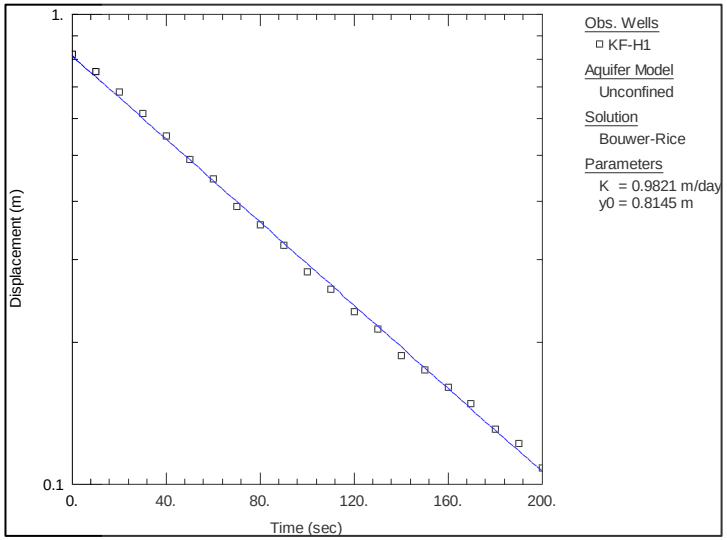

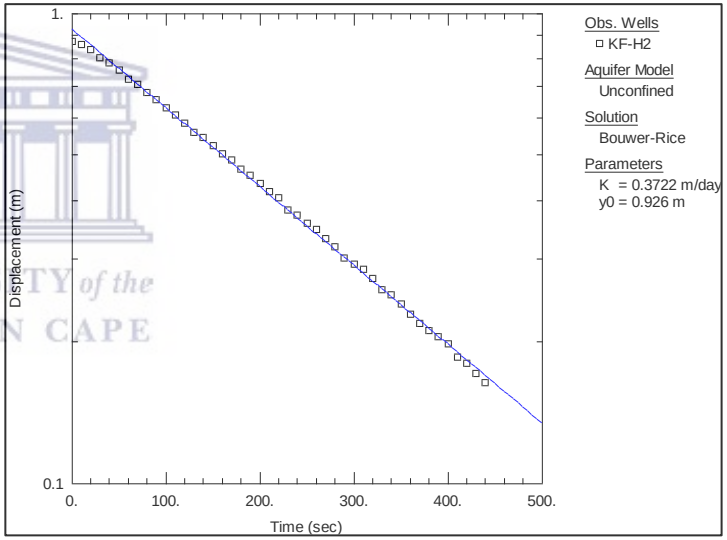

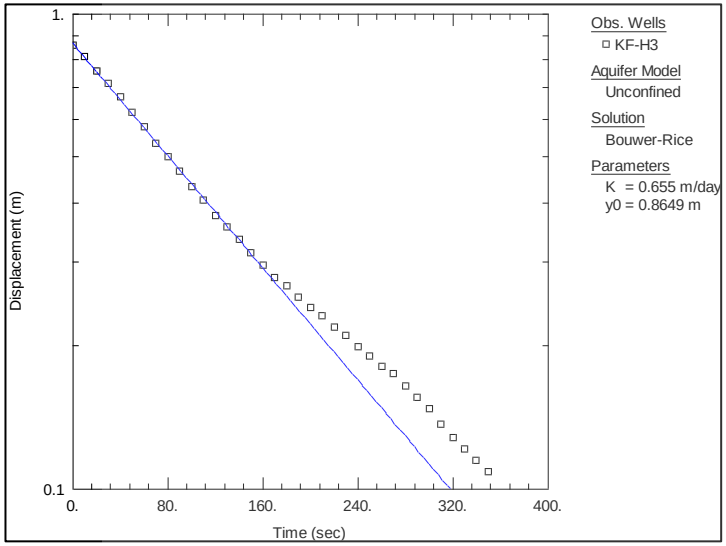

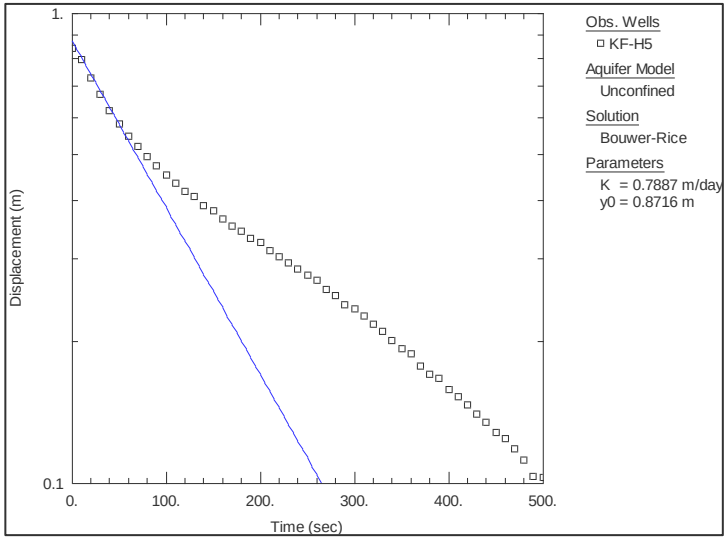

UNIVERSITY of the
WESTERN CAPE

https://etd.uwc.ac.za

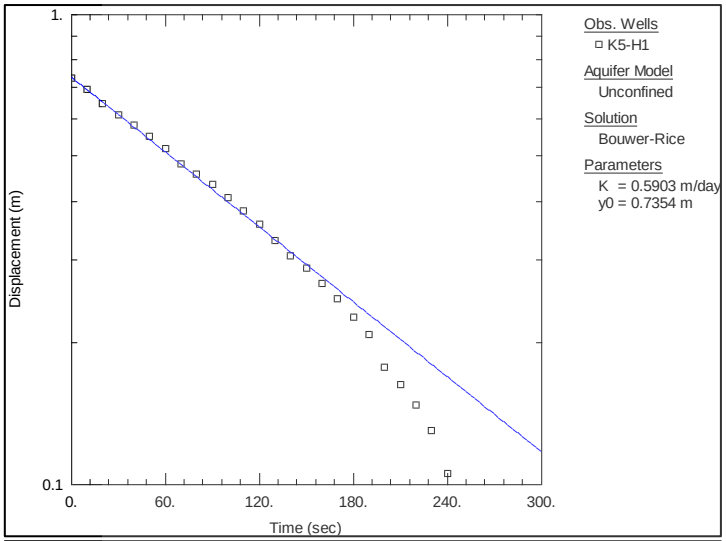

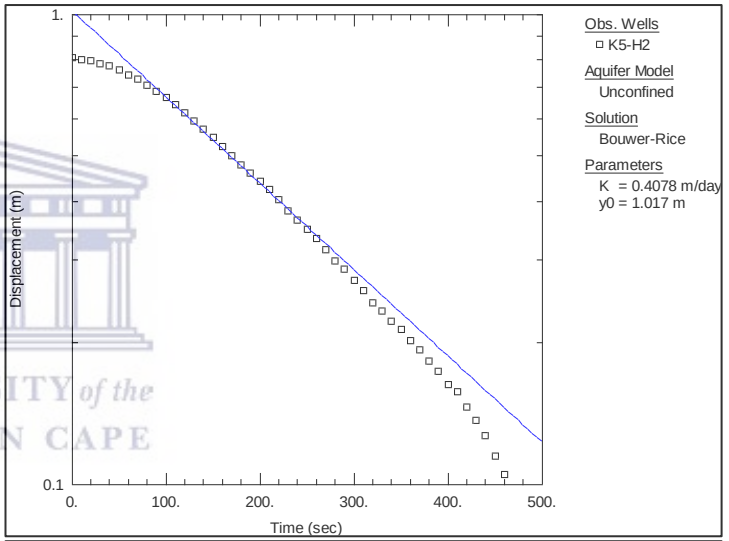

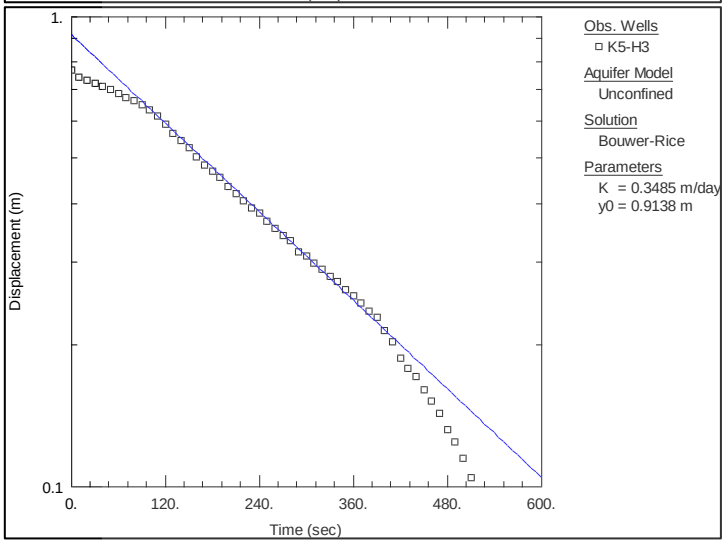

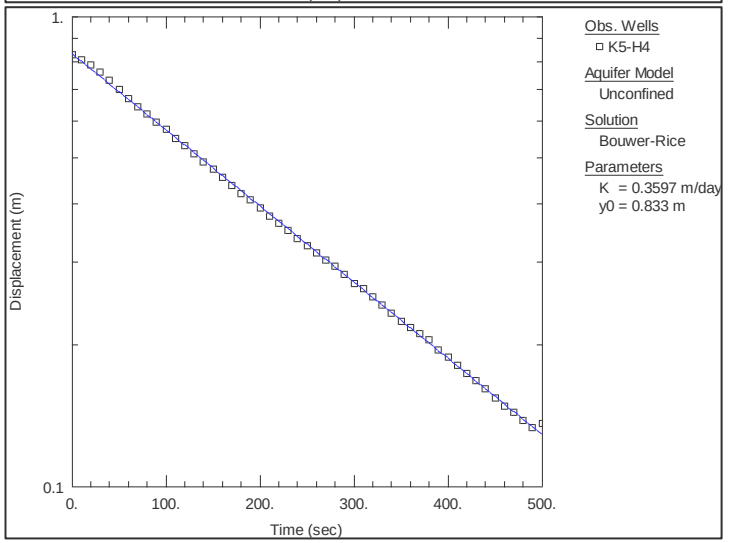

UNIVERSITY of the
WESTERN CAPE

https://etd.uwc.ac.za

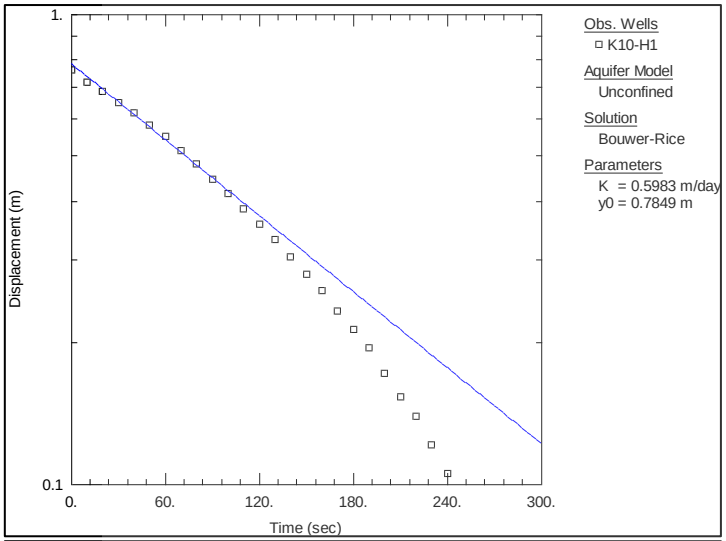

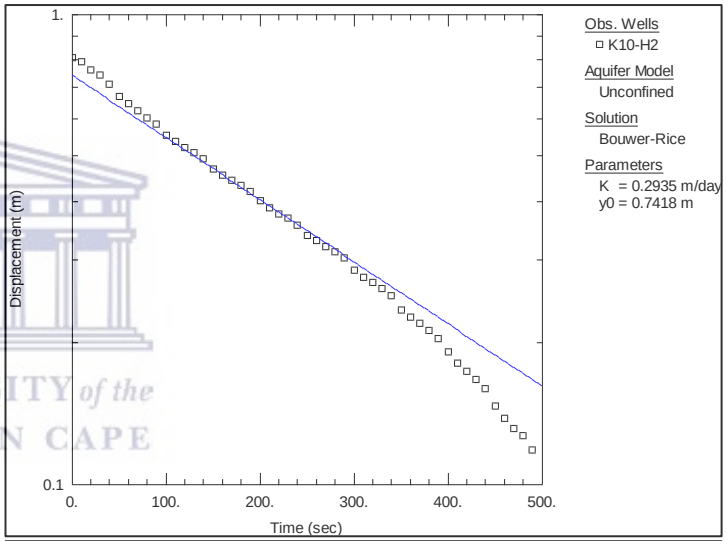

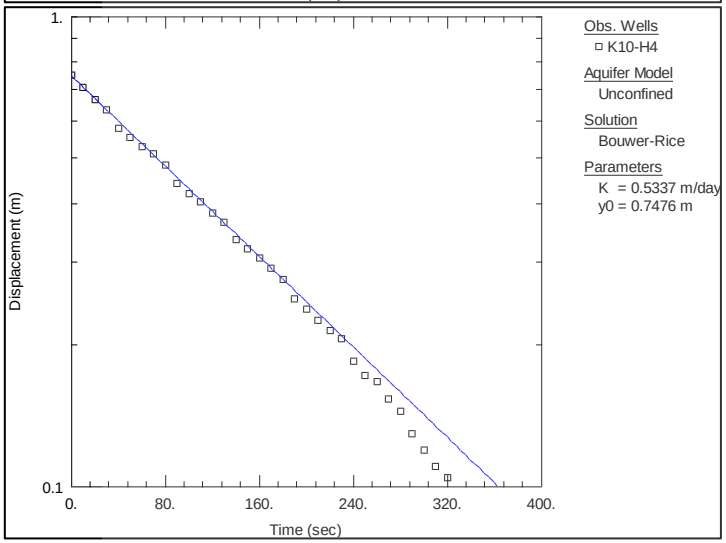

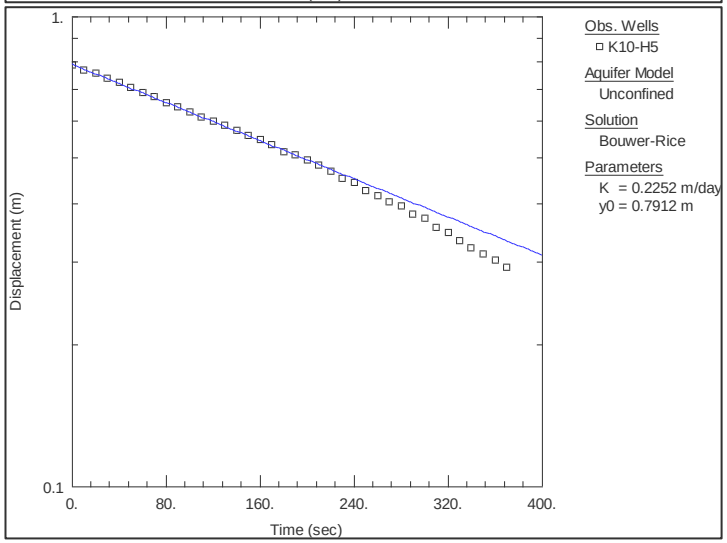

UNIVERSITY of the
WESTERN CAPE

https://etd.uwc.ac.za

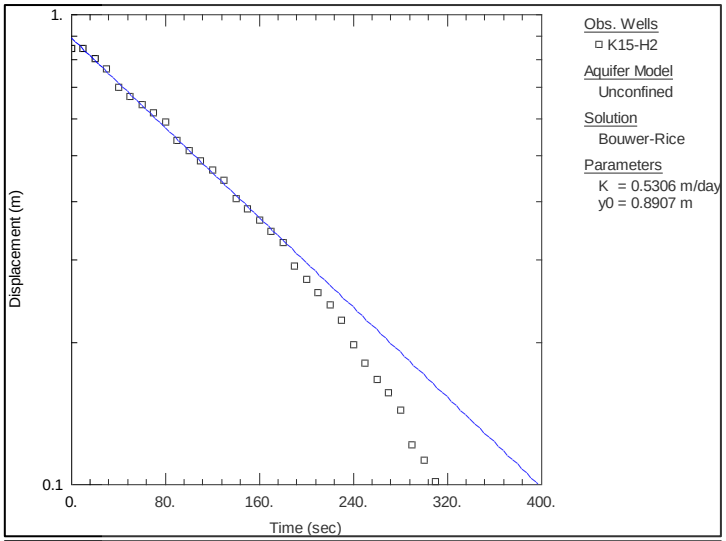

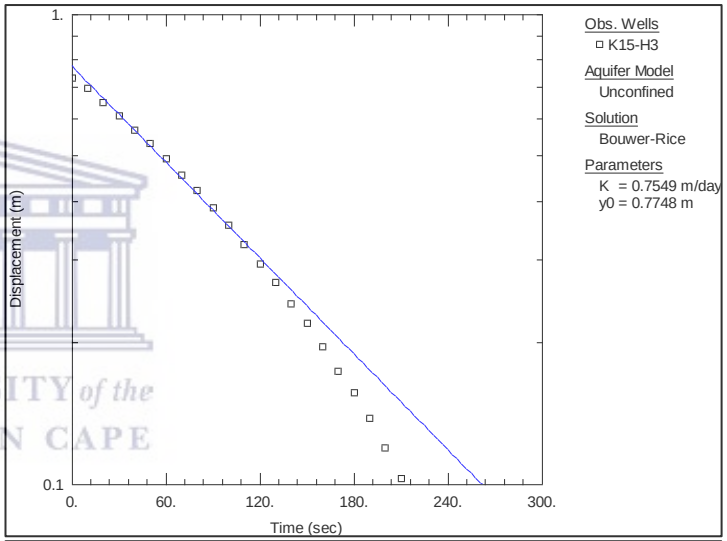

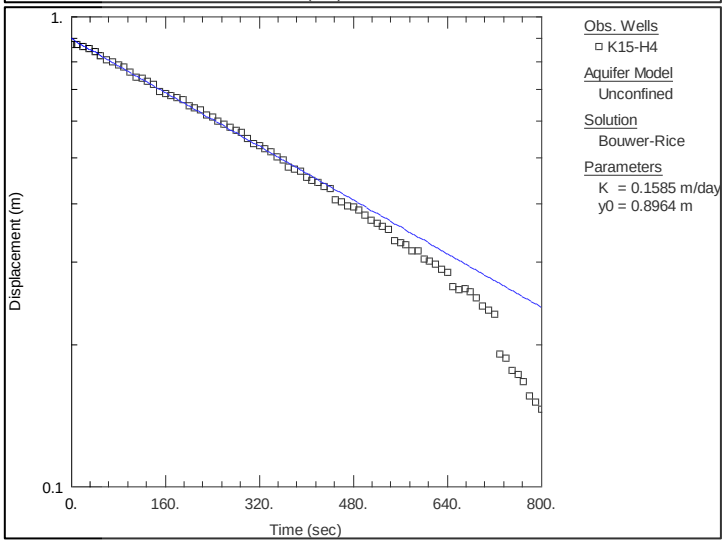

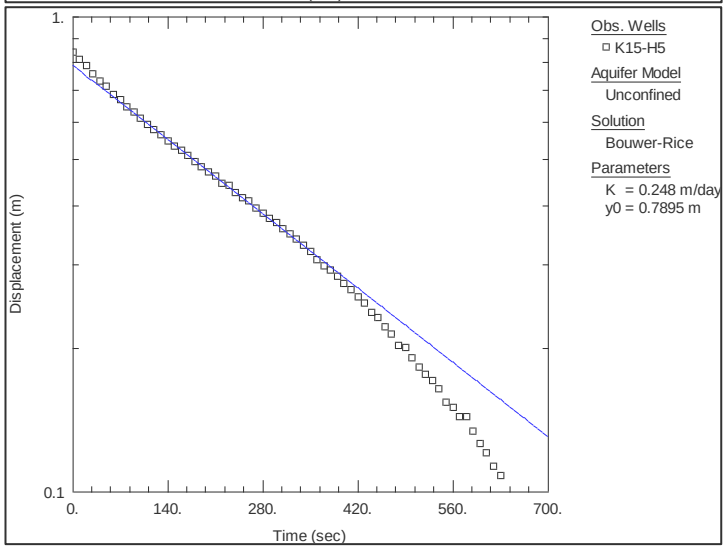

UNIVERSITY of the
WESTERN CAPE

https://etd.uwc.ac.za

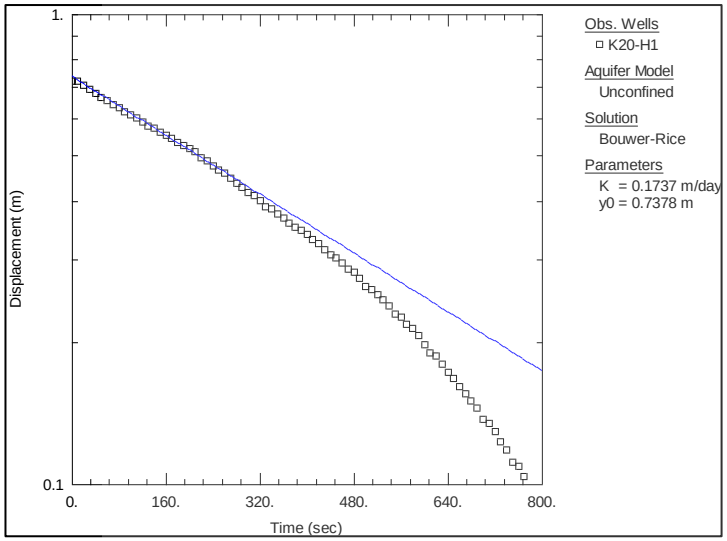

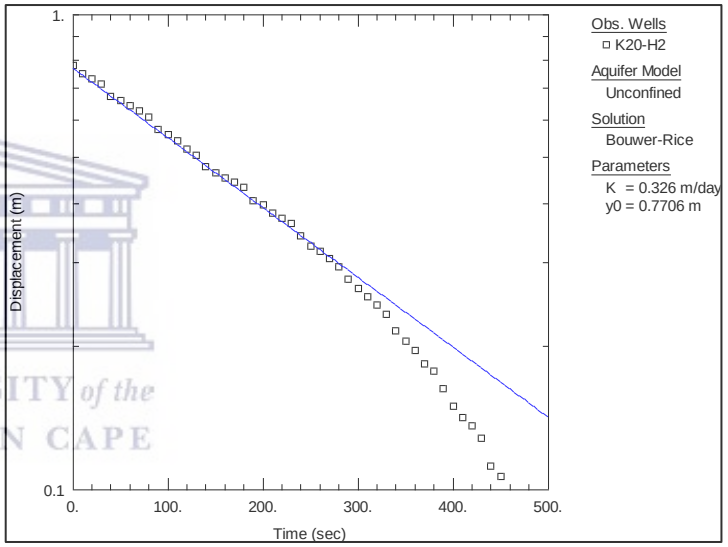

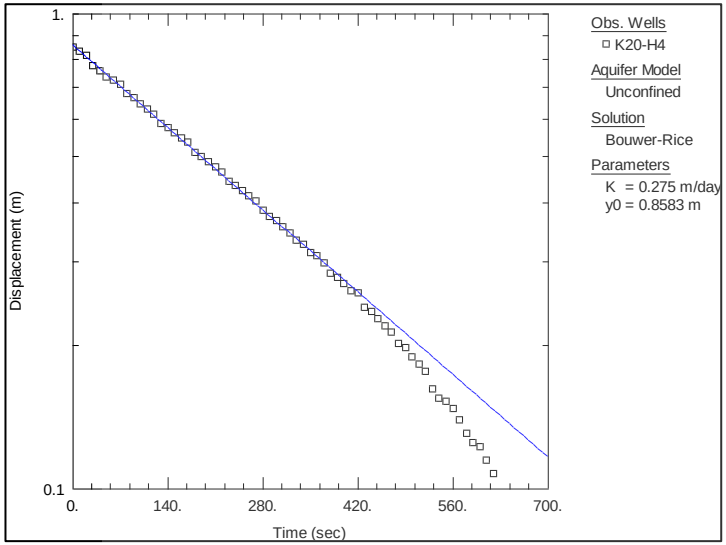

UNIVERSITY of the
WESTERN CAPE

https://etd.uwc.ac.za

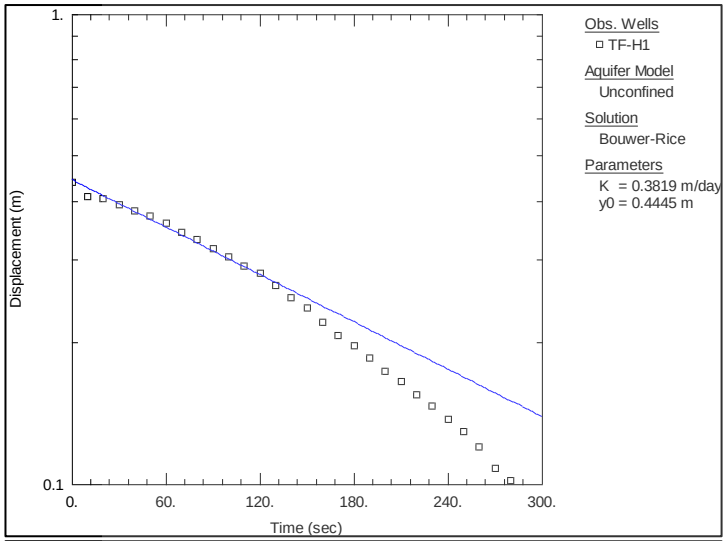

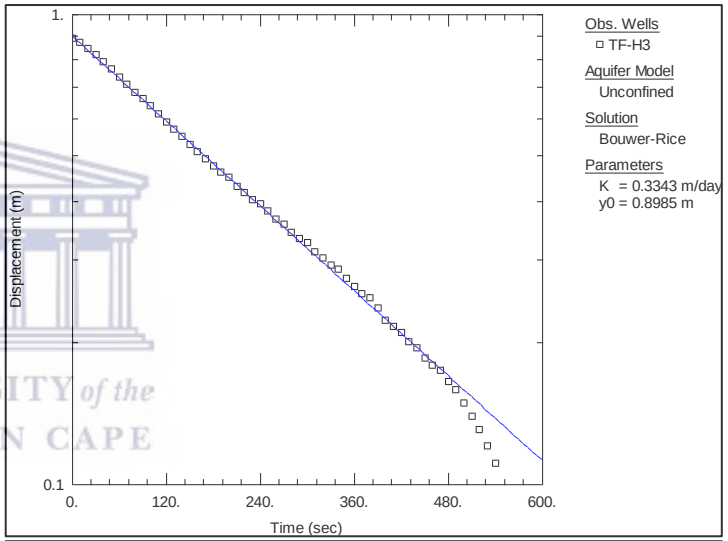

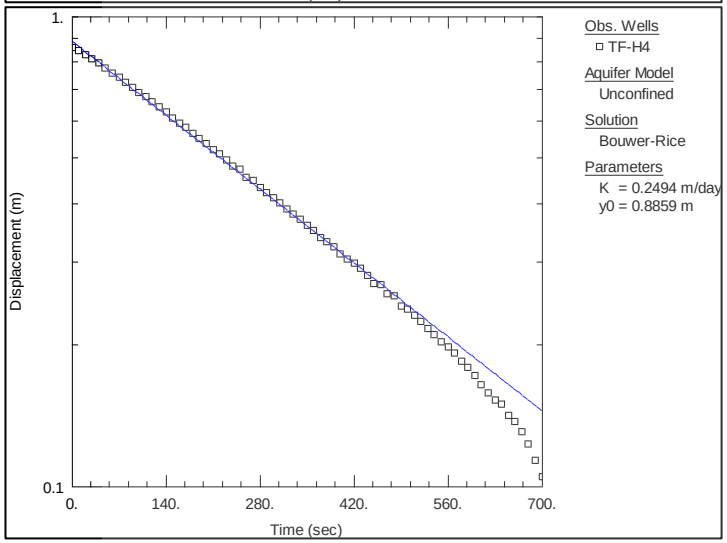

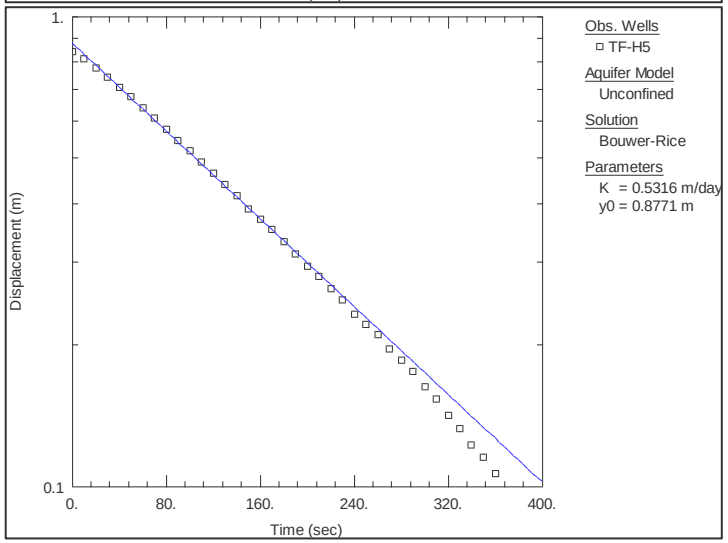

UNIVERSITY of the
WESTERN CAPE

https://etd.uwc.ac.za

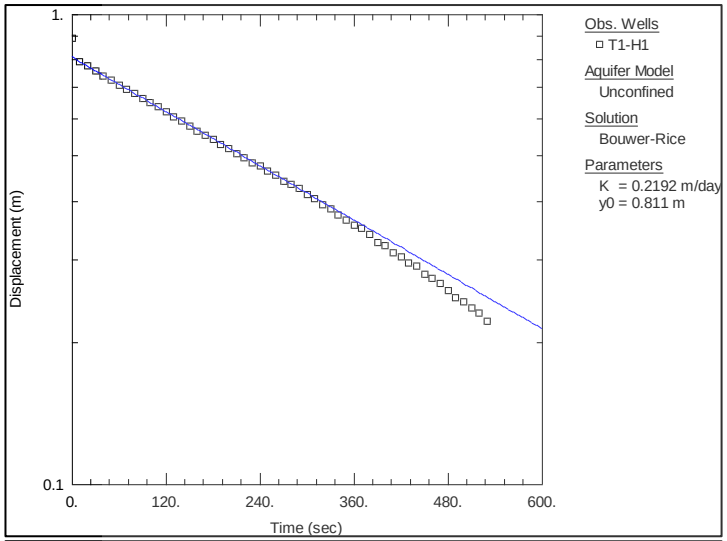

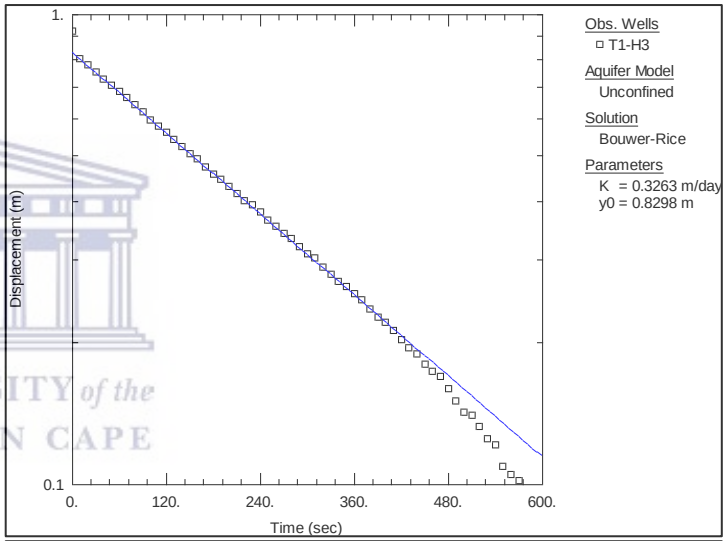

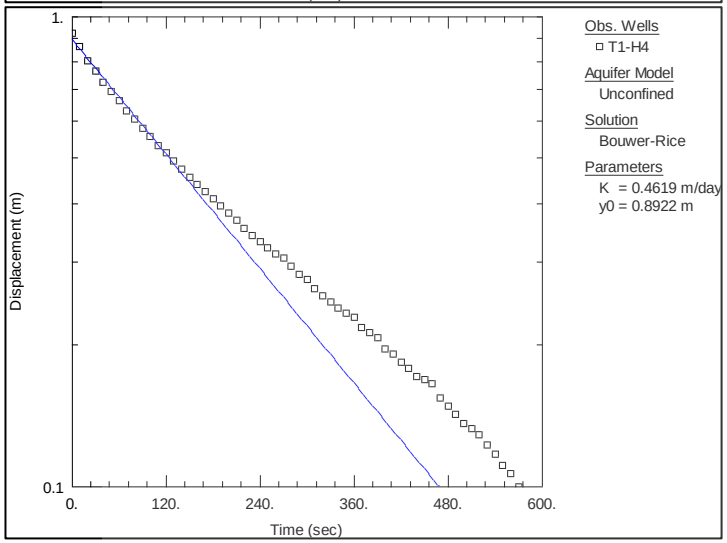

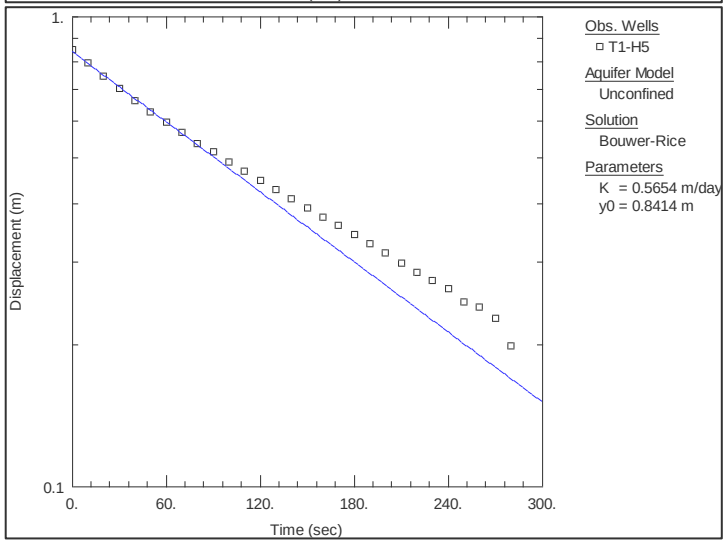

UNIVERSITY of the
WESTERN CAPE

https://etd.uwc.ac.za

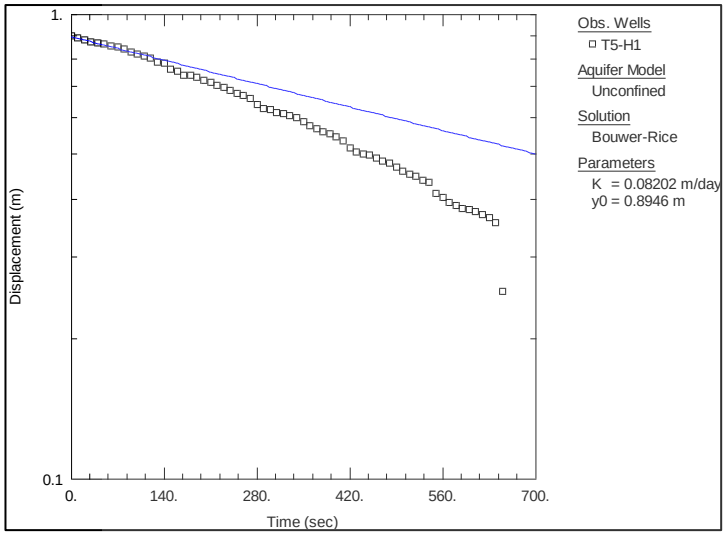

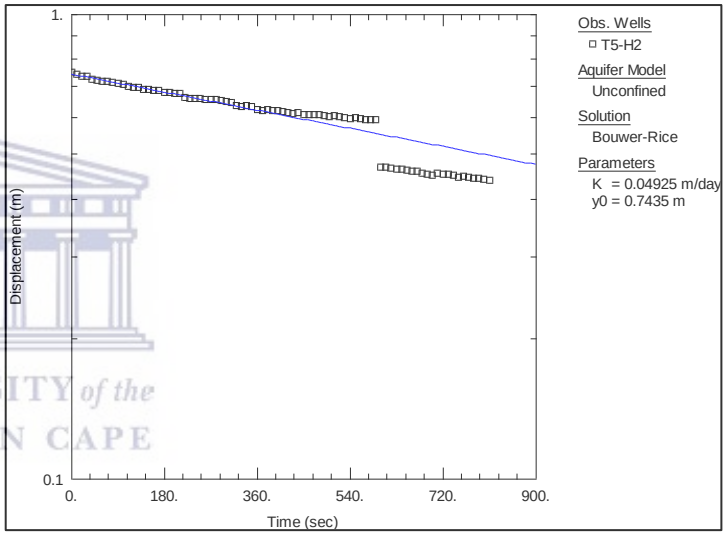

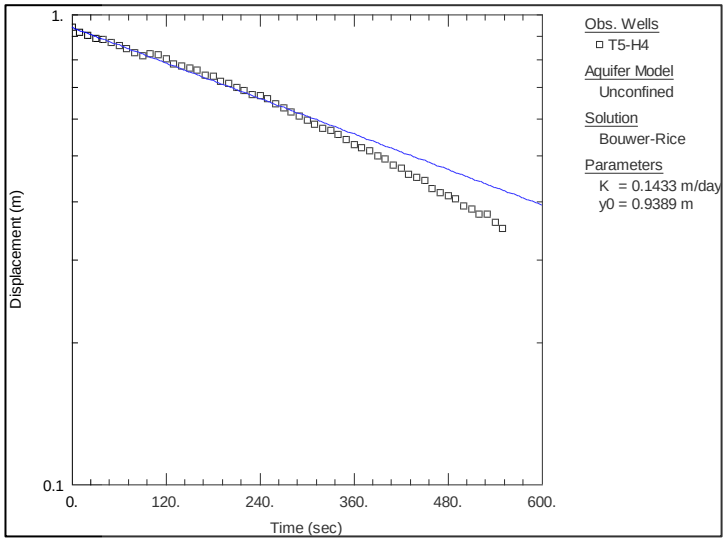

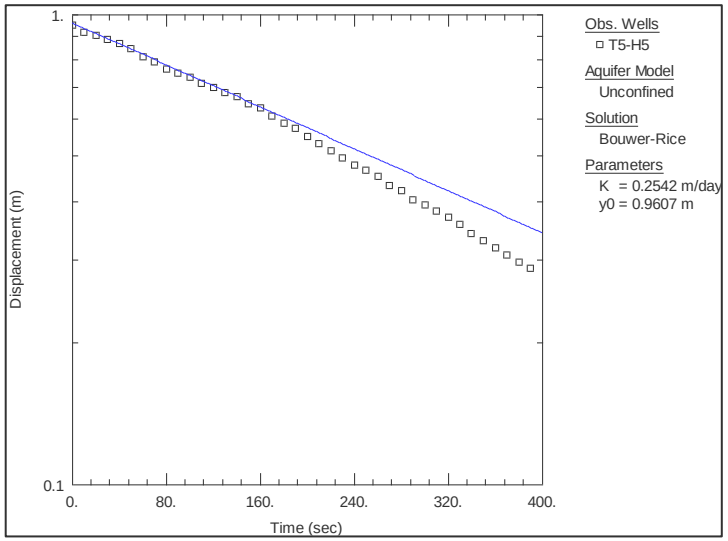

UNIVERSITY of the
WESTERN CAPE

https://etd.uwc.ac.za

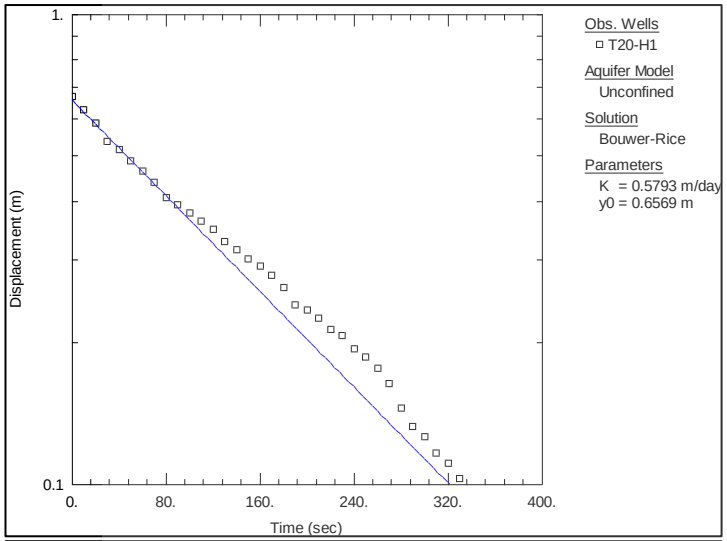

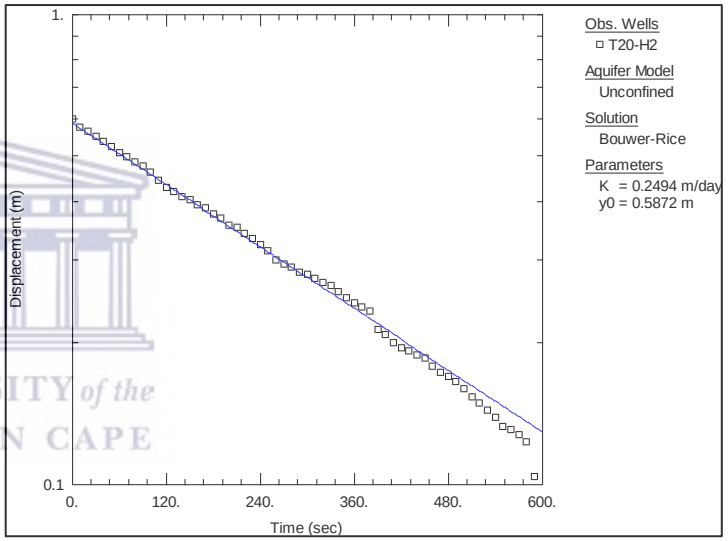

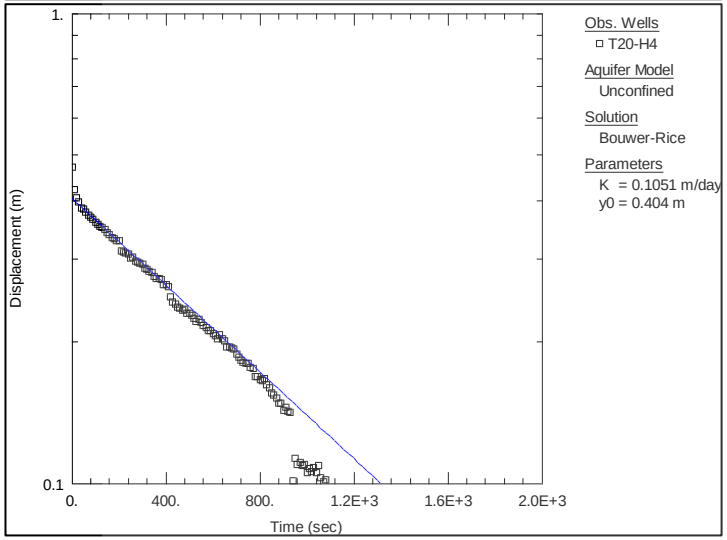

UNIVERSITY of the
WESTERN CAPE

https://etd.uwc.ac.za

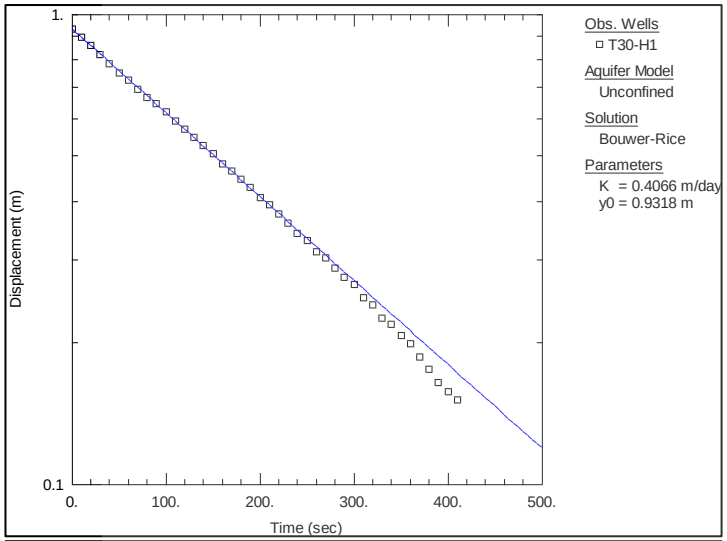

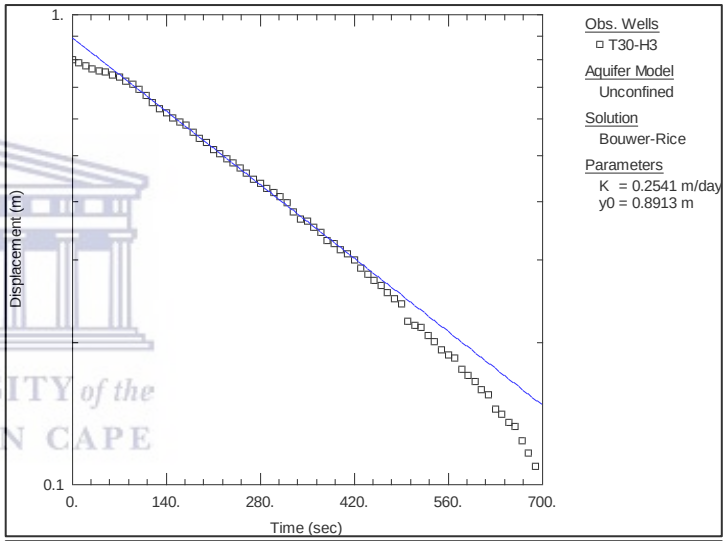

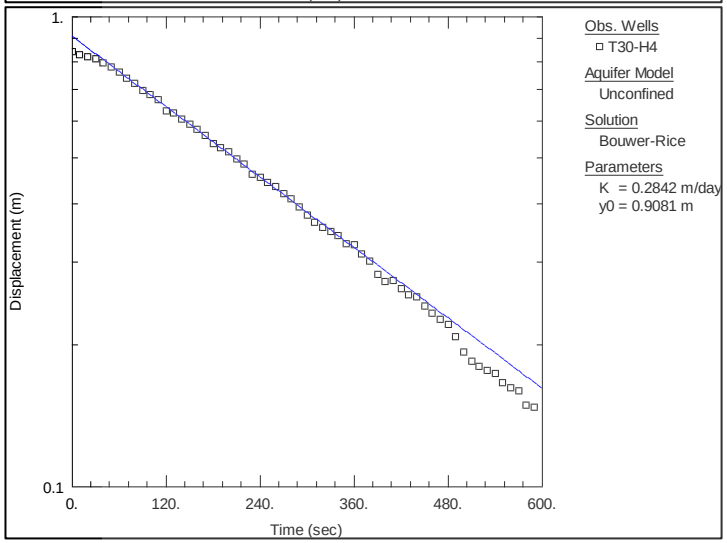

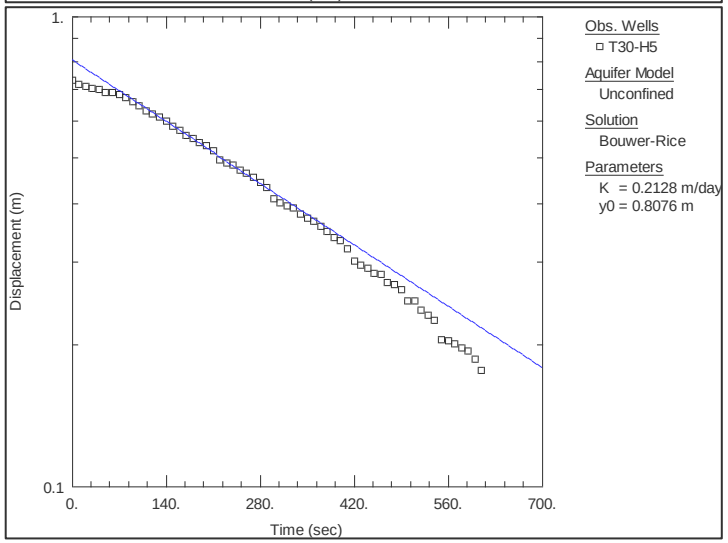

UNIVERSITY of the
WESTERN CAPE

https://etd.uwc.ac.za

APPENDIX C: Leachate samples quality data.

K50 Column												
Project		**Experiments**										
Parameters (mg/l)	**Sample ID**	**K50 15-09 01**	**K50 18-09 02**	**K50 19-09 03**	**K50 20-09 04**	**K50 03-10 05**	**K50 10-10 06**	**K50 20-10 07**	**K50 26-10 08**	**K50 06-11 09**	**K50 08-11 10**	**K50 15-11 11**
	Lab ID	**DUK 034**	**DUK 035**	**DUK 036**	**DUK 037**	**DUK 038**	**DUK 040**	**DUK 041**	**DUK 044**	**DUK 045**	**DUK 046**	**DUK 047**
Al		2.74	32.5	38.1	38.9	30.9	35.4	41.3	41.5	36.8	37.3	41.1
B		2.83	1.90	1.65	1.29	1.74	1.63	1.44	1.06	0.880	0.849	0.789
Ca		569	479	464	411	530	454	455	423	418	446	494
Cr		0.202	0.115	0.095	0.075	0.026	<0.01	<0.01	<0.01	<0.01	<0.01	<0.01
Fe		<0.06	0.064	0.067	0.092	0.098	0.157	0.685	1.55	8.89	12.4	21.3
K		7.12	5.71	4.72	4.34	7.48	6.02	5.95	5.35	5.38	5.80	7.16
Mg		306	251	261	233	246	257	303	267	275	293	325
Mn		5.38	28.4	32.5	31.1	39.1	55.8	72.8	69.1	74.4	84.8	94.2
Mo		0.030	0.049	0.081	0.073	0.033	0.032	0.038	0.052	0.053	0.011	0.027
Na		57.8	47.6	36.1	34.5	49.9	44.4	45.0	41.0	40.6	41.7	51.0
Ni		0.174	0.899	1.01	0.945	0.969	1.21	1.36	1.37	1.64	1.84	1.84
Si		0.511	3.80	4.21	4.50	3.54	3.51	4.01	3.82	3.99	3.98	4.52
Sr		3.61	3.38	3.08	2.65	4.76	3.82	3.75	3.47	3.86	4.33	3.92
V		0.035	0.019	0.034	0.024	0.027	<0.01	0.010	0.013	0.021	0.016	0.019
Zn		0.425	4.49	5.14	5.24	3.77	5.63	6.61	6.88	7.93	8.61	8.66
S as SO4		2 402	2 477	2 484	2 195	2 483	2 686	2 659	2 632	2 813	2 829	2 892

UNIVERSITY of the WESTERN CAPE

https://etd.uwc.ac.za

T50 Column															
Project		**Experiments**													
Parameters (mg/l)	**Sample ID**	**T50 15-09 01**	**T50 18-09 02**	**T50 19-09 03**	**T50 20-09 04**	**T50 03-10 05**	**T50 05-10 06**	**T50 10-10 07**	**T50 20-10 08**	**T50 23-10 9**	**T50 26-10 10**	**T50 30-10 11**	**T50 06-11 12**	**T50 15-11 13**	**T50 18-11 14**
	Lab ID	**DUK0 01**	**DUK0 02**	**DUK0 03**	**DUK0 04**	**DUK0 05**	**DUK0 06**	**DUK0 07**	**DUK0 08**	**DUK0 10**	**DUK0 11**	**DUK0 12**	**DUK0 13**	**DUK0 14**	**DUK0 15**
Al		0.547	31.8	38.6	34.0	20.9	29.3	51.5	61.1	64.5	69.5	72.6	60.7	70.0	76.0
B		2.52	1.90	2.05	1.76	1.50	1.78	1.31	0.679	0.473	0.373	0.303	0.184	0.125	0.101
Ca		514	481	510	463	440	485	455	410	449	466	456	350	395	305
Cr		0.187	0.074	0.052	0.038	<0.01	<0.01	<0.01	<0.01	<0.01	<0.01	<0.01	<0.01	<0.01	<0.01
Fe		<0.06	<0.06	0.082	0.089	0.096	0.123	0.235	0.309	0.350	0.339	0.340	2.65	6.00	5.28
K		9.25	6.42	7.11	6.56	7.91	6.67	5.58	6.21	11.03	5.34	5.61	4.76	4.62	5.17
Mg		305	298	313	277	233	309	313	258	272	281	284	199	197	166
Mn		23.9	26.6	32.4	29.3	30.3	45.9	69.8	117	126.1	128	119	77.8	64.4	50.5
Mo		0.039	0.067	0.053	0.075	0.069	0.051	0.095	0.030	0.074	0.074	0.065	0.094	0.136	0.133
Na		54.3	46.4	49.1	42.7	46.2	46.5	43.2	43.8	45.1	41.3	38.7	31.9	31.5	36.1
Ni		0.797	0.818	0.879	0.942	0.931	1.13	1.32	2.08	2.25	2.84	3.29	2.68	2.40	2.13
Si		1.68	3.11	4.15	3.33	2.51	2.95	4.11	4.54	5.13	5.62	5.80	5.42	5.24	4.57
Sr		4.45	3.27	3.31	3.60	4.74	3.87	3.12	3.32	2.99	3.05	2.93	2.63	2.60	2.24
V		0.043	0.017	0.032	0.035	0.031	0.019	0.021	<0.01	<0.01	0.018	0.029	0.020	0.029	0.024
Zn		2.41	4.11	4.62	4.66	4.59	5.59	6.79	8.75	9.26	12.5	14.6	18.1	16.2	13.7
S as SO4		2 735	2 678	2 824	2 796	2 609	2 691	2 811	2 959	2 817	2 979	3 010	2 627	2 572	2 260

UNIVERSITY of the WESTERN CAPE

https://etd.uwc.ac.za

K500 Column													
Project		**Experiments**											
Parameters (mg/l)	**Sample ID**	**K500 14-09 01**	**K500 15-09 02**	**K500 16-09 03**	**K500 20-09 04**	**K500 03-10 05**	**K500 10-10 06**	**K500 20-10 07**	**K500 26-10 08**	**K500 03-11 09**	**K500 06-11 10**	**K500 08-11 11**	**K500 15-11 12**
	Lab ID	**DUK048**	**DUK049**	**DUK050**	**DUK053**	**DUK054**	**DUK056**	**DUK057**	**DUK060**	**DUK062**	**DUK063**	**DUK064**	**DUK065**
Al		1.41	0.516	<0.06	0.121	<0.06	<0.06	0.202	<0.06	0.180	<0.06	<0.06	0.090
B		0.016	0.088	0.067	2.13	2.68	3.37	3.66	3.87	4.15	4.01	4.17	4.28
Ca		106	527	547	565	545	416	712	493	590	520	545	550
Cr		1.95	1.17	0.713	0.164	0.027	<0.01	<0.01	<0.01	<0.01	<0.01	<0.01	<0.01
Fe		0.094	<0.06	<0.06	<0.06	0.179	<0.06	<0.06	<0.06	0.027	<0.06	<0.06	0.071
K		40.0	22.3	14.8	10.2	12.4	6.87	17.3	10.0	9.46	10.2	8.56	7.77
Mg		0.987	1.08	1.18	119	109	215	305	229	270	265	216	312
Mn		0.213	<0.06	<0.06	<0.06	<0.06	<0.06	<0.06	<0.06	19.6	9.51	12.0	30.6
Mo		1.30	0.434	0.162	0.111	0.053	0.053	0.029	0.055	0.052	0.041	0.048	0.031
Na		51.8	57.1	69.1	45.0	45.2	37.0	70.0	48.3	49.8	50.2	47.0	56.3
Ni		<0.01	<0.01	<0.01	<0.01	<0.01	<0.01	0.023	<0.01	0.128	0.052	0.060	0.280
Si		0.555	1.69	1.89	-0.148	0.104	0.187	0.206	0.185	0.316	0.163	0.099	0.350
Sr		13.1	16.1	13.6	7.72	9.38	5.74	6.70	7.08	7.36	6.69	7.20	7.43
V		0.274	0.145	0.116	0.065	0.064	0.018	<0.01	0.022	0.030	0.026	0.012	<0.01
Zn		0.027	<0.01	<0.01	<0.01	0.032	<0.01	<0.01	<0.01	0.019	<0.01	<0.01	0.266
S as SO4		298	1 274	1 463	1 764	1 807	2 198	2 245	2 170	2 467	2 428	2 432	2 555

UNIVERSITY of the WESTERN CAPE

https://etd.uwc.ac.za

T500 Column															
Project		**Experiments**													
Parameters (mg/l)	**Sample ID**	**T500 14-09 01**	**T500 15-09 02**	**T500 16-09 03**	**T500 18-09 04**	**T500 20-09 05**	**T500 03-10 06**	**T500 05-10 07**	**T500 10-10 08**	**T500 20-10 09**	**T500 26-10 10**	**T500 03-11 11**	**T500 06-11 12**	**T500 08-11 13**	**T500 15-11 14**
	Lab ID	**DUK0 16**	**DUK0 17**	**DUK0 18**	**DUK0 19**	**DUK0 21**	**DUK0 22**	**DUK0 23**	**DUK0 24**	**DUK0 25**	**DUK0 28**	**DUK0 30**	**DUK0 31**	**DUK0 32**	**DUK0 33**
Al		0.763	0.438	0.200	<0.06	<0.06	<0.06	<0.06	0.120	0.114	0.138	6.65	9.58	14.9	14.8
B		0.289	0.268	0.537	2.27	2.66	2.82	3.15	3.29	3.86	3.943	3.23	3.21	2.67	2.66
Ca		158	542	580		506	556	587	539	545	538	439	496	416	435
Cr		4.95	1.69	0.793	0.480	0.203	0.049	0.070	0.027	<0.01	<0.01	<0.01	<0.01	<0.01	<0.01
Fe		<0.06	<0.06	<0.06	<0.06	<0.06	<0.06	<0.06	<0.06	<0.06	<0.06	0.069	<0.06	<0.06	0.099
K		86.5	26.6	11.0	9.27	8.43	11.4	8.19	8.88	8.95	8.10	6.08	7.04	6.37	6.52
Mg		1.23	2.49	13.7	104	140	141	253	271	250	276	278	361	332	329
Mn		0.246	0.018	<0.06	<0.06	<0.06	<0.06	4.39	15.3	17.4	26.4	22.8	28.2	26.5	30.7
Mo		1.00	0.335	0.166	0.138	0.098	0.037	0.064	0.042	0.044	0.049	0.011	<0.01	<0.01	0.013
Na		**447**	**137**	53.1	53.9	49.0	52.2	56.0	56.1	51.8	54.7	41.0	49.3	51.5	49.5
Ni		<0.01	<0.01	<0.01	<0.01	<0.01	<0.01	0.118	0.311	0.309	0.581	0.601	0.687	0.863	0.763
Si		1.04	1.06	1.17	0.901	0.432	0.735	0.519	0.613	0.541	0.844	1.46	1.74	1.47	1.72
Sr		9.85	13.8	12.1	8.71	8.03	8.54	6.53	5.87	6.67	6.42	4.61	4.24	4.71	4.14
V		0.566	0.200	0.147	0.113	0.070	0.018	0.013	0.030	0.031	<0.01	<0.01	<0.01	<0.01	<0.01
Zn		0.057	<0.01	<0.01	<0.01	<0.01	0.021	0.038	0.179	0.209	3.29	2.88	3.04	3.88	3.29
S as SO4		1 410	1 564	1 685	1 826	1 988	1 949	2 267	2 367	2 370	2 598	2 543	2 628	2 699	2 699

UNIVERSITY of the WESTERN CAPE

https://etd.uwc.ac.za